Flow-IEG Enables Programmable Thermodynamic Properties in Sequence-Defined Unimolecular Macromolecules

By

Amanda C. Wicker

B.S. Chemistry
Rice University, 2014

SUBMITTED TO THE DEPARTMENT OF CHEMISTRY IN PARTIAL FULFILLMENT OF THE REQUIREMENTS FOR THE DEGREE OF

MASTER OF SCIENCE IN CHEMISTRY
AT THE
MASSACHUSETTS INSTITUTE OF TECHNOLOGY

JUNE 2017

Signature of Author: Signature redacted

Department of Chemistry
April 14, 2017

Certified by: Signature redacted

Timothy F. Jamison
Department Head and Robert R. Taylor Professor of Chemistry
Thesis Supervisor

Accepted by: Signature redacted

Robert Warren Field
Robert T. Haslam and Bradley Dewey Professor of Chemistry
Director of Graduate Studies

Flow-IEG Enables Programmable Thermodynamic Properties in Sequence-Defined Unimolecular Macromolecules

By

Amanda C. Wicker

Submitted to the Department of Chemistry
on April 14, 2017 in Partial Fulfillment of the
Requirements for the Degree of
Master of Science in Chemistry

ABSTRACT

Flow-IEG has emerged as a powerful platform for the production of sequence-defined macromolecules and has demonstrated the utility of adapting continuous-flow methodologies to the production of materials for structure/function analysis. Our Flow-IEG system has been expanded to include both the ruthenium-catalyzed azide–alkyne cycloaddition (RuAAC), as well as a more operationally simple version of the copper-catalyzed analogue (CuAAC). These advances have enabled the rapid synthesis of a library of oligomers with systematic variations in triazole connectivity, allowing us to probe the consequences of sequential connectivity on material properties. In our investigation, we found that the crystallinity of the synthesized materials increased with higher proportions of 1,4- to 1,5-triazoles, from which a set of predictive design rules was developed and applied to a second library of diblock copolymers. Furthermore, we discovered that the crystallization properties of these macromolecules were highly dependent on both their monomer sequence and triazole substitution pattern. The results of these studies are reported herein.

Thesis Supervisor: Timothy F. Jamison
Title: Department Head and Robert R. Taylor Professor of Chemistry

TABLE OF CONTENTS

1. Introduction

The synthesis of monodisperse macromolecules of intermediate size is inherently challenging. Oligomers are too large for stepwise synthetic approaches, which can require days to produce a single oligomer, and traditional polymerization techniques lack the fine control of molecular structure necessary to produce unimolecular, sequence-defined materials. However, the ability to control the molecular structure and assembly of sequence-defined synthetic polymers holds significant potential in a number of applied areas and this demand has spurred many creative approaches to this contemporary challenge.[1–5]

A valuable method for the synthesis of sequence-defined unimolecular polymers is iterative exponential growth (IEG). First developed by Whiting[6,7] and expanded by Moore,[8,9] Tour,[10] Hawker,[11,12] and many others,[13] IEG methods combine a series of orthogonal deprotection and coupling methods to produce unimolecular, sequence-defined polymers. Fundamental to the success of this iterative approach are high-yielding reactions. As a result, the azide–alkyne 1,3-dipolar cycloaddition first developed by Huisgen[14] and made catalytic by both Sharpless et al.[15] and Meldal et al.,[16] has found great utility in IEG.[13,17–19] Despite its efficiency and long history, IEG has not become a routine method in polymer synthesis due to its laborious and repetitive nature which requires three reaction and purification steps for each doubling of molecular weight.

Continuous-flow chemistry was recognized as a promising area to simplify the redundancy of IEG due to its throughput, reproducibility, and ability to telescope reactions.[20–22] Our group previously reported the application of flow chemistry to IEG to create a continuous-flow system that performs one cycle of IEG (two deprotection steps, in-line purification, and one coupling step) in an uninterrupted fashion (Figure 1).[23] Referred to as Flow-IEG, the first

generation continuous system demonstrated the utility of this hybrid approach through the synthesis of an alternating polyester/oligo(ethylene glycol) hexadecamer with a molecular weight of 4,023 g/mol in a 28% overall yield from the monomer in four cycles.

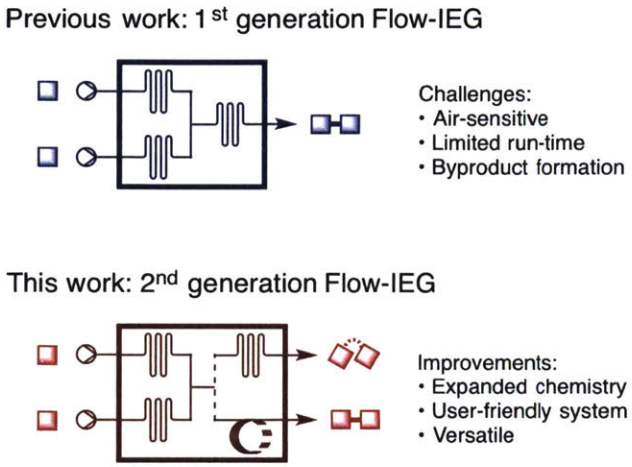

Figure 1. The evolution of the Flow-IEG platform.

With the concept of Flow-IEG established, there exist significant opportunities to exploit the molecular-level control over sequence and connectivity to synthesize materials with systematic variations in structure and enable a semi-automated method to tune the thermal and mechanical properties of soft materials. Herein we report an improved Flow-IEG platform which incorporates new coupling chemistry and facilitates the rapid synthesis of libraries of structurally isomeric oligomers with systematic variations in both sequence and connectivity. Using a telescoped continuous-flow series of reactions, the structure–property relationships of these soft materials were prepared for investigation in an expedited fashion, with the ultimate goal of understanding the consequence of monomer sequence and connectivity on material function. The second generation Flow-IEG system described here offers a number of inherent advantages in pursuit of this goal, namely the plug-and-play nature of the platform and its expanded reactivity, which enables facile variation in sequence (through the use of different starting monomers) and connectivity (through the introduction of new chemical reactions).

2. Results and Discussion

Design and Optimization of Flow-IEG Click Reactors. In pursuit of a more robust and user-friendly system, we first sought to modify the copper-catalyzed azide–alkyne cycloaddition (CuAAC) utilized in the first generation Flow-IEG platform. Despite its efficiency and utility, the choice of copper(I) iodide as a catalyst for the CuAAC presented a number of challenges: the iodide counterion participated in a Finkelstein reaction with the bromide functionality of the growing polymer chain, the Cu(I)/ligand complex became increasingly insoluble over the course of hours, and the system required oxygen-free conditions. We sought to develop a continuous CuAAC that was homogeneous, chemoselective, tolerant to air, and could run uninterrupted.

There are a number of reports in the literature[24,25] of using copper(0) metal to generate an active copper(I) catalytic species for the CuAAC reaction. In a typical batch procedure, the coupling partners are introduced to a polar, aprotic solvent along with an elemental copper catalyst and stirred for 12–48 h.[15,26] This procedure can be accelerated by a variety of techniques, including: microwave heating,[27–29] continuous flow,[30,31] and even mechanochemical conditions.[32] We initiated our studies under continuous-flow conditions employing copper tubing as both a reactor and catalyst source. All reactions were conducted in a 1:1 mixture of toluene/polar solvent with the temperature, time, and ligand identity noted in Table 1. The flow reactors were pressurized to 100 psi using a Zaiput® back pressure regulator (BPR) to allow the superheating of solvents. Conducting the reaction in the absence of a multidentate amine ligand did not generate the 1,4-disubstituted 1,2,3-triazole product (Table 1, entry 1) and the addition of tris[2-(dimethylamino)ethyl]amine (Me_6TREN)[33] as a ligand did not appreciably improve conversion (entry 2). Changing the identity of the ligand to tris(2-benzimidazolylmethyl)amine [$(Bim)_3$], a ligand reported to be highly effective in CuAAC reactions,[34] was likewise ineffective (entry 3).

To increase the concentration of active catalyst in solution, we supplied a soluble, external copper(II) source. Previous work has demonstrated that the comproportionation of copper(II) and copper(0) can generate a soluble and active copper(I) catalyst in solution.[27,31,35] Initial trials using 10 mol% of copper(II) bromide ($CuBr_2$) passed through the copper tubing at 150 °C produced 85% conversion of starting material terminal alkyne (**1**) and aliphatic azide (**2**) into the 1,4-disubstituted triazole (**3**), with no side products detected (entry 4). We discovered that the substitution of dimethylsulfoxide (DMSO) with acetonitrile (ACN) resulted in a further increase in conversion (entries 5–9). Moreover, we found that this method was tolerant of oxygen in solution, negating the need to rigorously degas the reagents prior to use and thus making the system operationally simpler. Subsequent optimization of temperature, solvent, residence time, ligand amount, and catalyst loading allowed us to lower the amount of $CuBr_2$ while still achieving high conversion (Table 1, entries 5–7). Reagent concentration was varied from 0.1 to 0.5 M with no decrease in reactivity. Minimal conversion was obtained in the absence of copper tubing (Table 1, entry 8). For practical utility in the telescoped sequence of reactions, we selected the conditions in entry 9 for the CuAAC reaction. Our efforts in catalyst development have significantly improved the Flow-IEG system. The air-stable nature of the catalyst system makes setup more facile and substantially less time-consuming. The improved reaction conditions are consistent enough to be run without any user interference for up to 11 hours, retaining high conversion and yields throughout the length of the run.

Table 1. Optimization table of the CuAAC reaction in flow with copper metal tubing.

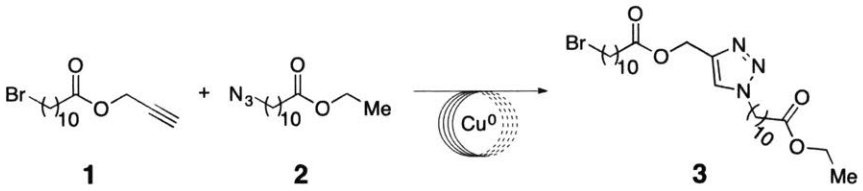

1 **2** **3**

#	$CuBr_2$, mol%	Polar Solvent	Ligand	Ligand, mol%	Temperature, °C	Residence Time, min	Conversion, %
1	0	DMSO	–	0	135	7.5	0
2	0	DMSO	Me_6TREN	25	150	7.5	10
3	0	DMSO	$(Bim)_3$	25	150	7.5	3
4	10	DMSO	Me_6TREN	60	150	7.5	85
5	10	ACN	Me_6TREN	60	150	3.8	97
6	10	ACN	Me_6TREN	0	150	3.8	–*
7	5	ACN	Me_6TREN	15	150	2.5	96
8	10	ACN	Me_6TREN	60	150	5	8†
9	5	ACN	Me_6TREN	15	140	3.3	94

Conversion of starting material to product **3** was determined through ^1H NMR. All reactions conducted in 1:1 toluene/polar solvent. *Although quantitative conversion of starting material was achieved, significant byproduct formation occurred. Additionally, $CuBr_2$ is less soluble in absence of the ligand. †PFA tubing of equal internal volume was used in lieu of copper tubing.

In order to synthesize designer materials with tunable thermal and mechanical properties, we sought to develop a complementary coupling chemistry that alters the physical properties of the synthesized oligomers while remaining isostructural in composition. The ruthenium-catalyzed azide–alkyne cycloaddition (RuAAC), developed by Fokin et al.,[36] held strong appeal for this objective as the reaction utilizes the same starting materials but produces a 1,5-disubstituted 1,2,3-triazole, which is a structural isomer of the CuAAC product. The consequences of the structural differences between these linkages has been demonstrated in their incorporation into proteins; the 1,5-triazole was utilized as a surrogate for cis-prolyl peptide bonds, whereas installation of the 1,4-isomer was found to alter the native structure of the protein.[37] Therefore, we envisioned that incorporating one or more of the 1,5-triazole linkages in an oligomer would lead to significant differences in physical properties.

We elected to use Cp*RuCl(COD) (COD = 1,5-cyclooctadiene) as our catalyst due to the reported regioselective generation of the 1,5-triazole from alkyl azides and terminal alkynes.[38] Optimization of catalyst loading, temperature, solvent, and reaction time under continuous-flow conditions (Table 2, entries 1–4) led to a method that produced high conversion from **1** and **2** to **4** at 70 °C in only 1 min (Table 2, entry 5).

Table 2. Optimization table of the RuAAC reaction in flow.

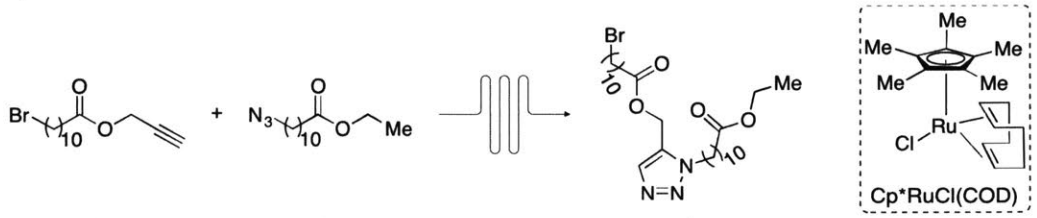

1 **2** **4**

#	Cp*RuCl(COD), mol%	Temperature, °C	Solvent	Residence Time, min	Conversion, %
1	0.5	60	Toluene	2.5	59
2	2.5	60	Toluene	2.5	95
3	2.5	70	Toluene	1.5	97
4	2.5	80	Toluene	1.5	95
5	3	70	4:1 Toluene/THF	1	96

Conversion of starting material to product **4** was determined through ^{1}H NMR.

The water sensitivity of the Cp*RuCl(COD) catalyst presented challenges that we did not observe in the copper system. Although the RuAAC reaction functions with high conversion in isolation, the telescoped Flow-IEG system necessitates that the coupling reaction be conducted after an in-line liquid–liquid extraction. Initial experiments running the Flow-IEG system with the RuAAC gave only low conversions (~10–15%) of starting material to the 1,5-triazole product. We discovered that ~2500 ppm of water (quantified by Karl Fischer titration) remained in the reaction stream after in-line liquid–liquid separation, which hindered reactivity in our initial experiments. This challenge could be overcome by increasing the catalyst loading to 5 mol% in conjunction with the addition of a column of 3 Å molecular sieves immediately after the in-line separation which reduced the water content to <120 ppm and restored reactivity

commensurate with Table 2, entry 5. Reactions were run under these conditions for up to 2 h with no decrease in reactivity or yield.

Scheme 1. Flow-IEG three-reaction sequence to produce 1,4 or 1,5 alkyl ester dimer. Box: graphical notation key.

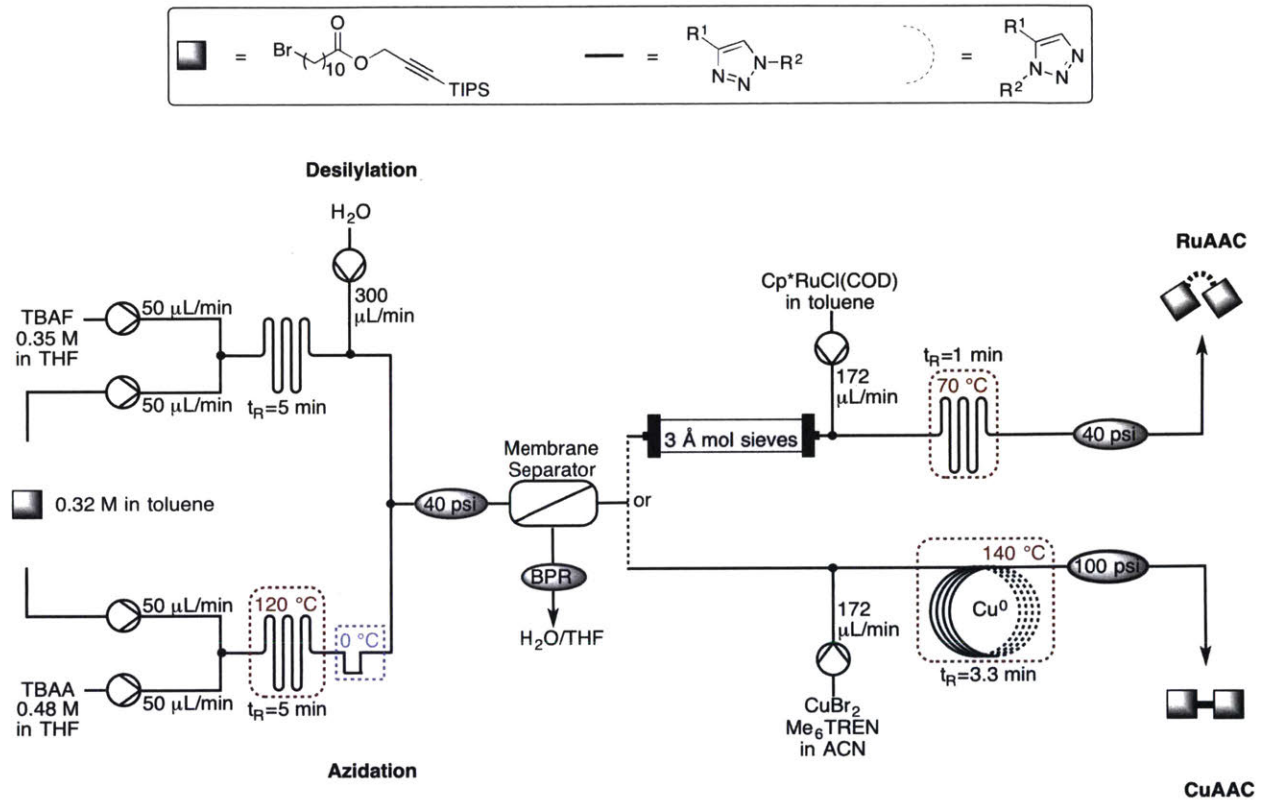

Library Synthesis of Oligomers and Investigation of Structure–Property Relationships. With two distinct modes of reactivity now amenable to Flow-IEG, we sought to systematically vary connectivity in monodisperse oligomers in order to investigate its influence on material properties. For the di-functional aliphatic ester depicted in Figure 2, its tetrameric species have eight possible structural isomers derived solely from differences in triazole connectivity. Incorporating the newly optimized coupling reactions into the Flow-IEG framework, we were able to rapidly synthesize a library of oligoesters with a variety of 1,4- and 1,5-triazole linkages (Figure 2).

The first steps of triazole formation in flow are the same for both isomers. The reagents are loaded into syringes, then pumped into two separate reactors. In the first, a triisopropylsilyl ether (TIPS) protecting group is removed to reveal a free alkyne, while in the other reactor the bromide end group is substituted by an azide (Scheme 1). Water is introduced directly after the deprotection reactions to quench excess reagents and remove tetrabutylammonium salts. The alkyne and azide streams are combined and passed through an in-line, membrane-based, liquid–liquid separator.[39] The aqueous stream containing excess tetrabutylammonium fluoride (TBAF) and tetrabutylammonium azide (TBAA) is collected as waste. For the formation of the 1,4-triazole, the organic stream containing the deprotected monomers then mix with the catalyst and proceed directly into the copper CuAAC reactor. Alternatively, to form the 1,5-triazole, the organic stream passes through a column of 3 Å molecular sieves immediately after the in-line separator to further reduce water content, and continues into a shorter PFA tubing reactor after mixing with the ruthenium catalyst. In the final system, comprised of three reactions and one in-line purification, 1,4- and 1,5-triazoles can be synthesized in just 10 and 15 minutes, respectively. By combining three reactions into one cycle of this semi-automated system, tetramers can be produced quickly and efficiently in two cycles. Using this divergent Flow-IEG system, all eight aliphatic ester tetramers were synthesized, with yields averaging 86–94% per step (Figure 2).

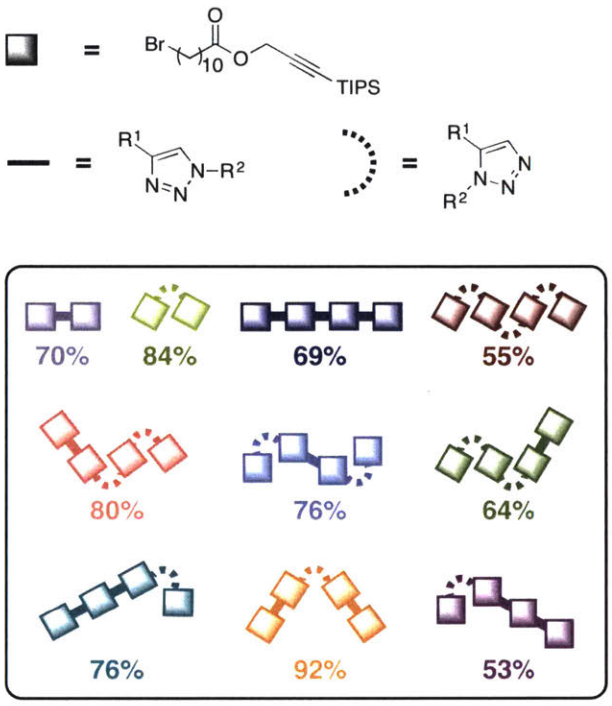

Figure 2. Top: graphical notation key for oligomers. Bottom: yields of oligoesters. Yields are given for the three-step Flow-IEG cycle that directly produced the given oligomer.

We characterized all oligomers by gel-permeation chromatography (GPC), differential scanning calorimetry (DSC), thermogravimetric analysis (TGA), high-resolution mass spectrometry (HR-MS), and ^{1}H and ^{13}C nuclear magnetic resonance (NMR). We found GPC traces and ^{1}H NMR spectra particularly informative: the GPC traces of the 1,4-tetramers displayed sharp, monomodal peaks that matched with previously determined values[23] and confirmed the unimolecular nature of the oligomers, and the ^{1}H NMR spectra revealed distinct triazole and propargylic peaks that aided in confirming structures of the new oligomers and synthetic intermediates. Concurrently with the method development and optimization of these platforms, we wanted to explore the thermal properties of the oligoesters to examine the variation in thermal properties as a function of both connectivity and structure.

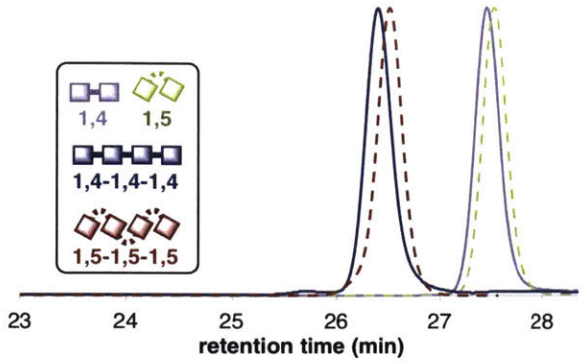

Figure 3. Overlaid GPC traces of alkyl ester 1,4 and 1,5 oligomers.

The properties of the all 1,4 series are distinct from those of the all 1,5 series. The 1,5 species adopt a smaller hydrodynamic radius than their 1,4 analogues as observed from the GPC traces in Figure 3, most likely due to the change in chain conformation induced by the 1,5- vs. 1,4-triazole linkage. Although the eight structurally isomeric tetramers differ only in the connectivity between monomers (Figure 4a), they displayed remarkably different physical properties, namely glass transition temperature (T_g), melting temperature (T_m), and crystallization behavior (Figure 4b). The T_g of all materials increased proportionally to molecular weight, as expected,[40] and were similar across the series of tetramers. Crystallization behavior, however, was significantly influenced by changes in connectivity between the monomers. The 1,4-1,4-1,4 tetramer displayed a melting point in the DSC, and is a waxy solid at room temperature (T_m = 69.0 °C, all DSC data reported from 3rd heating scan at a heating rate of 5 °C/min). All of the species with two 1,4-triazoles and one 1,5-triazole exhibit melting transitions ranging from 48.9 to 58.0 °C, which are lower than those of the parent 1,4-1,4-1,4 tetramer. Only small differences in thermal properties are observed between these three tetramers, indicating that the sequence of triazole connectivity within these oligomers has only a moderate impact on properties. The species with one 1,4-triazole and two 1,5-triazoles, as well as the 1,5-1,5-1,5 tetramer, only

display a melting peak during the first heating cycle of the DSC, but do not recrystallize during subsequent heating and cooling cycles. Further, the melting transitions observed during this slow crystallization process range from 54.5–61.1 °C, all surprisingly lower than the slow crystallization of the parent 1,5-1,5-1,5 tetramer (67.9 °C). Based on these data, we hypothesize that the relatively linear 1,4-triazole linkages increase the compound's propensity to crystallize due to greater ease in packing as compared to the distortion from linearity imparted by the 1,5-triazole linkages.

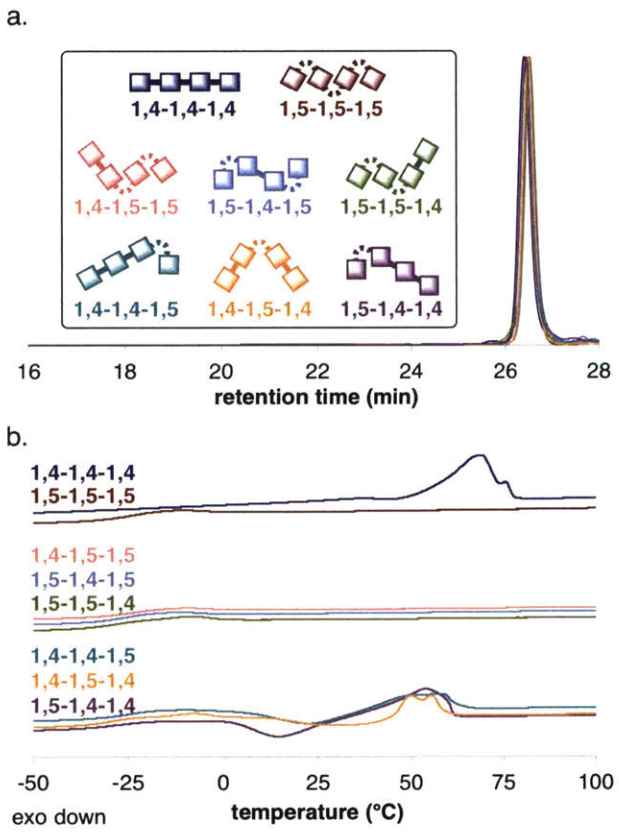

Figure 4. Physical properties vary with triazole connectivity. (a) Monomodal GPC traces of alkyl ester tetramers. (b) DSC traces of alkyl ester tetramers grouped by triazole connectivity.

Having probed one parameter—the sequence of various triazole linkages—we sought to further utilize the rapid library-synthesis capabilities of the Flow-IEG platform to produce a more complex library of tetramers. We chose to construct an isomeric series of perfectly

alternating alkyl ester/oligo(ethylene glycol) oligomers, with the hope that the added variable of monomer sequence would result in more disparate properties between the ABAB tetramers and furthermore, that our knowledge of the previous alkyl ester series would enable us to better rationalize the thermal properties of the new ABAB tetramer series. We expected that tetramers with a ratio of 1,4:1,5-triazoles <1 would not be crystalline, and that the T_ms of those species would be lower than the T_ms of tetramers with a ratio of 1,4:1,5-triazoles >1. Additionally, we predicted that both the T_ms and T_gs would increase with molecular weight. With the Flow-IEG system, we were able to quickly produce both AB dimers and all eight ABAB tetramers, averaging 83–91% yield per step (Figure 5). Notably, the added complexity of the product oligomers did not add complexity to the operation of the Flow-IEG platform—a syringe of the alkyl ester monomer was merely exchanged with one of oligo(ethylene glycol) monomer. Again, the Flow-IEG system produced unimolecular oligomers, as confirmed by GPC (Figure 6a).

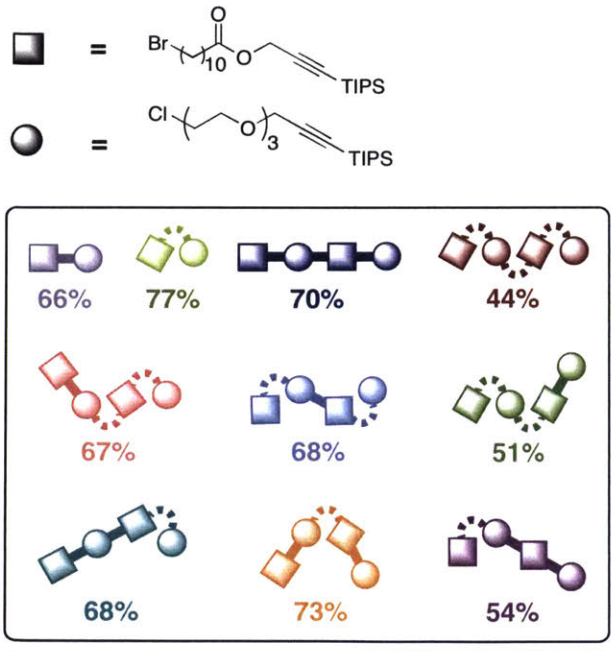

Figure 5. Top: graphical notation key for alternating oligomers. Bottom: yields of alternating oligomers. Yields are given for the three-step Flow-IEG cycle that directly produced the given oligomer.

We were pleased to discover that the properties of the ABAB tetramers followed similar trends to the aliphatic ester series of oligomers (Figure 6b). In particular, the 1,4-1,4-1,4 ABAB tetramer underwent a cold crystallization and was a waxy solid at room temperature with a T_m = 26.7 °C. All alternating oligomers containing two 1,4-triazoles and one 1,5-triazole exhibited cold crystallizations and a melting transitions (T_ms ranging from 0.3 to 16.6 °C) that were lower than that of the 1,4-1,4-1,4 ABAB tetramer. Here, the sequence of monomer connectivity did indeed appear to alter the thermal properties as the T_ms are non-identical for the 1,4-1,4-1,5 and the 1,5-1,4-1,4 ABAB tetramers. The species with one 1,4-triazole and two 1,5-triazoles did not possess crystallization or melting transitions, even on the first DSC heating cycle. 1,5-1,5-1,5 ABAB tetramer did not crystallize under any of the conditions tested and was a viscous liquid even at –70 °C. By changing the order of triazole linkages within these alternating oligomers, we were able to tune the melting transitions of isomeric species.

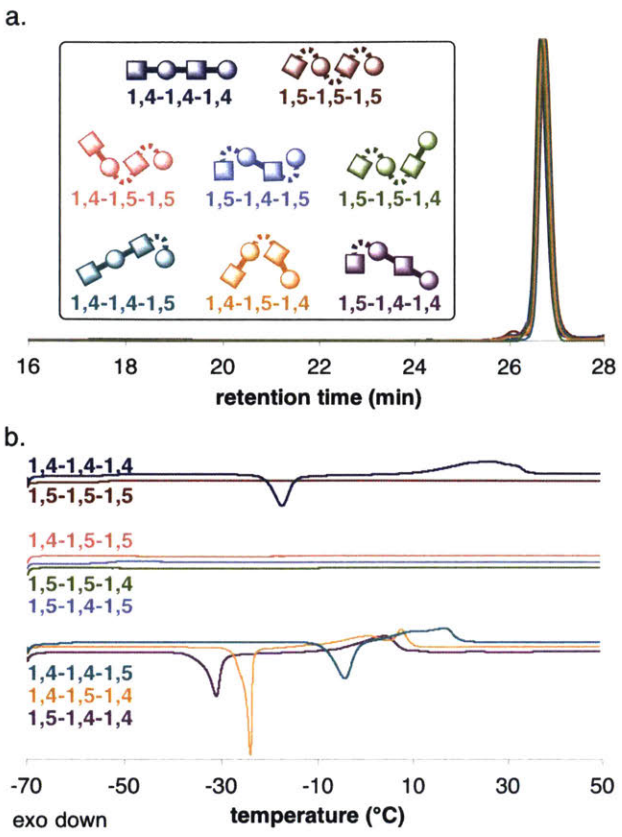

Figure 6. Physical properties vary with both triazole and monomer connectivity. (a) Monomodal GPC traces of ABAB tetramers. (b) DSC traces of ABAB tetramers grouped by triazole connectivity.

From these data, we posit that it is not the absolute number of triazole linkages, but rather the proportion of 1,4:1,5-triazole linkages that determines physical properties, and that the sequence of monomers or triazole linkages can further tune those values. In simple macromolecules such as the alkyl ester oligomers, it was predominantly the combination of triazole linkages, more than the order in which they occurred, that governed the properties discussed. However, in more complex systems like the alternating oligomers, the types of triazoles and the order in which they occur can be combined to allow programmable control over the physical properties of these soft materials.

3. Conclusion

This work demonstrates the utility of the Flow-IEG system for making unimolecular, defined macromolecules and the ability to diversify structure through the use of plug-and-play reactors. Oligomers of >1000 g/mol were manufactured quickly, efficiently, and in a semi-automated-manner. Production of monodisperse oligomers of this size is inherently challenging: iterative synthetic approaches require days to produce a single oligomer, and polymer chemistry approaches struggle to produce truly monodisperse products. By developing technology for the rapid production of libraries of oligomers, we were able to isolate the variables of sequence and connectivity and study how they independently influence the properties of soft materials. Predictive rules emerged from these studies that can be used to synthesize materials with programmable properties. This work validates Flow-IEG as a uniquely valuable tool in the production of libraries of materials for structure/function analysis, and displays the benefits of merging continuous processes and polymer chemistry to enable fundamental studies that are inaccessible through traditional means.

4. Experimental

Materials

All commercially obtained solvents and reagents were used without further purification, with the exception of the TBAA, which was dissolved to in tetrahydrofuran (THF) and filtered through a VWR 13 mm Syringe Filter with 0.2 μm PTFE membrane prior to use. (3-Bromoprop-1-yn-1-yl)triisopropylsilane[41], the oligo(ethylene glycol) monomer,[19] and 3-(triisopropylsilyl)prop-2-yn-1-yl 11-bromoundecanoate[23] were prepared according to previously published procedures. The TBAF deprotection and azide displacement reactions were conducted as previously described, although higher equivalents of TBAA (1.5 eq) were used.[23] Anhydrous THF, toluene, DMSO, and ACN were purified in a SG Water USA solvent column system. Flash column chromatography was performed using either Silicycle silica gel (230–400 mesh) or a Biotage Isolera flash purification system on SNAP Ultra columns. Analytical TLC was performed on TLC Silica gel 60 F_{254} plates and visualized using a UV lamp (254 nm) and $KMnO_4$ stain.

Flow equipment

Harvard Apparatus syringe pumps, model PHD 2000, with 8 mL stainless-steel syringes (four syringes in two pumps) were used to flow the substrate solutions and the TBAF and TBAA solutions. VICI Model M6 Liquid Handling Pumps were used to flow the CuAAC or RuAAC solution and the water utilized for separation. FloZF™ software was used to control the flow rates of the M6 pumps. Spring-based BPRs, PFA tubing, connectors, mixers, etc. were purchased from IDEX Health & Science. PFA tubing with a 0.03 in inner diameter was used unless otherwise noted. Copper-metal tubing of 0.0345 in inner diameter and 1/16 in outer diameter was purchased from Small Parts, and activated by injection of 10 mL 1 M HCl through the reactor

before use. Stainless-steel nuts, unions, and ferrules were purchased from Swagelok. T-mixers with an internal diameter of 0.02 in were used for mixing all of the reagents. Heating the reactors was accomplished by immersion in an oil bath with temperature regulation provided by an IKA hot plate equipped with a thermocouple probe. The membrane-based liquid–liquid separator and BPRs were purchased from Zaiput Flow Technologies.

Copper-catalyzed azide–alkyne cycloaddition optimization

The coupling partners were prepared and mixed in solution at a total concentration of 0.2 M in toluene and loaded into an 8 mL stainless-steel syringe. A mixture of $CuBr_2$, ligand, and solvent was prepared and loaded into an 8 mL stainless-steel syringe. The two reagent streams were allowed to mix in a T-mixer before continuing into a copper-metal tubing reactor. The residence time was varied by adjusting the flow rate. The system was allowed to equilibrate for 3 residence times to reach steady state before the product was collected for analysis. The results of the trials are shown in Table 1.

Ruthenium-catalyzed azide–alkyne cycloaddition optimization

The coupling partners were prepared and mixed in solution at a total concentration of 0.2 M in toluene. The Cp*RuCl(COD) catalyst was weighed out into a vial, capped, evacuated, and backfilled with argon two times before the introduction of toluene. All solvent and reagent solutions were degassed by sparging with argon for 20 min before being loaded into 8 mL stainless-steel syringes. The reagent streams were allowed to mix in a T-mixer before continuing into a PFA tubing reactor. The residence time was varied by adjusting the flow rate. The system

was allowed to equilibrate for 3 residence times to reach steady state before the product was collected for analysis. The results of the trials are shown in Table 2.

General notes for running the Flow-IEG reactions

The substrates of interest, TBAF, and TBAA solutions were all pumped using Harvard PHD 2000 pumps equipped with 8 mL stainless-steel syringes at 50 μL/min. The deionized water for the separation was pumped at 300 μL/min using an M6 pump. The organic stream exiting the separator was recorded as flowing at 172 μL/min, and so the catalyst stream was also pumped at 172 μL/min, using an M6 pump. The catalyst loading is calculated from the concentration of the reagent stream post-separation in order to account for the concentrating effect of the separator. The system was allowed to equilibrate for 3 residence times to reach steady state before product was collected for anlaysis. Reactions generating alkyl ester tetramers were generally conducted at monomer concentrations of 0.15 M in chlorobenzene to maintain solubility in the flow system. For reactions involving the alkyl ester/oligo(ethylene glycol) series, a substrate concentration of 0.32 M in toluene was found to be necessary to ensure reactivity.

Example procedure for running the CuAAC Flow-IEG system

Two 0.32 M solutions of 3-(triisopropylsilyl)prop-2-yn-1-yl 11-bromoundecanoate were prepared by dissolving 1.47 g of 3-(triisopropylsilyl)prop-2-yn-1-yl 11-bromoundecanoate in 5 mL toluene per solution. A 0.35 M (1.1 eq) solution of TBAF was prepared by dissolving 0.55 g TBAF•$3H_2O$ in a 2:1 THF/toluene solution for a total volume of 5 mL. A 0.48 M (1.5 eq) solution of TBAA was prepared by dissolving 0.68 g TBAA in THF at a total volume of 5 mL, then filtered to remove undissolved particles. A 5 mol% $CuBr_2$/15 mol% Me_6TREN solution was

prepared by dissolving 42 mg of $CuBr_2$ and 129 mg of Me_6TREN in 20 mL ACN. The pumps were turned on and the system was allowed to equilibrate for 3 residence times to reach steady state. The product was collected for 2 h. The solvent was evaporated, and the product was loaded directly on a column and run at 10% EtOAc/Hex to remove byproducts, and then ramped to 40% EtOAc/Hex to yield the product as a waxy white solid (70% yield). A photograph of the setup can be seen in Figure 7, and the diagram of the system can be viewed in Scheme 1.

Figure 7. Photograph of CuAAC system with labeled components.

Example procedure for running the RuAAC Flow-IEG system

Two 0.15 M solutions of 3-(triisopropylsilyl)prop-2-yn-1-yl 11-bromoundecanoate were prepared by dissolving 0.69 g of 3-(triisopropylsilyl)prop-2-yn-1-yl 11-bromoundecanoate in 5

mL toluene for each. A 0.165 M (1.1 eq) solution of TBAF was prepared by dissolving 0.26 g TBAF•$3H_2O$ in a 2:1 THF/toluene solution for a total volume of 5 mL. A 0.225 M (1.5 eq) solution of TBAA was prepared by dissolving 0.32 g TBAA in THF at a total volume of 5 mL, then filtered to remove undissolved particles. A 5 mol% solution of Cp*RuCl(COD) was prepared as described above with 33 mg Cp*RuCl(COD) in 20 mL toluene. All reagent and solvent solutions were degassed for 20 min before use. The pumps were turned on, and the system was allowed to equilibrate for 3 residence times to reach steady state. The product was collected for 2 h. The solvent was evaporated, and the product was loaded directly on a column and run at 10% EtOAc/Hex to remove byproducts, and then ramped to 40% EtOAc/Hex to yield the product as an amber viscous liquid (84% yield). A photograph of the setup can be seen in Figure 8, and a diagram of the system can be viewed in Scheme 1.

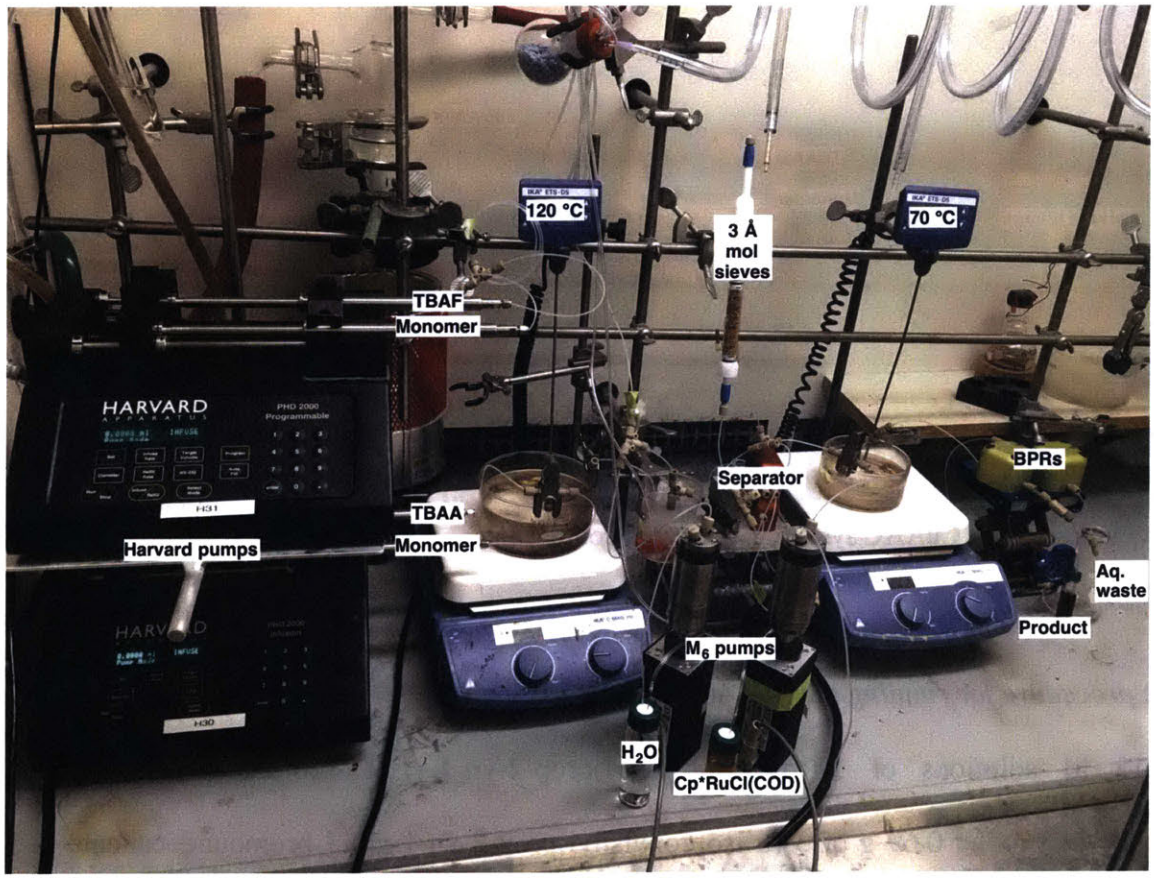

Figure 8. Photograph of the RuAAC setup with labeled components.

Characterization

^{1}H NMR and ^{13}C NMR spectra were recorded on a Bruker 400 or a JEOL 500 NMR spectrometer. Chemical shifts are reported in δ, parts per million (ppm) relative to the residual solvent peak of $CDCl_3$. Data are reported as follows: chemical shift, multiplicity (s = singlet, d = doublet, t = triplet, q = quartet, dd = doublet of doublets, dt = doublet of triplets, ddt = doublet of doublet of triplets, dtd = doublet of triplet of doublets, m = multiplet), coupling constant (*J*) in Hertz (Hz), and integration. GPC was performed in THF on an HP/Agilent series 1100 GPC system and analyzed using a HP/Agilent refractive index detector. TGA was performed on a TA Instruments Discovery TGA. Samples were run in platinum TGA pans at a ramp rate of 10 °C/min from 50 °C to 600 °C. DSC was performed on a TA Instruments Discovery DSC. Samples were run in Tzero aluminum pans with hermetic lids. Data for the alkyl ester oligomers were taken from the third heating cycle of a run where the sample was cycled at a rate of 5 °C/min from –70 °C to 150 °C; data for the alkyl ester/oligo(ethylene glycol) oligomers were taken from the third heating cycle of a run where the sample was cycled at a rate of 5 °C/min from –70 °C to 50 °C. High-resolution mass spectrometry data were acquired in the Department of Chemistry Instrumentation Facility, Massachusetts Institute of Technology on a Bruker Daltonics APEXIV 4.7 Tesla FT-ICR Mass Spectrometer. Water content was calculated with a Mettler Toledo C20 Coulometric KF Titrator.

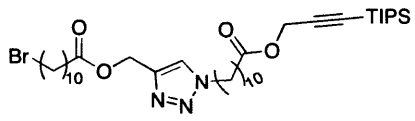

1,4 alkyl ester dimer

^{1}H NMR (500 MHz, $CDCl_3$) δ 7.57 (s, 1H), 5.21 (s, 2H), 4.70 (s, 2H), 4.33 (t, J = 7.4 Hz, 2H), 3.40 (t, J = 6.9 Hz, 2H), 2.37 – 2.28 (m, 4H), 1.93 – 1.80 (m, 4H), 1.65 – 1.58 (m, 4H), 1.44 – 1.37 (m, 2H), 1.34 – 1.22 (m, 22H), 1.06 (s, 21H). ^{13}C NMR (126 MHz, $CDCl_3$) δ 173.8, 173.0, 143.0, 123.6, 101.2, 88.1, 57.6, 52.7, 50.5, 34.2, 34.1, 32.8, 30.4, 29.41, 29.37, 29.2, 29.12, 29.07, 29.0, 28.8, 28.2, 26.5, 24.94, 24.88, 18.6, 11.2. GPC: T_{ret} = 27.4 min, $Đ$ = 1.007. HR-MS (m/z) $[M + H]^+$ calcd for $C_{37}H_{66}BrN_3O_4Si$: 726.4082; found: 726.4055.

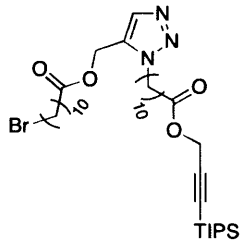

1,5 alkyl ester dimer

^{1}H NMR (500 MHz, $CDCl_3$) δ 7.69 (s, 1H), 5.16 (s, 2H), 4.70 (s, 2H), 4.33 (t, J = 7.4 Hz, 2H), 3.40 (t, J = 6.8 Hz, 2H), 2.36 – 2.29 (m, 4H), 1.93 – 1.80 (m, 4H), 1.64 – 1.60 (m, 4H), 1.44 – 1.37 (m, 2H), 1.34 – 1.24 (m, 22H), 1.06 (s, 21H). ^{13}C NMR (126 MHz, $CDCl_3$) δ 173.00, 172.97, 134.8, 131.5, 101.2, 88.1, 53.4, 52.7, 48.5, 34.1, 34.0, 32.8, 30.3, 29.43, 29.40, 29.35, 29.3, 29.2, 29.14, 29.09, 28.8, 28.2, 26.7, 24.9, 24.8, 18.6, 11.1. GPC: T_{ret} = 27.5 min, $Đ$ = 1.007. HR-MS (m/z) $[M + H]^+$ calcd for $C_{37}H_{66}BrN_3O_4Si$: 726.4082; found: 726.4053.

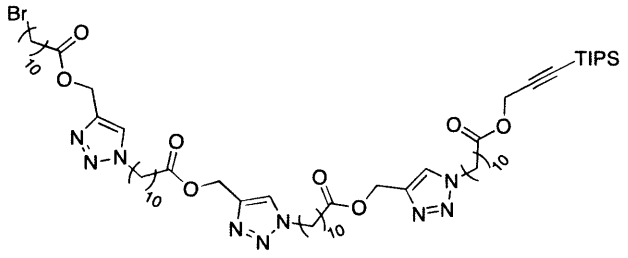

1,4-1,4-1,4 alkyl ester tetramer

^{1}H NMR (500 MHz, $CDCl_3$) δ 7.57 (s, 3H), 5.21 (s, 6H), 4.70 (s, 2H), 4.33 (t, J = 7.3 Hz, 6H), 3.40 (t, J = 6.9 Hz, 2H), 2.36 – 2.28 (m, 8H), 1.92 – 1.81 (m, 8H), 1.65 – 1.58 (m, 8H), 1.44 – 1.37 (m, 2H), 1.32 – 1.23 (m, 46H), 1.06 (s, 21H). ^{13}C NMR (126 MHz, $CDCl_3$) δ 173.73, 173.70, 172.9, 142.89, 142.86, 123.6, 101.2, 88.1, 57.5, 52.6, 50.4, 34.13, 34.07, 32.8, 30.3, 29.4, 29.3, 29.2, 29.14, 29.06, 29.04, 28.98, 28.9, 28.7, 28.2, 26.49, 26.46, 24.9, 24.8, 18.5, 11.1. GPC: T_{ret} = 26.4 min, $Đ$ = 1.011. HR-MS (m/z) $[M + H]^+$ calcd for $C_{65}H_{112}BrN_9O_8Si$: 1256.7673; found: 1256.7712.

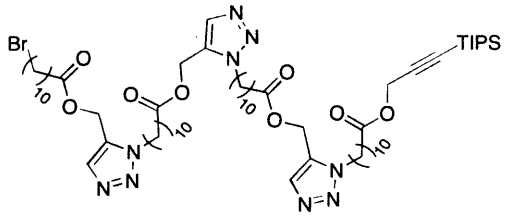

1,5-1,5-1,5 alkyl ester tetramer

^{1}H NMR (500 MHz, $CDCl_3$) δ 7.69 (s, 3H), 5.16 (s, 6H), 4.70 (s, 2H), 4.33 (t, J = 7.4 Hz, 6H), 3.40 (t, J = 6.8 Hz, 2H), 2.36 – 2.28 (m, 8H), 1.92 – 1.79 (m, 8H), 1.62 – 1.56 (m, 8H), 1.44 – 1.36 (m, 2H), 1.34 – 1.22 (m, 46H), 1.06 (s, 21H). ^{13}C NMR (126 MHz, $CDCl_3$) δ 173.0, 134.8, 131.5, 101.2, 88.1, 53.4, 52.6, 48.4, 34.11, 34.08, 34.0, 32.8, 30.31, 30.28, 29.39, 29.36, 29.3, 29.24, 29.20, 29.10, 29.06, 28.7, 28.2, 26.62, 26.59, 24.9, 24.8, 18.6, 11.1. GPC: T_{ret} = 26.5 min, $Đ$ = 1.009. HR-MS (m/z) $[M + H]^+$ calcd for $C_{65}H_{112}BrN_9O_8Si$: 1256.7673; found: 1256.7705.

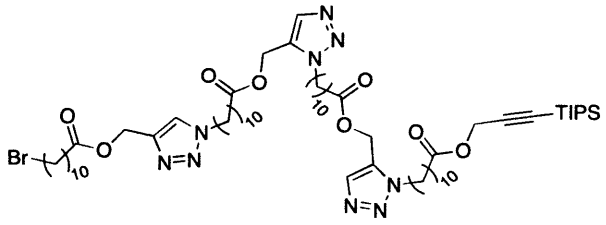

1,4-1,5-1,5 alkyl ester tetramer

^{1}H NMR (400 MHz, $CDCl_3$) δ 7.69 (s, 2H), 7.57 (s, 1H), 5.23 – 5.14 (m, 6H), 4.70 (s, 2H), 4.34 (t, J = 7.6 Hz, 6H), 3.40 (t, J = 6.9 Hz, 2H), 2.37 – 2.28 (m, 8H), 1.95 – 1.80 (m, 8H), 1.67 – 1.57 (m, 8H), 1.45 – 1.16 (m, 48H), 1.07 (s, 21H). ^{13}C NMR (126 MHz, $CDCl_3$) δ 173.6, 172.9, 142.8, 134.7, 131.4, 123.5, 101.1, 88.0, 57.5, 53.4, 52.5, 50.3, 48.4, 34.1, 34.04, 33.99, 33.9, 32.8, 30.2, 29.3, 29.24, 29.21, 29.15, 29.1, 29.01, 28.96, 28.9, 28.7, 28.1, 26.53, 26.50, 26.4, 24.82, 24.76, 24.7, 18.5, 11.0. GPC: T_{ret} = 26.5 min, $Đ$ = 1.009. HR-MS (m/z) $[M + H]^+$ calcd for $C_{65}H_{112}BrN_9O_8Si$: 1256.7673; found: 1256.7700.

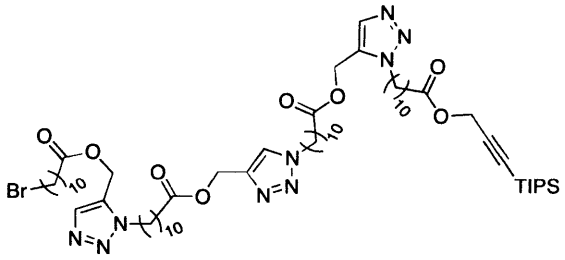

1,5-1,4-1,5 alkyl ester tetramer

^{1}H NMR (400 MHz, $CDCl_3$) δ 7.69 (s, 2H), 7.58 (s, 1H), 5.22 – 5.14 (m, 6H), 4.70 (s, 2H), 4.33 (t, J = 7.6 Hz, 6H), 3.40 (t, J = 6.8 Hz, 2H), 2.36 – 2.28 (m, 8H), 1.95 – 1.80 (m, 8H), 1.65 – 1.58 (m, 8H), 1.45 – 1.20 (m, 48H), 1.07 (s, 21H). ^{13}C NMR (126 MHz, $CDCl_3$) δ 173.7, 172.97, 172.95, 142.9, 134.8, 131.5, 123.6, 101.2, 88.1, 57.5, 53.4, 52.6, 50.4, 48.5, 34.14, 34.10, 34.07, 34.0, 32.8, 30.3, 29.38, 29.35, 29.3, 29.23, 29.18, 29.1, 29.04, 28.96, 28.7, 28.1, 26.6, 26.5, 24.9,

24.82, 24.78, 18.6, 11.1. GPC: T_{ret} = 26.5 min, $Đ$ = 1.010. HR-MS (m/z) [M + H]$^+$ calcd for $C_{65}H_{112}BrN_9O_8Si$: 1256.7673; found: 1256.7637.

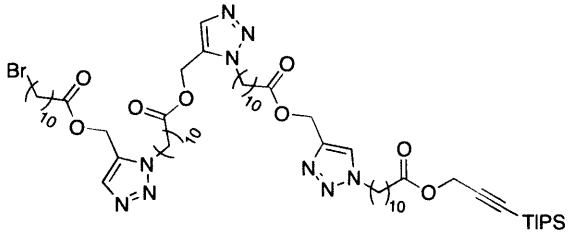

1,5-1,5-1,4 alkyl ester tetramer

^{1}H NMR (500 MHz, $CDCl_3$) δ 7.69 (s, 2H), 7.57 (s, 1H), 5.23 – 5.13 (m, 6H), 4.70 (s, 2H), 4.37 – 4.30 (m, 6H), 3.40 (t, J = 6.9 Hz, 2H), 2.37 – 2.27 (m, 8H), 1.93 – 1.80 (m, 8H), 1.66 – 1.61 (m, 8H), 1.44 – 1.21 (m, 48H), 1.06 (s, 21H). ^{13}C NMR (126 MHz, $CDCl_3$) δ 173.8, 173.02, 172.99, 142.9, 134.8, 131.5, 123.6, 101.2, 88.2, 57.6, 53.5, 52.7, 50.5, 48.5, 34.2, 34.1, 34.0, 32.8, 30.33, 30.30, 29.4, 29.3, 29.2, 29.1, 29.0, 28.8, 28.2, 26.6, 26.5, 24.93, 24.86, 24.8, 18.6, 11.1. GPC: T_{ret} = 26.5 min, $Đ$ = 1.012. HR-MS (m/z) [M + H]$^+$ calcd for $C_{65}H_{112}BrN_9O_8Si$: 1256.7673; found: 1256.7691.

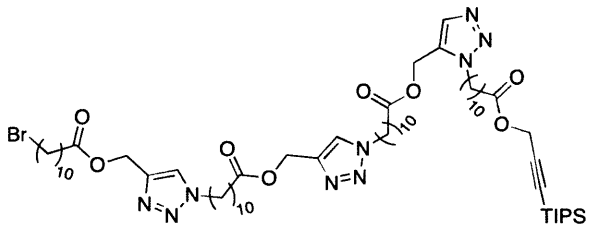

1,4-1,4-1,5 alkyl ester tetramer

^{1}H NMR (400 MHz, $CDCl_3$) δ 7.69 (s, 1H), 7.57 (s, 2H), 5.23 – 5.14 (m, 6H), 4.70 (s, 2H), 4.33 (t, J = 7.4 Hz, 6H), 3.40 (t, J = 6.9 Hz, 2H), 2.37 – 2.27 (m, 8H), 1.94 – 1.80 (m, 8H), 1.66 – 1.56 (m, 8H), 1.45 – 1.20 (m, 48H), 1.07 (s, 21H). ^{13}C NMR (126 MHz, $CDCl_3$) δ 173.68,

173.66, 172.89, 172.87, 142.85, 142.83, 134.7, 131.4, 123.6, 101.1, 88.0, 57.5, 53.4, 52.6, 50.4, 48.4, 34.10, 34.09, 34.06, 34.0, 33.9, 32.8, 30.2, 29.7, 29.4, 29.32, 29.28, 29.27, 29.25, 29.24, 29.19, 29.15, 29.12, 29.05, 29.03, 28.99, 28.9, 28.7, 28.1, 26.6, 26.4, 24.9, 24.80, 24.78, 24.7, 18.5, 11.1. GPC: T_{ret} = 26.5 min, $Đ$ = 1.013. HR-MS (m/z) $[M + H]^+$ calcd for $C_{65}H_{112}BrN_9O_8Si$: 1256.7673; found: 1256.7679.

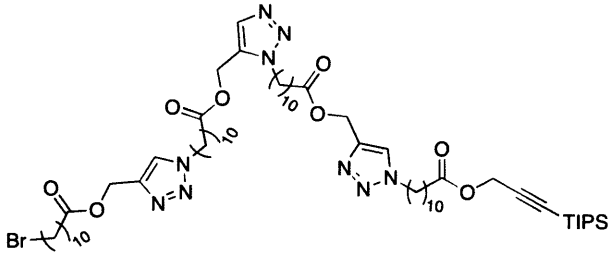

1,4-1,5-1,4 alkyl ester tetramer

^1H NMR (400 MHz, $CDCl_3$) δ 7.68 (s, 1H), 7.57 (d, J = 1.8 Hz, 2H), 5.21 (s, 4H), 5.16 (s, 2H), 4.70 (s, 2H), 4.38 – 4.29 (m, 6H), 3.40 (t, J = 6.9 Hz, 2H), 2.36 – 2.28 (m, 8H), 1.94 – 1.80 (m, 8H), 1.66 – 1.57 (m, 8H), 1.45 –1.22 (m, 48H), 1.06 (s, 21H). ^{13}C NMR (126 MHz, $CDCl_3$) δ 173.7, 173.6, 172.9, 142.84, 142.80, 134.7, 131.4, 123.5, 101.1, 88.0, 57.5, 53.4, 52.6, 50.4, 48.4, 34.1, 34.0, 33.9, 32.8, 30.2, 29.3, 29.2, 29.1, 29.01, 28.97, 28.93, 28.90, 28.7, 28.1, 26.5, 26.44, 26.41, 24.85, 24.78, 24.7, 18.5, 11.0. GPC: T_{ret} = 26.5 min, $Đ$ = 1.007. HR-MS (m/z) $[M + H]^+$ calcd for $C_{65}H_{112}BrN_9O_8Si$: 1256.7673; found: 1256.7662.

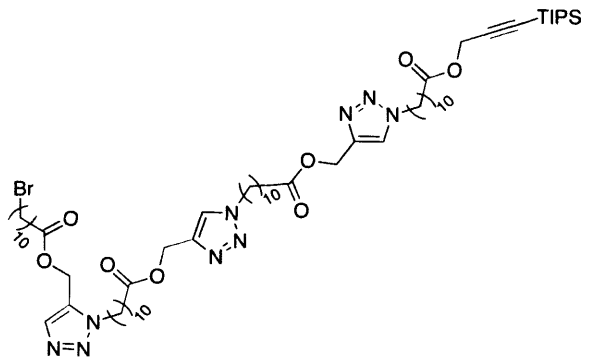

1,5-1,4-1,4 alkyl ester tetramer

^{1}H NMR (400 MHz, $CDCl_3$) δ 7.69 (s, 1H), 7.57 (s, 2H), 5.22 – 5.15 (m, 6H), 4.70 (s, 2H), 4.33 (t, *J* = 7.3 Hz, 6H), 3.40 (t, *J* = 6.9 Hz, 2H), 2.36 – 2.27 (m, 8H), 1.94 – 1.80 (m, 8H), 1.65 – 1.57 (m, 8H), 1.45 – 1.19 (m, 48H), 1.07 (s, 21H). ^{13}C NMR (101 MHz, $CDCl_3$) δ 173.7, 172.93, 172.90, 142.9, 134.7, 131.5, 123.5, 101.2, 88.1, 57.6, 53.4, 52.6, 50.4, 48.5, 34.13, 34.07, 34.05, 34.0, 32.8, 30.3, 29.4, 29.33, 29.29, 29.27, 29.20, 29.17, 29.15, 29.05, 29.02, 28.98, 28.95, 28.7, 28.2, 26.6, 26.49, 26.47, 24.9, 24.82, 24.79, 18.6, 11.1. GPC: T_{ret} = 26.5 min, $Đ$ = 1.011. HR-MS (m/z) $[M + H]^+$ calcd for $C_{65}H_{112}BrN_9O_8Si$: 1256.7673; found: 1256.7699.

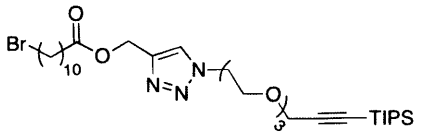

1,4 alkyl ester/oligo(ethylene glycol) dimer

^{1}H NMR (500 MHz, $CDCl_3$) δ 7.78 (s, 1H), 5.21 (s, 2H), 4.54 (t, *J* = 5.1 Hz, 2H), 4.24 (s, 2H), 3.87 (t, *J* = 5.0 Hz, 2H), 3.73 – 3.70 (m, 2H), 3.67 – 3.64 (m, 2H), 3.64 – 3.60 (s, 4H), 3.40 (t, *J* = 6.9 Hz, 2H), 2.31 (t, *J* = 7.6 Hz, 2H), 1.88 – 1.81 (m, 2H), 1.64 – 1.58 (m, 2H), 1.44 – 1.37 (m, 2H), 1.33 – 1.23 (m, 10H), 1.06 (s, 21H). ^{13}C NMR (126 MHz, $CDCl_3$) δ 173.7, 142.8, 125.0, 103.2, 87.9, 70.65, 70.58, 70.55, 69.5, 68.8, 59.3, 57.5, 50.4, 34.23, 34.18, 32.9, 29.5, 29.4, 29.3,

29.2, 28.8, 28.3, 24.9, 18.7, 11.2. GPC: T_{ret} = 27.6 min, $Đ$ = 1.004. HR-MS (m/z) $[M + H]^+$ calcd for $C_{32}H_{58}BrN_3O_5Si$: 674.3403; found: 674.3407.

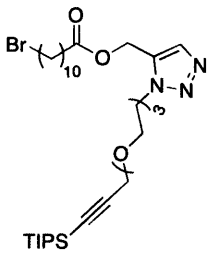

1,5 alkyl ester/oligo(ethylene glycol) dimer

^1H NMR (500 MHz, $CDCl_3$) δ 7.66 (s, 1H), 5.26 (s, 2H), 4.59 (t, J = 5.1 Hz, 2H), 4.23 (s, 2H), 3.87 (t, J = 5.2 Hz, 2H), 3.70 – 3.66 (m, 2H), 3.62 – 3.58 (m, 2H), 3.55 (s, 4H), 3.40 (t, J = 6.9 Hz, 2H), 2.31 (t, J = 7.5 Hz, 2H), 1.89 – 1.80 (m, 2H), 1.62 – 1.57 (m, 2H), 1.44 – 1.37 (m, 2H), 1.31 – 1.24 (m, 10H), 1.07 (s, 21H). ^{13}C NMR (126 MHz, $CDCl_3$) δ 173.1, 134.2, 133.6, 103.2, 87.8, 70.7, 70.5, 70.2, 68.7, 59.2, 54.1, 48.8, 34.2, 34.1, 32.9, 29.45, 29.40, 29.3, 29.1, 28.8, 28.2, 24.9, 18.7, 11.2. GPC: T_{ret} = 27.7 min, $Đ$ = 1.007. HR-MS (m/z) $[M + H]^+$ calcd for $C_{32}H_{58}BrN_3O_5Si$: 674.3403; found: 674.3397.

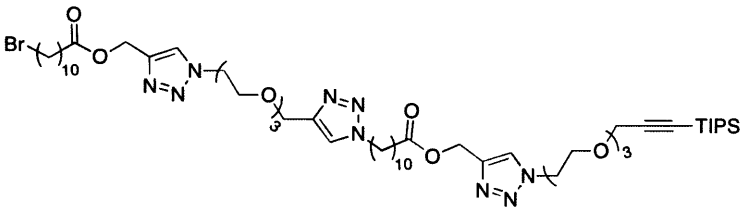

1,4-1,4-1,4 alkyl ester/oligo(ethylene glycol) tetramer

^1H NMR (500 MHz, $CDCl_3$) δ 7.78 (s, 2H), 7.53 (s, 1H), 5.20 (d, J = 3.0 Hz, 4H), 4.67 (s, 2H), 4.56 – 4.50 (m, 4H), 4.33 (t, J = 7.4 Hz, 2H), 4.23 (s, 2H), 3.87 (t, J = 5.0 Hz, 4H), 3.73 – 3.59 (m, 16H), 3.40 (t, J = 6.9 Hz, 2H), 2.31 (t, J = 7.5 Hz, 4H), 1.92 – 1.80 (m, 4H), 1.64 – 1.59 (m, 4H), 1.44 – 1.37 (m, 2H), 1.33 – 1.22 (m, 22H), 1.06 (s, 21H). ^{13}C NMR (126 MHz, $CDCl_3$) δ

173.7, 173.6, 144.9, 142.8, 125.0, 124.9, 122.5, 103.2, 87.8, 70.58, 70.55, 70.53, 70.49, 69.7, 69.5, 68.7, 64.6, 59.2, 57.5, 50.4, 50.3, 34.2, 32.9, 30.4, 29.40, 29.35, 29.2, 29.1, 29.0, 28.8, 28.2, 26.6, 24.9, 18.6, 11.2. T_{ret} = 26.6 min, $Đ$ = 1.009. HR-MS (m/z) [M + Na]$^+$ calcd for $C_{55}H_{96}BrN_9O_{10}Si$: 1174.6135; found: 1174.6094.

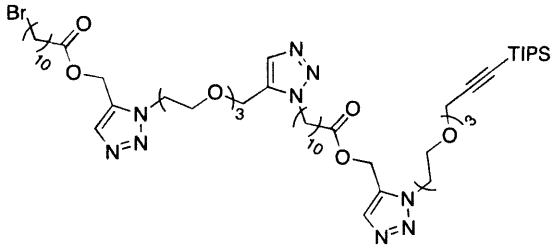

1,5-1,5-1,5 alkyl ester/oligo(ethylene glycol) tetramer

^{1}H NMR (500 MHz, $CDCl_3$) δ 7.65 (d, J = 4.0 Hz, 2H), 7.61 (s, 1H), 5.26 (s, 2H), 5.23 (s, 2H), 4.63 – 4.56 (m, 6H), 4.33 (t, J = 7.4 Hz, 2H), 4.22 (s, 2H), 3.87 (t, J = 5.2 Hz, 4H), 3.71 – 3.66 (m, 2H), 3.62 – 3.48 (m, 14H), 3.40 (t, J = 6.8 Hz, 2H), 2.34 – 2.28 (m, 4H), 1.92 – 1.80 (m, 4H), 1.62 – 1.57 (m, 4H), 1.44 – 1.37 (m, 2H), 1.32 – 1.22 (m, 22H), 1.06 (s, 21H). ^{13}C NMR (126 MHz, $CDCl_3$) δ 173.08, 173.05, 134.3, 134.1, 133.5, 133.3, 132.8, 103.2, 87.7, 70.60, 70.57, 70.5, 70.4, 70.11, 70.05, 69.5, 68.7, 61.1, 59.2, 54.00, 53.96, 48.7, 48.6, 48.5, 34.1, 34.0, 32.8, 30.1, 29.4, 29.3, 29.2, 29.11, 29.06, 28.7, 28.2, 26.6, 24.8, 18.6, 11.2. GPC: T_{ret} = 26.8 min, $Đ$ = 1.016. HR-MS (m/z) [M + H]$^+$ calcd for $C_{55}H_{96}BrN_9O_{10}Si$: 1152.6316; found: 1152.6324.

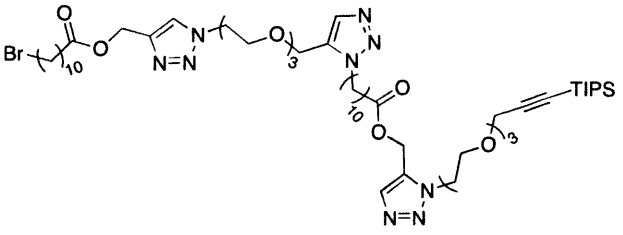

1,4-1,5-1,5 alkyl ester/oligo(ethylene glycol) tetramer

^{1}H NMR (500 MHz, $CDCl_3$) δ 7.74 (s, 1H), 7.66 (s, 1H), 7.62 (s, 1H), 5.26 (s, 2H), 5.20 (s, 2H), 4.64 – 4.56 (m, 4H), 4.53 (t, J = 5.0 Hz, 2H), 4.34 (t, J = 7.3 Hz, 2H), 4.23 (s, 2H), 3.87 (q, J = 5.4 Hz, 4H), 3.70 – 3.65 (m, 2H), 3.61 – 3.53 (m, 14H), 3.40 (t, J = 6.7 Hz, 2H), 2.31 (t, J = 7.6 Hz, 4H), 1.93 – 1.80 (m, 4H), 1.63 – 1.58 (m, 4H), 1.43 – 1.37 (m, 2H), 1.34 – 1.22 (m, 22H), 1.06 (s, 21H). ^{13}C NMR (126 MHz, $CDCl_3$) δ 173.7, 173.0, 142.8, 134.3, 134.2, 133.4, 132.7, 124.8, 103.2, 87.7, 70.6, 70.54, 70.47, 70.4, 70.1, 69.5, 69.4, 68.6, 61.1, 59.2, 57.4, 54.0, 50.3, 48.7, 48.5, 34.2, 34.0, 32.8, 30.1, 29.4, 29.3, 29.2, 29.10, 29.05, 28.7, 28.2, 26.6, 24.85, 24.79, 18.6, 11.2. GPC: T_{ret} = 26.7 min, $Đ$ = 1.015. HR-MS (m/z) $[M + H]^+$ calcd for $C_{55}H_{96}BrN_9O_{10}Si$: 1152.6316; found: 1152.6321.

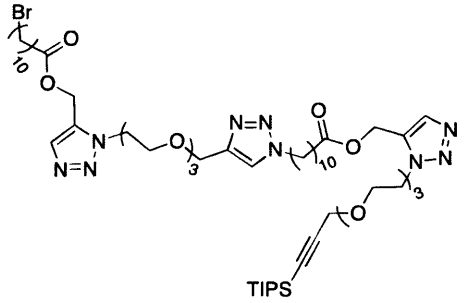

1,5-1,4-1,5 alkyl ester/oligo(ethylene glycol) tetramer

^{1}H NMR (500 MHz, $CDCl_3$) δ 7.65 (d, J = 6.3 Hz, 2H), 7.54 (s, 1H), 5.26 (d, J = 2.9 Hz, 4H), 4.67 (s, 2H), 4.61 – 4.57 (m, 4H), 4.33 (t, J = 7.3 Hz, 2H), 4.23 (s, 2H), 3.87 (t, J = 5.1 Hz, 4H), 3.69 – 3.64 (m, 4H), 3.61 – 3.52 (m, 12H), 3.40 (t, J = 6.8 Hz, 2H), 2.31 (t, J = 7.6 Hz, 4H), 1.93 – 1.80 (m, 4H), 1.62 – 1.57 (m, 4H), 1.43 – 1.38 (m, 2H), 1.34 – 1.23 (m, 22H), 1.06 (s, 21H). ^{13}C NMR (126 MHz, $CDCl_3$) δ 173.01, 172.98, 144.9, 134.2, 133.41, 133.37, 122.4, 103.2, 87.7, 70.60, 70.58, 70.45, 70.42, 70.36, 70.3, 70.1, 69.6, 68.6, 64.6, 59.1, 54.0, 50.3, 48.6, 34.1, 33.9, 32.8, 30.3, 29.32, 29.26, 29.1, 29.00, 28.95, 28.7, 28.1, 26.5, 24.8, 18.6, 11.1. GPC: T_{ret} = 26.7

min, $Đ$ = 1.015. HR-MS (m/z) $[M + H]^+$ calcd for $C_{55}H_{96}BrN_9O_{10}Si$: 1152.6316; found: 1152.6357.

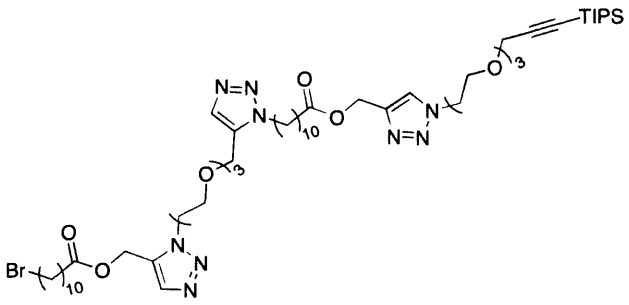

1,5-1,5-1,4 alkyl ester/oligo(ethylene glycol) tetramer

^{1}H NMR (500 MHz, $CDCl_3$) δ 7.78 (s, 1H), 7.65 (s, 1H), 7.61 (s, 1H), 5.23 (s, 2H), 5.20 (s, 2H), 4.61 (s, 2H), 4.58 (t, J = 5.1 Hz, 2H), 4.54 (t, J = 5.1 Hz, 2H), 4.34 (t, J = 7.4 Hz, 2H), 4.24 (s, 2H), 3.89 – 3.85 (m, 4H), 3.74 – 3.69 (m, 2H), 3.68 – 3.64 (m, 2H), 3.62 (s, 4H), 3.56 – 3.49 (m, 8H), 3.40 (t, J = 6.8 Hz, 2H), 2.31 (t, J = 7.6 Hz, 4H), 1.92 – 1.80 (m, 4H), 1.64 – 1.57 (m, 4H), 1.44 – 1.37 (m, 2H), 1.34 – 1.21 (m, 22H), 1.06 (s, 21H). ^{13}C NMR (126 MHz, $CDCl_3$) δ 173.6, 173.0, 142.7, 134.3, 134.1, 133.2, 132.7, 124.8, 103.1, 87.7, 70.52, 70.45, 70.41, 70.35, 70.0, 69.5, 69.4, 68.6, 61.0, 59.1, 57.5, 53.9, 50.3, 48.6, 48.4, 34.1, 33.9, 32.8, 30.0, 29.4, 29.31, 29.27, 29.2, 29.14, 29.07, 29.0, 28.7, 28.1, 26.6, 24.80, 24.75, 18.6, 11.1. GPC: T_{ret} = 26.8 min, $Đ$ = 1.015. HR-MS (m/z) $[M + H]^+$ calcd for $C_{55}H_{96}BrN_9O_{10}Si$: 1152.6316; found: 1152.6340.

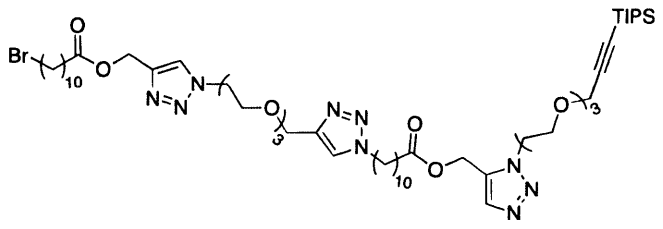

1,4-1,4-1,5 alkyl ester/oligo(ethylene glycol) tetramer

^{1}H NMR (500 MHz, $CDCl_3$) δ 7.78 (s, 1H), 7.66 (s, 1H), 7.53 (s, 1H), 5.26 (s, 2H), 5.19 (s, 2H), 4.67 (s, 2H), 4.59 (t, J = 5.1 Hz, 2H), 4.53 (t, J = 5.0 Hz, 2H), 4.33 (t, J = 7.4 Hz, 2H), 4.22 (s, 2H), 3.87 (q, J = 4.7 Hz, 4H), 3.71 – 3.51 (m, 16H), 3.40 (t, J = 6.8 Hz, 2H), 2.31 (t, J = 7.5 Hz, 4H), 1.92 – 1.79 (m, 4H), 1.61 – 1.54 (m, 4H), 1.44 – 1.21 (m, 24H), 1.06 (s, 21H). ^{13}C NMR (126 MHz, $CDCl_3$) δ 173.6, 173.0, 144.8, 142.7, 134.3, 133.4, 124.9, 122.4, 103.1, 87.7, 70.6, 70.50, 70.46, 70.3, 70.0, 69.6, 69.4, 68.60, 64.59, 59.1, 57.4, 54.0, 50.3, 50.2, 48.6, 34.1, 33.9, 32.8, 30.3, 29.31, 29.27, 29.24, 29.16, 29.1, 29.04, 28.98, 28.9, 28.7, 28.1, 26.5, 24.8, 24.7, 18.6, 11.1. GPC: T_{ret} = 26.7 min, $Đ$ = 1.010. HR-MS (m/z) $[M + H]^+$ calcd for $C_{55}H_{96}BrN_9O_{10}Si$: 1152.6316; found: 1152.6314.

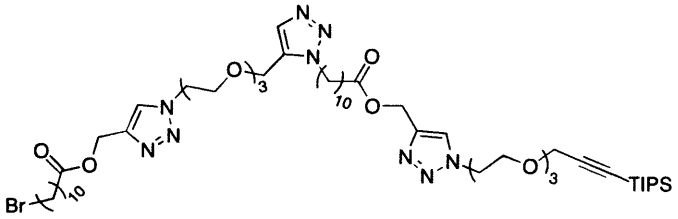

1,4-1,5-1,4 alkyl ester/oligo(ethylene glycol) tetramer

^{1}H NMR (500 MHz, $CDCl_3$) δ 7.78 (s, 1H), 7.74 (s, 1H), 7.62 (s, 1H), 5.20 (d, J = 2.2 Hz, 4H), 4.63 (s, 2H), 4.55 – 4.51 (m, 4H), 4.34 (t, J = 7.4 Hz, 2H), 4.23 (s, 2H), 3.89 – 3.84 (m, 4H), 3.73 – 3.69 (m, 2H), 3.68 – 3.64 (m, 2H), 3.63 – 3.56 (m, 12H), 3.40 (t, J = 6.7 Hz, 2H), 2.31 (t, J = 7.6 Hz, 4H), 1.93 – 1.80 (m, 4H), 1.63 – 1.58 (m, 4H), 1.44 – 1.37 (m, 2H), 1.34 – 1.21 (m, 22H), 1.06 (s, 21H). ^{13}C NMR (126 MHz, $CDCl_3$) δ 173.6, 173.5, 142.8, 142.7, 134.1, 132.7,

124.84, 124.80, 103.1, 87.7, 70.5, 70.43, 70.41, 69.5, 69.4, 68.6, 61.0, 59.1, 57.45, 57.40, 50.3, 50.2, 48.4, 34.1, 32.8, 30.0, 29.34, 29.32, 29.28, 29.2, 29.0, 28.7, 28.1, 26.6, 24.8, 18.6, 11.1. GPC: T_{ret} = 26.7 min, $Đ$ = 1.013. HR-MS (m/z) $[M + H]^+$ calcd for $C_{55}H_{96}BrN_9O_{10}Si$: 1152.6316; found: 1152.6352.

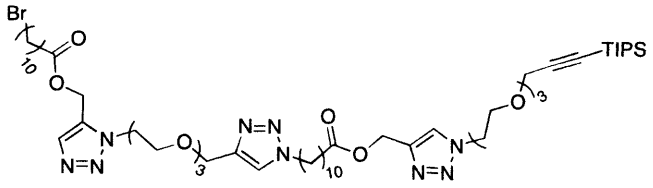

1,5-1,4-1,4 alkyl ester/oligo(ethylene glycol) tetramer

^{1}H NMR (500 MHz, $CDCl_3$) δ 7.78 (s, 1H), 7.65 (s, 1H), 7.54 (s, 1H), 5.25 (s, 2H), 5.20 (s, 2H), 4.67 (s, 2H), 4.59 (t, J = 5.1 Hz, 2H), 4.54 (t, J = 5.0 Hz, 2H), 4.33 (t, J = 7.4 Hz, 2H), 4.24 (s, 2H), 3.90 – 3.84 (m, 4H), 3.74 – 3.69 (m, 2H), 3.68 – 3.52 (m, 14H), 3.40 (t, J = 6.8 Hz, 2H), 2.31 (t, J = 7.5 Hz, 4H), 1.92 – 1.81 (m, 4H), 1.64 – 1.59 (m, 4H), 1.44 – 1.21 (m, 24H), 1.06 (s, 21H). ^{13}C NMR (126 MHz, $CDCl_3$) δ 173.6, 173.1, 145.0, 142.8, 134.4, 133.4, 124.9, 122.4, 103.2, 87.8, 70.65, 70.58, 70.52, 70.48, 70.1, 69.7, 69.5, 68.7, 64.7, 59.2, 57.5, 54.0, 50.4, 50.3, 48.7, 34.2, 34.0, 32.8, 30.4, 29.4, 29.3, 29.2, 29.12, 29.08, 29.0, 28.8, 28.2, 26.6, 24.9, 24.8, 18.6, 11.2. GPC: T_{ret} = 26.7 min, $Đ$ = 1.010. HR-MS (m/z) $[M + Na]^+$ calcd for $C_{55}H_{96}BrN_9O_{10}Si$: 1174.6135; found: 1174.6125.

5. References

(1) Lutz, J. F.; Ouchi, M.; Liu, D. R.; Sawamoto, M. Sequence-Controlled Polymers. *Science* **2013**, *341*, 1238149-1–1238149-8.

(2) Solleder, S. C.; Schneider, R. V.; Wetzel, K. S.; Boukis, A. C.; Meier, M. A. R. Recent Progress in the Design of Monodisperse, Sequence-Defined Macromolecules. *Macromol. Rapid Commun.* **2017**, 1600711.

(3) Hibi, Y.; Ouchi, M.; Sawamoto, M. A Strategy for Sequence Control in Vinyl Polymers via Iterative Controlled Radical Cyclization. *Nat. Commun.* **2016**, *7*, 11064-1–11064-9.

(4) Porel, M.; Thornlow, D. N.; Phan, N. N.; Alabi, C. A. Sequence-Defined Bioactive Macrocycles via an Acid-Catalysed Cascade Reaction. *Nat. Chem.* **2016**, *8*, 590–596.

(5) Edwardson, T. G. W.; Carneiro, K. M. M.; Serpell, C. J.; Sleiman, H. F. An Efficient and Modular Route to Sequence-Defined Polymers Appended to DNA. *Angew. Chem., Int. Ed.* **2014**, *53*, 4567–4571.

(6) Paynter, O. I.; Simmonds, D. J.; Whiting, M. C. The Synthesis of Long-Chain Unbranched Aliphatic Compounds by Molecular Doubling. *J. Chem. Soc., Chem. Commun.* **1982**, 1165–1166.

(7) Bidd, I.; Whiting, M. C. The Synthesis of Pure n-Paraffins with Chain-Lengths Between One and Four Hundred. *J. Chem. Soc., Chem. Commun.* **1985**, 543–544.

(8) Zhang, J.; Moore, J. S.; Xu, Z.; Aguirre, R. A. Nanoarchitectures. 1. Controlled Synthesis of Phenylacetylene Sequences. *J. Am. Chem. Soc.* **1992**, *114*, 2273–2274.

(9) Zhang, J.; Pesak, D. J.; Ludwick, J. L.; Moore, J. S. Geometrically-Controlled and Site Specifically-Functionalized Phenylacetylene Macrocycles. *J. Am. Chem. Soc.* **1994**, *116*, 4227–4239.

(10) Schumm, J. S.; Pearson, D. L.; Tour, J. M. Iterative Divergent/Convergent Approach to Linear Conjugated Oligomers by Successive Doubling of the Molecular Length: A Rapid Route to a 128Å-Long Potential Molecular Wire. *Angew. Chem., Int. Ed.* **1994**, *33*, 1360–1363.

(11) Takizawa, K.; Tang, C.; Hawker, C. J. Molecularly Defined Caprolactone Oligomers and Polymers: Synthesis and Characterization. *J. Am. Chem. Soc.* **2008**, *130*, 1718–1726.

(12) Takizawa, K.; Nulwala, H.; Hu, J.; Yoshinaga, K.; Hawker, C. J. Molecularly Defined (L)-Lactic Acid Oligomers and Polymers: Synthesis and Characterization. *J. Polym. Sci., Part A: Polym. Chem.* **2008**, *46*, 5977–5990.

(13) Binauld, S.; Damiron, D.; Connal, L. A.; Hawker, C. J.; Drockenmuller, E. Precise Synthesis of Molecularly Defined Oligomers and Polymers by Orthogonal Iterative Divergent/Convergent Approaches. *Macromol. Rapid Commun.* **2011**, *32*, 147–168.

(14) Huisgen, R. In *1,3-Dipolar Cycloaddition Chemistry*; Padwa, Albert; Ed.; Wiley: New York, 1984; pp 1–176.

(15) Rostovtsev, V. V.; Green, L. G.; Fokin, V. V.; Sharpless, K. B. A Stepwise Huisgen Cycloaddition Process: Copper(I)-Catalyzed Regioselective "Ligation" of Azides and Terminal Alkynes. *Angew. Chem., Int. Ed.* **2002**, *41*, 2596–2596.

(16) Tornøe, C. W.; Christensen, C.; Meldal, M. Peptidotriazoles on Solid Phase: [1,2,3]-Triazoles by Regiospecific Copper(I)-Catalyzed 1,3-Dipolar Cycloadditions of Terminal Alkynes to Azides. *J. Org. Chem.* **2002**, *67*, 3057–3064.

(17) Barnes, J. C.; Ehrlich, D. J. C.; Gao, A. X.; Leibfarth, F. A.; Jiang, Y.; Zhou, E.; Jamison, T. F.; Johnson, J. A. Iterative Exponential Growth of Stereo- and Sequence-Controlled Polymers. *Nat. Chem.* **2015**, *7*, 810–815.

(18) Jiang, Y.; Golder, M. R.; Nguyen, H. V. T.; Wang, M.; Zhong, M.; Barnes, J. C.; Ehrlich, D. J. C.; Johnson, J. A. Iterative Exponential Growth Synthesis and Assembly of Uniform Diblock Copolymers. *J. Am. Chem. Soc.* **2016**, *138*, 9369–9372.

(19) Binauld, S.; Hawker, C. J.; Fleury, E.; Drockenmuller, E. A Modular Approach to Functionalized and Expanded Crown Ether Based Macrocycles Using Click Chemistry. *Angew. Chem., Int. Ed.* **2009**, *48*, 6654–6658.

(20) Webb, D.; Jamison, T. F. Continuous Flow Multi-step Organic Synthesis. *Chem. Sci.* **2010**, *1*, 675–680.

(21) Gutmann, B.; Cantillo, D.; Kappe, C. O. Continuous-Flow Technology—A Tool for the Safe Manufacturing of Active Pharmaceutical Ingredients. *Angew. Chem., Int. Ed.* **2015**, *54*, 6688–6728.

(22) McQuade, D. T.; Seeberger, P. H. Applying Flow Chemistry: Methods, Materials, and Multistep Synthesis. *J. Org. Chem.* **2013**, *78*, 6384–6389.

(23) Leibfarth, F. A.; Johnson, J. A.; Jamison, T. F. Scalable Synthesis of Sequence-Defined, Unimolecular Macromolecules by Flow-IEG. *Proc. Natl. Acad. Sci. U.S.A.* **2015**, *112*, 10617–10622.

(24) Hein, J. E.; Fokin, V. V. Copper-Catalyzed Azide–Alkyne Cycloaddition (CuAAC) and Beyond: New Reactivity of Copper(I) Acetylides. *Chem. Soc. Rev.* **2010**, *39*, 1302–1315.

(25) Haldón, E.; Nicasio, M. C.; Pérez, P. J. Copper-Catalysed Azide–Alkyne Cycloadditions (CuAAC): an Update. *Org. Biomol. Chem.* **2015**, *13*, 9528–9550.

(26) Himo, F.; Lovell, T.; Hilgraf, R.; Rostovtsev, V. V.; Noodleman, L.; Sharpless, K. B.; Fokin, V. V. Copper(I)-Catalyzed Synthesis of Azoles. DFT Study Predicts Unprecedented Reactivity and Intermediates. *J. Am. Chem. Soc.* **2005**, *127*, 210–216.

(27) Appukkuttan, P.; Dehaen, W.; Fokin, V. V.; Van der Eycken, E. A Microwave-Assisted Click Chemistry Synthesis of 1,4-Disubstituted 1,2,3-Triazoles via a Copper(I)-Catalyzed Three-Component Reaction. *Org. Lett.* **2004**, *6*, 4223–4225.

(28) Cravotto, G.; Fokin, V. V.; Garella, D.; Binello, A.; Boffa, L.; Barge, A. Ultrasound-Promoted Copper-Catalyzed Azide–Alkyne Cycloaddition. *J. Comb. Chem.* **2010**, *12*, 13–15.

(29) Lee, C. Y.; Held, R.; Sharma, A.; Baral, R.; Nanah, C.; Dumas, D.; Jenkins, S. Upadhaya, S.; Du, W. Copper-Granule-Catalyzed Microwave-Assisted Click Synthesis of Polyphenol Dendrimers. *J. Org. Chem.* **2013**, *78*, 11221–11228.

(30) Zhang, P.; Russell, M. G.; Jamison, T. F. Continuous Flow Total Synthesis of Rufinamide. *Org. Process Res. Dev.* **2014**, *18*, 1567–1570.

(31) Fuchs, M.; Goessler, W.; Pilger, C.; Kappe, C. O. Mechanistic Insights into Copper(I)-Catalyzed Azide-Alkyne Cycloadditions using Continuous Flow Conditions. *Adv. Synth. Catal.* **2010**, *352*, 323–328.

(32) Cook, T. L.; Walker, J. A.; Mack, J. Scratching the Catalytic Surface of Mechanochemistry: a Multi-Component CuAAC Reaction Using a Copper Reaction Vial. *Green Chem.* **2013**, *15*, 617–619.

(33) Candelon, N.; Lastécouères, D.; Diallo, A. K.; Aranzaes, J. R.; Astruc, D.; Vincent, J. M. A Highly Active and Reusable Copper(I)-tren Catalyst for the "Click" 1,3-Dipolar Cycloaddition of Azides and Alkynes. *Chem. Commun.* **2008**, 741–743.

(34) Presolski, S. I.; Hong, V.; Cho, S.-H.; Finn, M. G. Tailored Ligand Acceleration of the Cu-Catalyzed Azide–Alkyne Cycloaddition Reaction: Practical and Mechanistic Implications. *J. Am. Chem. Soc.* **2010**, *132*, 14570–14576.

(35) Matyjaszewski, K.; Tsarevsky, N. V.; Braunecker, W. A.; Dong, H.; Huang, J.; Jakubowski, W.; Kwak, Y.; Nicolay, R.; Tang, W.; Yoon, J. A. Role of Cu^0 in Controlled/"Living" Radical Polymerization. *Macromolecules* **2007**, *40*, 7795–7806.

(36) Zhang, L.; Chen, X.; Xue, P.; Sun, H. H. Y.; Williams, I. D.; Sharpless, K. B.; Fokin, V. V.; Jia, G. Ruthenium-Catalyzed Cycloaddition of Alkynes and Organic Azides. *J. Am. Chem. Soc.* **2005**, *127*, 15998–15999.

(37) Tam, A.; Arnold, U.; Soellner, M. B.; Raines, R. T. Protein Prosthesis: 1,5-Disubstituted[1,2,3]triazoles as *cis*-Peptide Bond Surrogates. *J. Am. Chem. Soc.* **2007**, *129*, 12670–12671.

(38) Boren, B. C.; Narayan, S.; Rasmussen, L. K.; Zhang, L.; Zhao, H.; Lin, Z.; Jia, G.; Fokin, V. V. Ruthenium-Catalyzed Azide–Alkyne Cycloaddition: Scope and Mechanism. *J. Am. Chem. Soc.* **2008**, *130*, 8923–8930.

(39) Adamo, A.; Heider, P. L.; Weeranoppanant, N.; Jensen, K. F. Membrane-based, liquid–liquid separator with integrated pressure control. *Ind. Eng. Chem. Res.* **2013**, *52*, 10802–10808.

(40) Fox, T. G.; Flory, P. J. Second-order transition temperatures and related properties of polystyrene. I. Influence of molecular weight. *J. Appl. Phys.* **1950**, *21*, 581–591.

(41) Hoogboom, J.; Swager, T. M. Increased Alignment of Electronic Polymers in Liquid Crystals via Hydrogen Bonding Extension. *J. Am. Chem. Soc.* **2006**, *128*, 15058–15059.

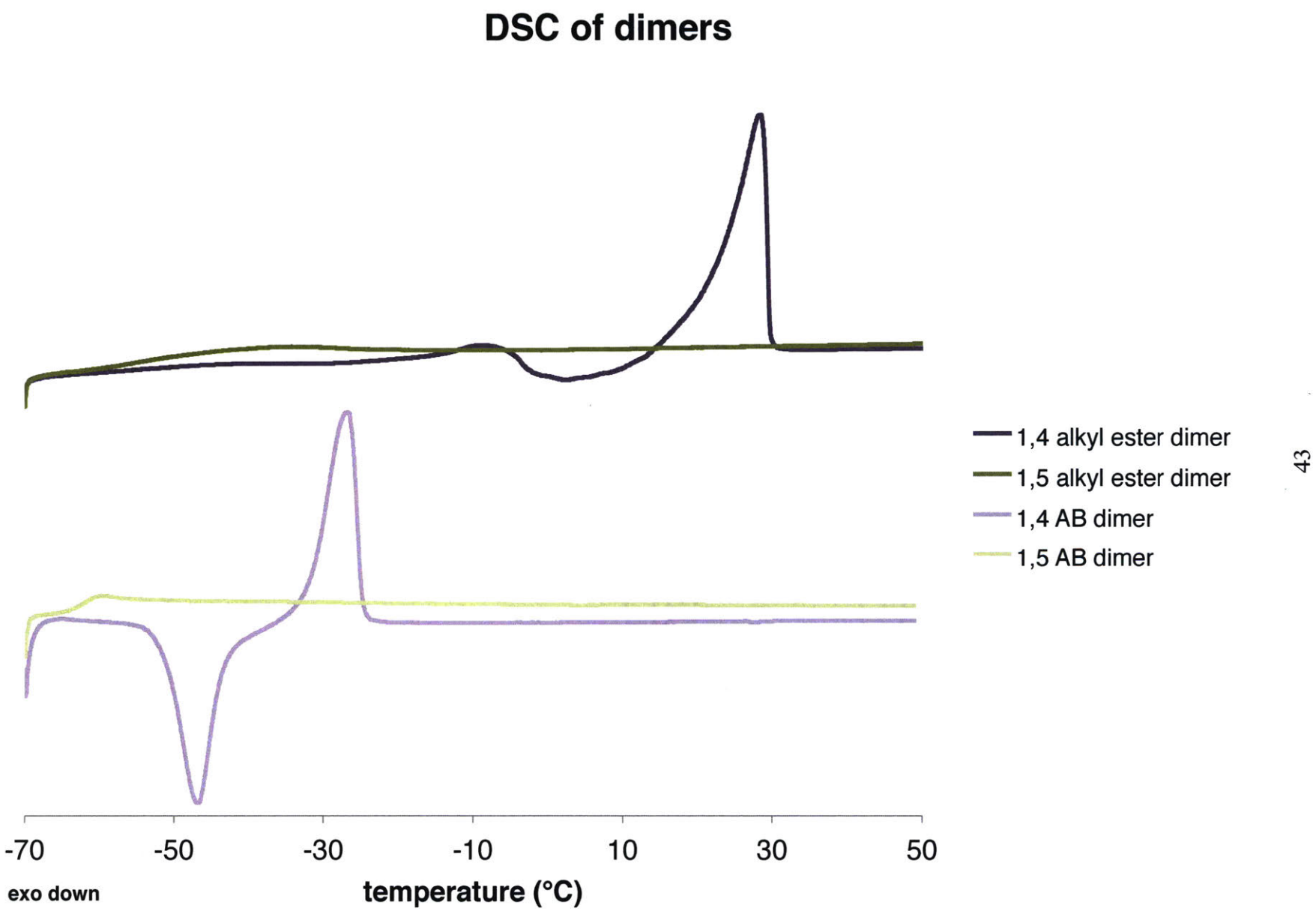
DSC of dimers
1,4 alkyl ester dimer
1,5 alkyl ester dimer
1,4 AB dimer
1,5 AB dimer
-70
-50
-30
-10
10
30
50
exo down
temperature (°C)

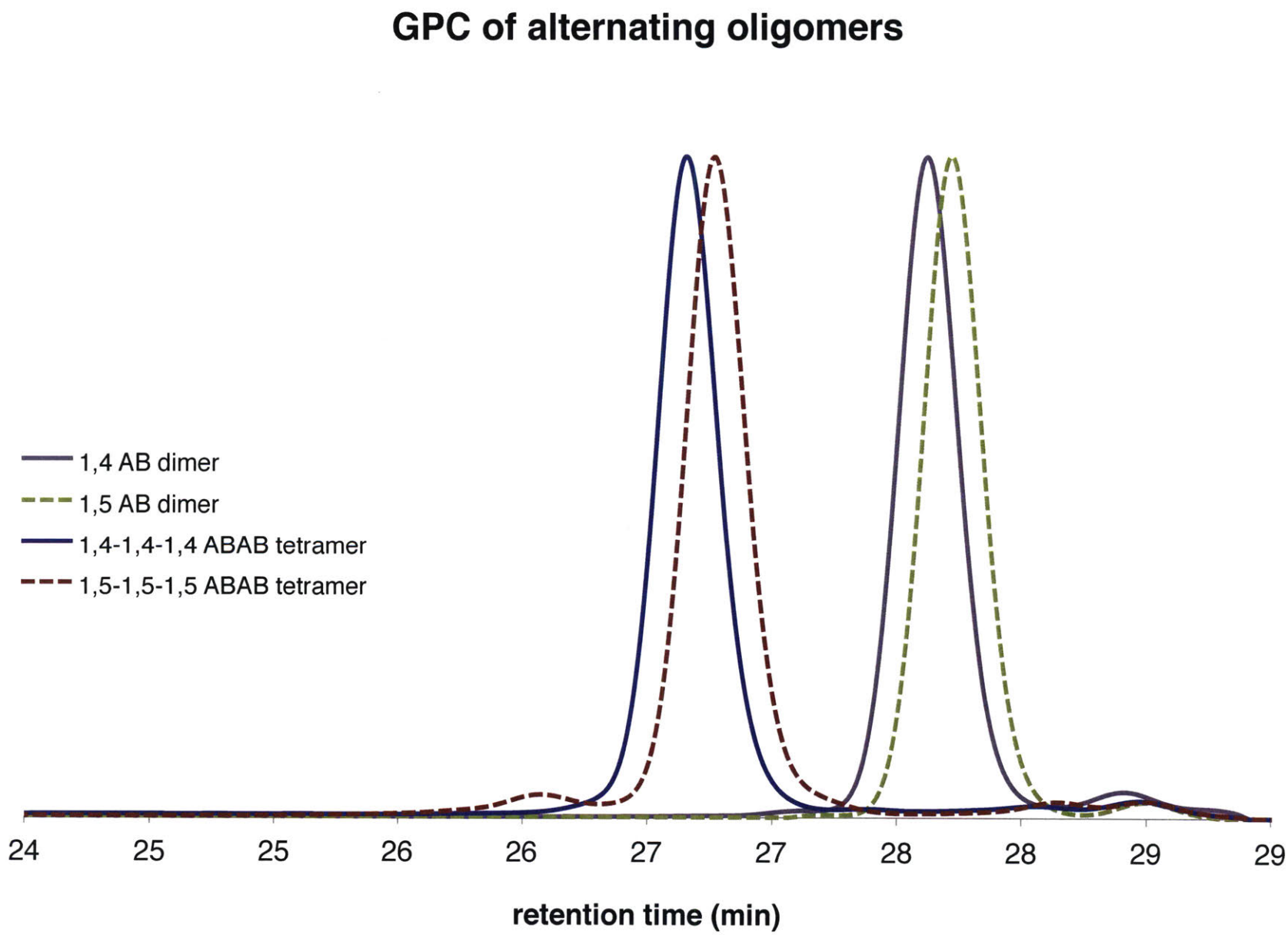
GPC of alternating oligomers
1,4 AB dimer
1,5 AB dimer
1,4-1,4-1,4 ABAB tetramer
1,5-1,5-1,5 ABAB tetramer
24
25
25
26
26
27
27
28
28
29
29
retention time (min)

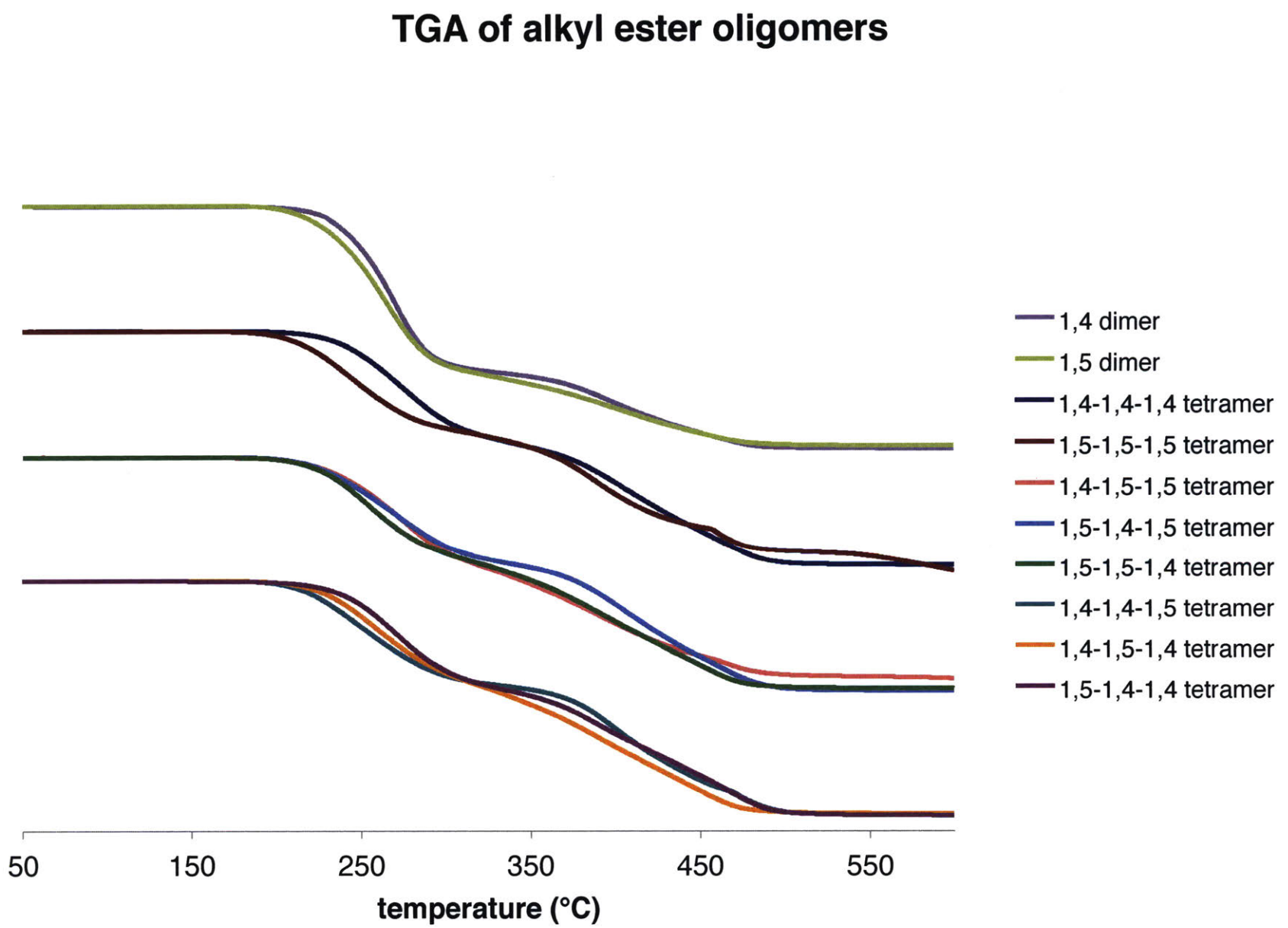
TGA of alkyl ester oligomers
1,4 dimer
1,5 dimer
1,4-1,4-1,4 tetramer
1,5-1,5-1,5 tetramer
1,4-1,5-1,5 tetramer
1,5-1,4-1,5 tetramer
1,5-1,5-1,4 tetramer
1,4-1,4-1,5 tetramer
1,4-1,5-1,4 tetramer
1,5-1,4-1,4 tetramer
50
150
250
350
450
550
temperature (°C)

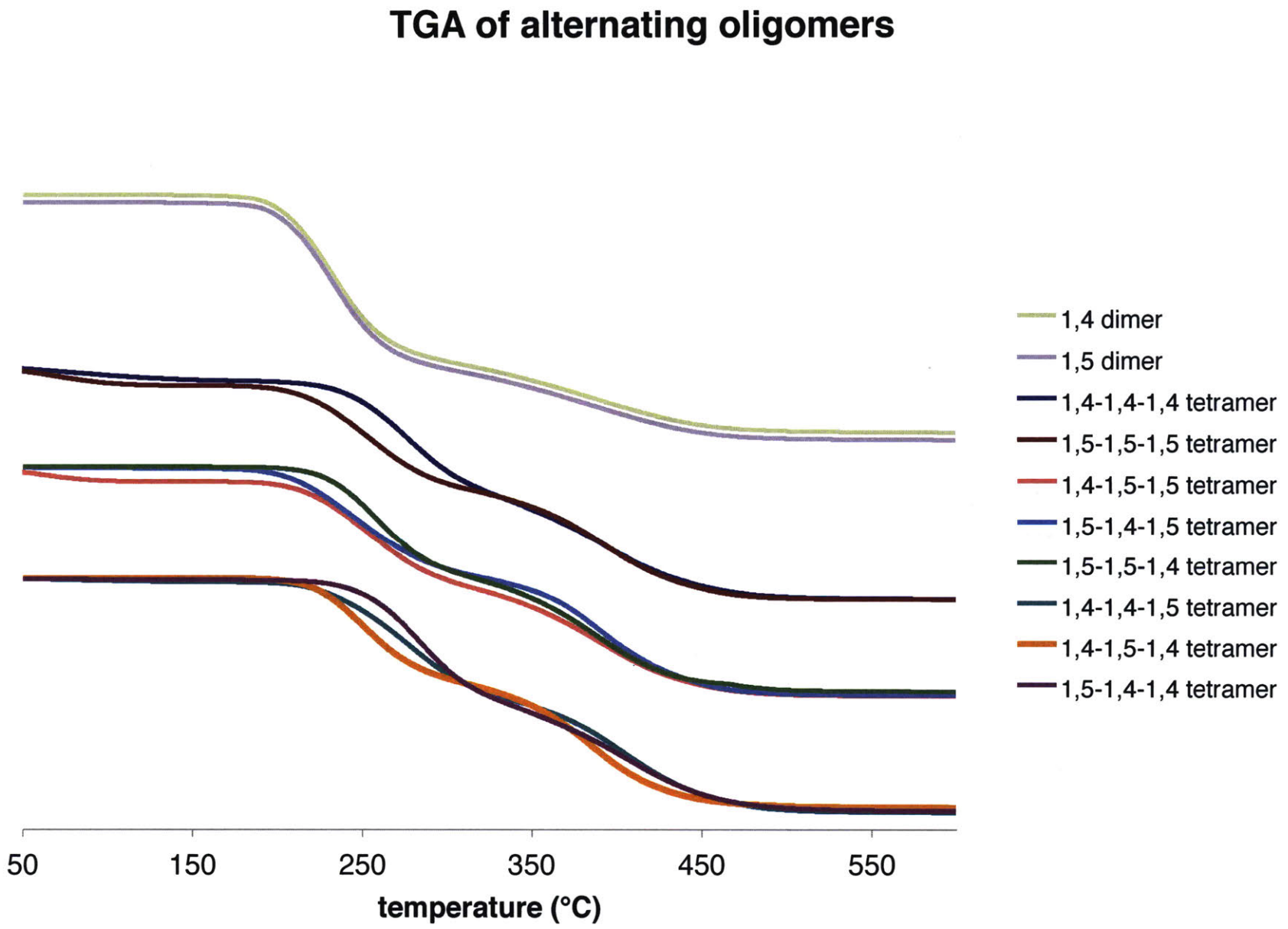
TGA of alternating oligomers
1,4 dimer
1,5 dimer
1,4-1,4-1,4 tetramer
1,5-1,5-1,5 tetramer
1,4-1,5-1,5 tetramer
1,5-1,4-1,5 tetramer
1,5-1,5-1,4 tetramer
1,4-1,4-1,5 tetramer
1,4-1,5-1,4 tetramer
1,5-1,4-1,4 tetramer
50
150
250
350
450
550
temperature (°C)

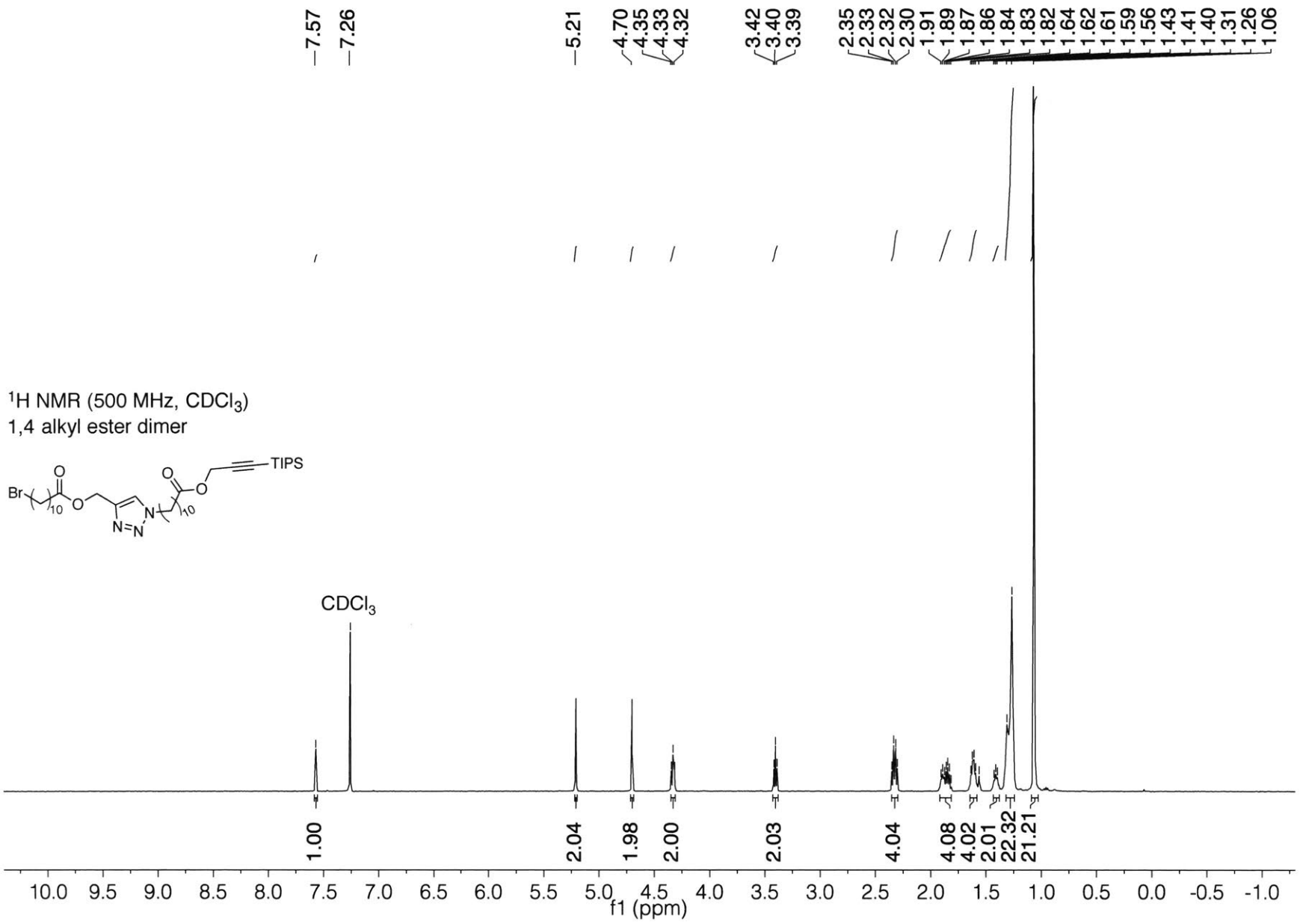
7.57
7.26
5.21
4.70
4.35
4.33
4.32
3.42
3.40
3.39
2.35
2.33
2.32
2.30
1.91
1.89
1.87
1.86
1.84
1.83
1.82
1.64
1.62
1.61
1.59
1.56
1.43
1.41
1.40
1.31
1.26
1.06
1H NMR (500 MHz, CDCl3)
1,4 alkyl ester dimer
TIPS
CDCl3
1.00
2.04
1.98
2.00
2.03
4.04
4.08
4.02
2.01
22.32
21.21
10.0 9.5 9.0 8.5 8.0 7.5 7.0 6.5 6.0 5.5 5.0 4.5 4.0 3.5 3.0 2.5 2.0 1.5 1.0 0.5 0.0 -0.5 -1.0
f1 (ppm)

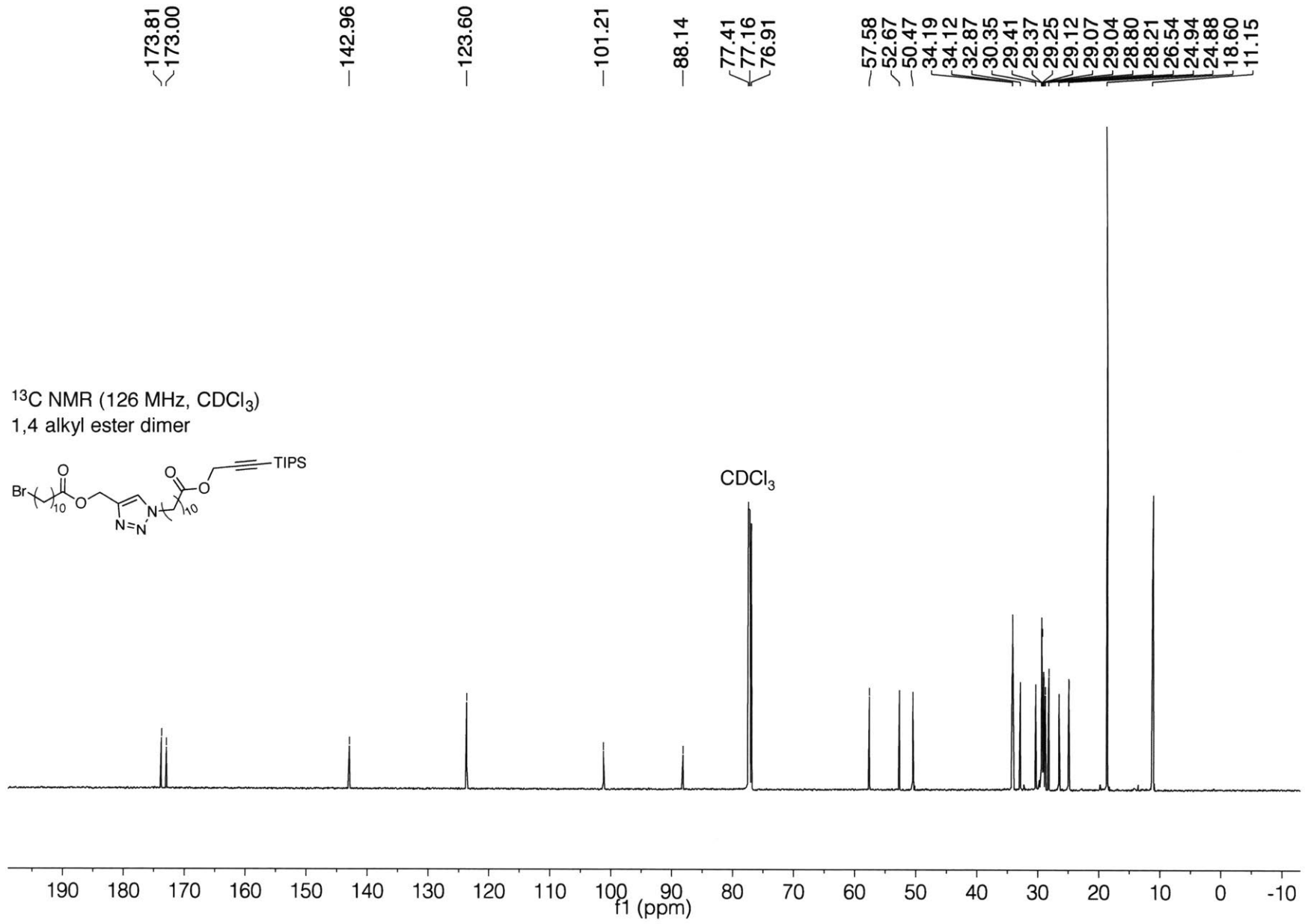
173.81
173.00
142.96
123.60
101.21
88.14
77.41
77.16
76.91
57.58
52.67
50.47
34.19
34.12
32.87
30.35
29.41
29.37
29.25
29.12
29.07
29.04
28.80
28.21
26.54
24.94
24.88
18.60
11.15
13C NMR (126 MHz, CDCl3)
1,4 alkyl ester dimer
Br
O
10
O
N
N=N
O
O
10
TIPS
CDCl3
190
180
170
160
150
140
130
120
110
100
90
80
70
60
50
40
30
20
10
0
-10
f1 (ppm)

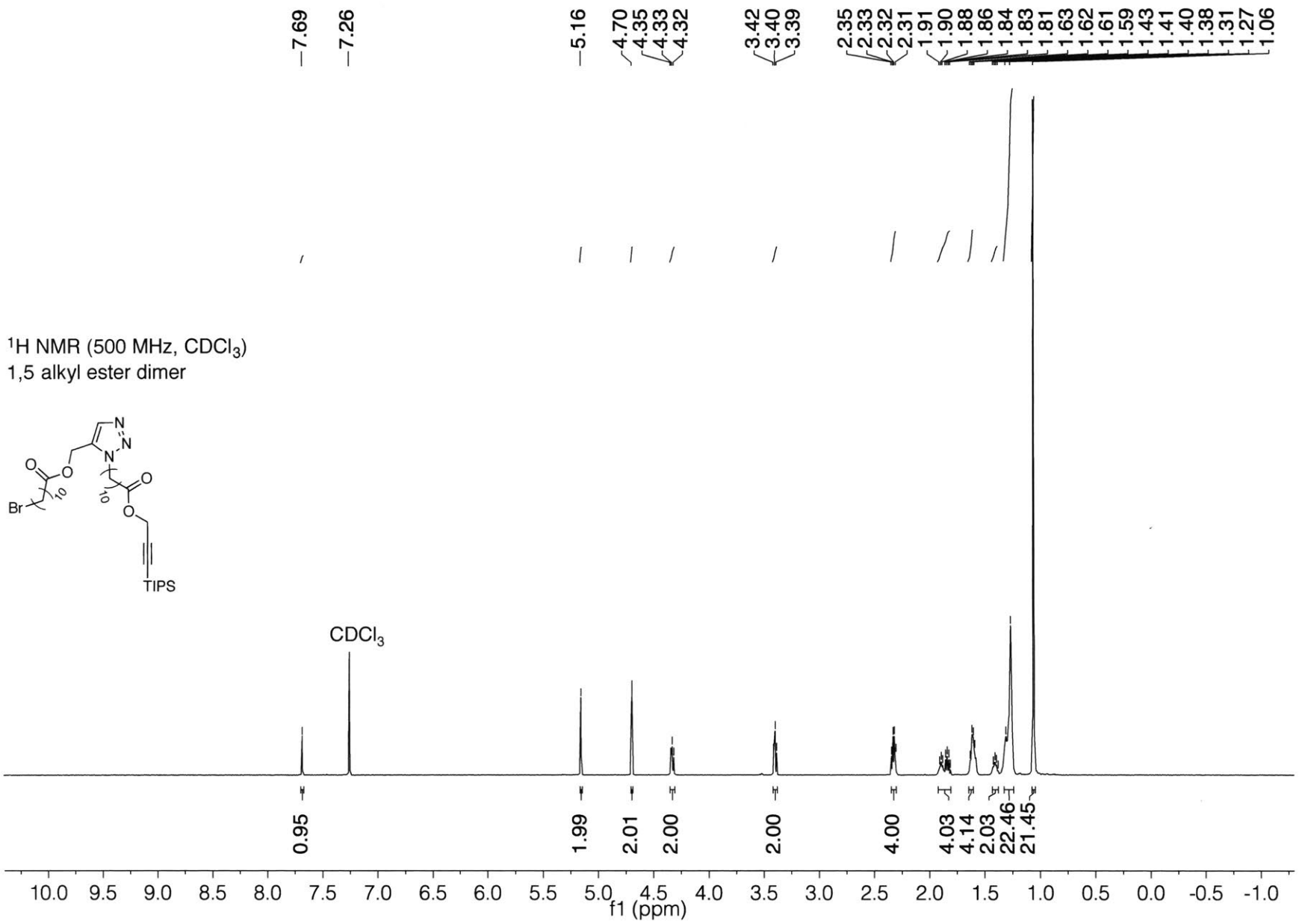
7.69
7.26
5.16
4.70
4.35
4.33
4.32
3.42
3.40
3.39
2.35
2.33
2.32
2.31
1.91
1.90
1.88
1.86
1.84
1.83
1.81
1.63
1.62
1.61
1.59
1.43
1.41
1.40
1.38
1.31
1.27
1.06
1H NMR (500 MHz, CDCl3)
1,5 alkyl ester dimer
Br
TIPS
CDCl3
0.95
1.99
2.01
2.00
2.00
4.00
4.03
4.14
2.03
22.46
21.45
10.0 9.5 9.0 8.5 8.0 7.5 7.0 6.5 6.0 5.5 5.0 4.5 4.0 3.5 3.0 2.5 2.0 1.5 1.0 0.5 0.0 -0.5 -1.0
f1 (ppm)

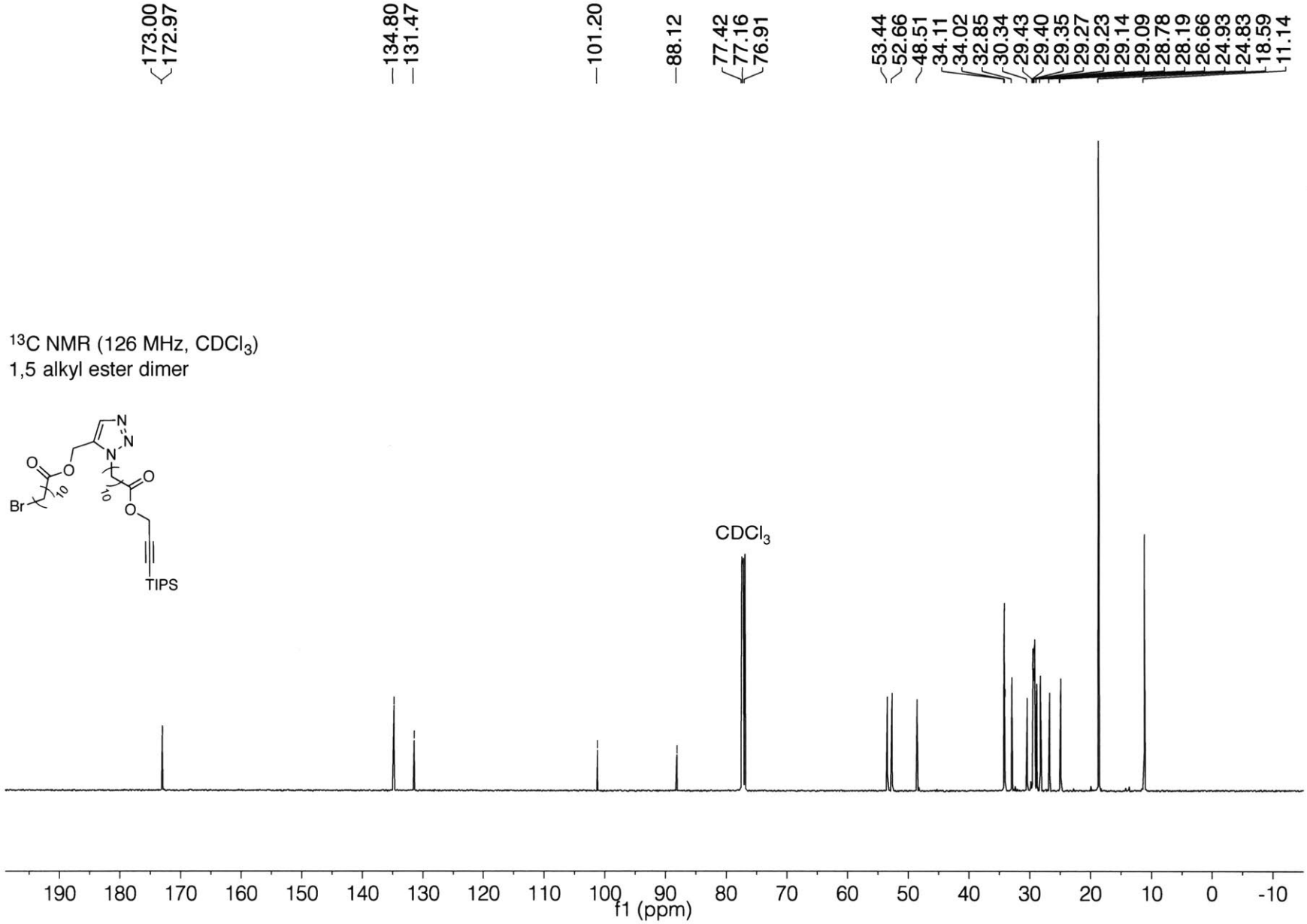
173.00
172.97
134.80
131.47
101.20
88.12
77.42
77.16
76.91
53.44
52.66
48.51
34.11
34.02
32.85
30.34
29.43
29.40
29.35
29.27
29.23
29.14
29.09
28.78
28.19
26.66
24.93
24.83
18.59
11.14
^{13}C NMR (126 MHz, $CDCl_3$)
1,5 alkyl ester dimer
Br
TIPS
$CDCl_3$
190 180 170 160 150 140 130 120 110 100 90 80 70 60 50 40 30 20 10 0 -10
f1 (ppm)

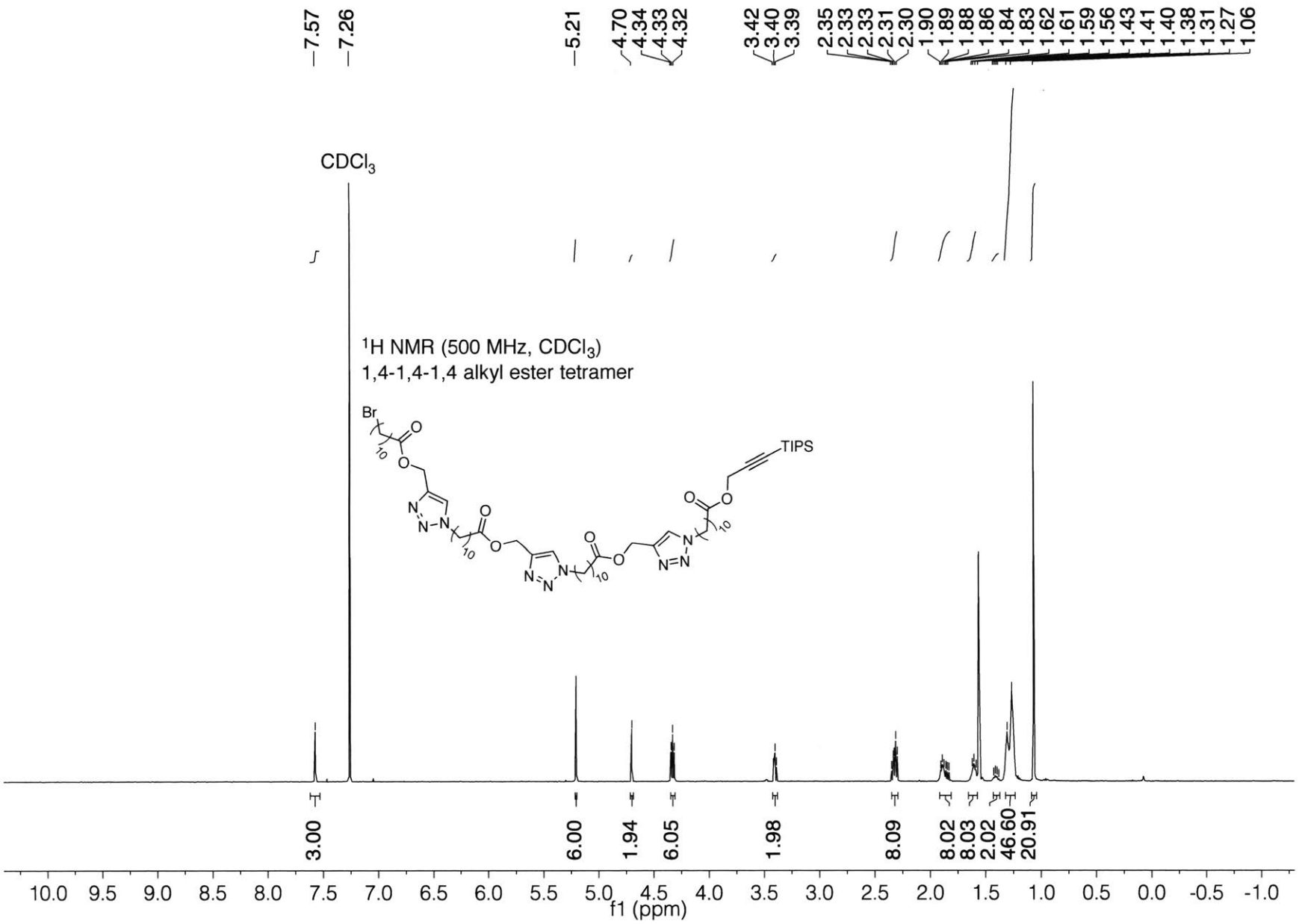
7.57
7.26
5.21
4.70
4.34
4.33
4.32
3.42
3.40
3.39
2.35
2.33
2.33
2.31
2.30
1.90
1.89
1.88
1.86
1.84
1.83
1.62
1.61
1.59
1.56
1.43
1.41
1.40
1.38
1.31
1.27
1.06
CDCl3
1H NMR (500 MHz, CDCl3)
1,4-1,4-1,4 alkyl ester tetramer
Br
TIPS
3.00
6.00
1.94
6.05
1.98
8.09
8.02
8.03
2.02
46.60
20.91
10.0 9.5 9.0 8.5 8.0 7.5 7.0 6.5 6.0 5.5 5.0 4.5 4.0 3.5 3.0 2.5 2.0 1.5 1.0 0.5 0.0 -0.5 -1.0
f1 (ppm)

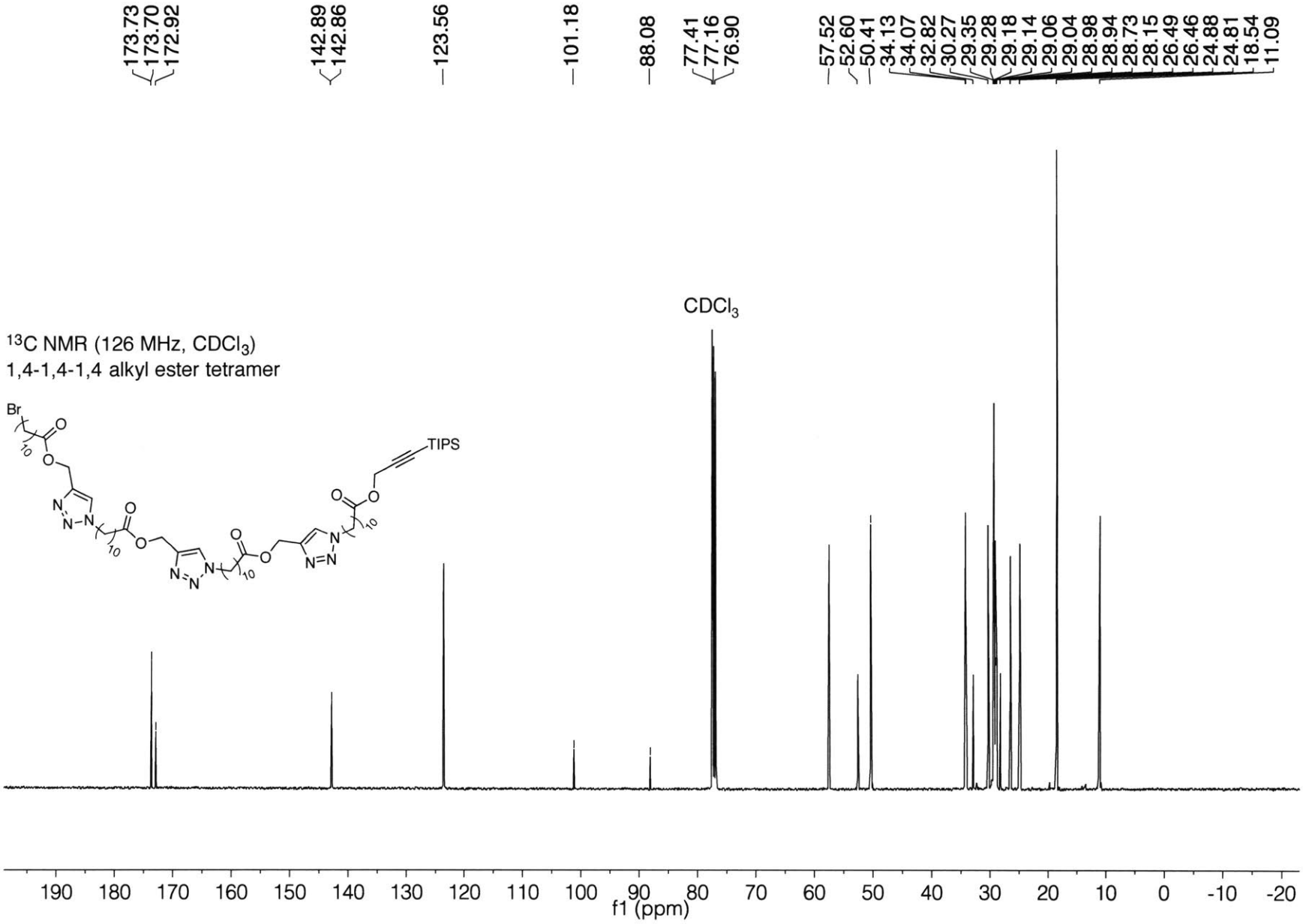
173.73
173.70
172.92
142.89
142.86
123.56
101.18
88.08
77.41
77.16
76.90
57.52
52.60
50.41
34.13
34.07
32.82
30.27
29.35
29.28
29.18
29.14
29.06
29.04
28.98
28.94
28.73
28.15
26.49
26.46
24.88
24.81
18.54
11.09
CDCl3
13C NMR (126 MHz, CDCl3)
1,4-1,4-1,4 alkyl ester tetramer
Br
TIPS
190 180 170 160 150 140 130 120 110 100 90 80 70 60 50 40 30 20 10 0 -10 -20
f1 (ppm)

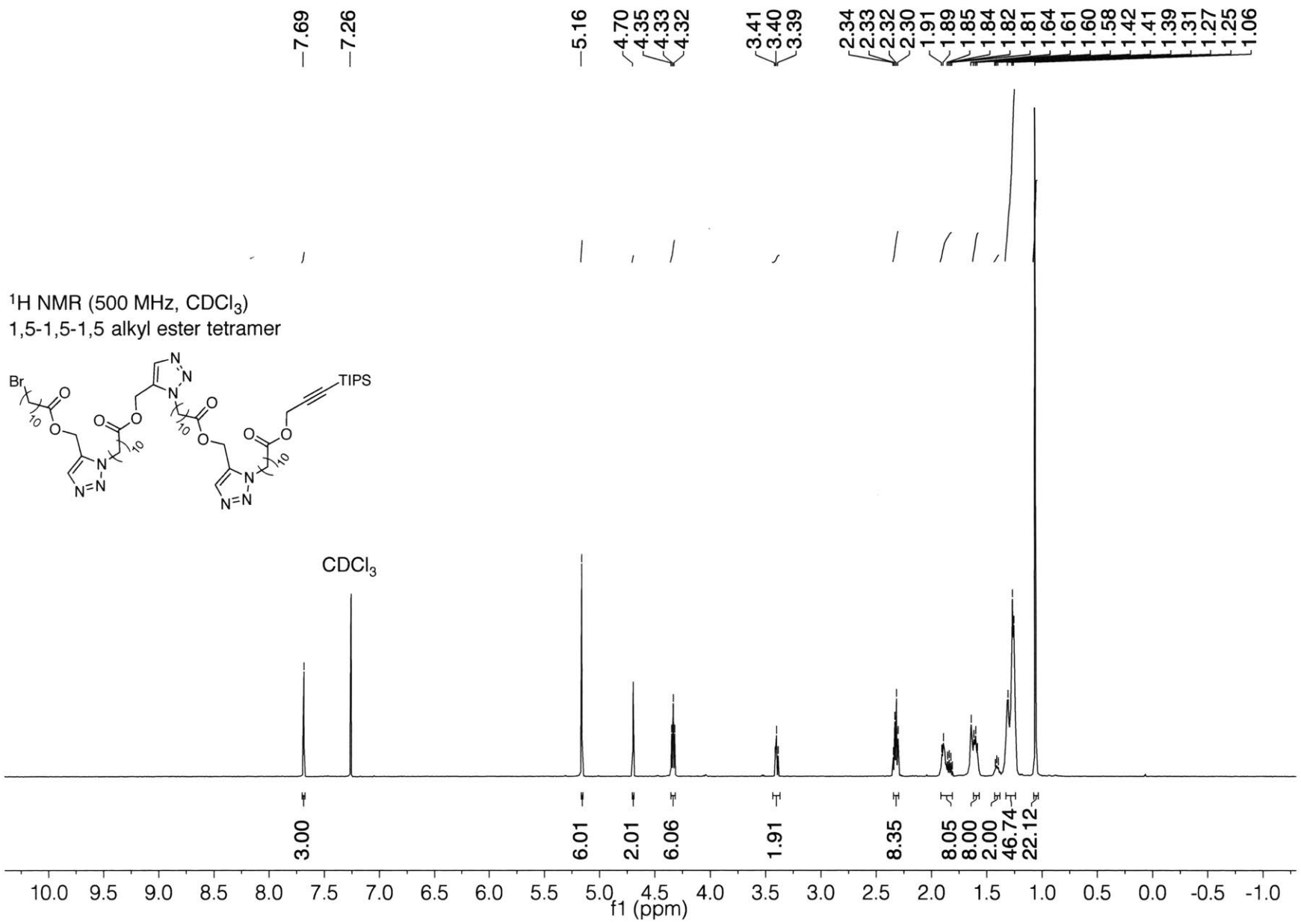
7.69
7.26
5.16
4.70
4.35
4.33
4.32
3.41
3.40
3.39
2.34
2.33
2.32
2.30
1.91
1.89
1.85
1.84
1.82
1.81
1.64
1.61
1.60
1.58
1.42
1.41
1.39
1.31
1.27
1.25
1.06
1H NMR (500 MHz, CDCl3)
1,5-1,5-1,5 alkyl ester tetramer
Br
TIPS
CDCl3
3.00
6.01
2.01
6.06
1.91
8.35
8.05
8.00
2.00
46.74
22.12
10.0 9.5 9.0 8.5 8.0 7.5 7.0 6.5 6.0 5.5 5.0 4.5 4.0 3.5 3.0 2.5 2.0 1.5 1.0 0.5 0.0 -0.5 -1.0
f1 (ppm)

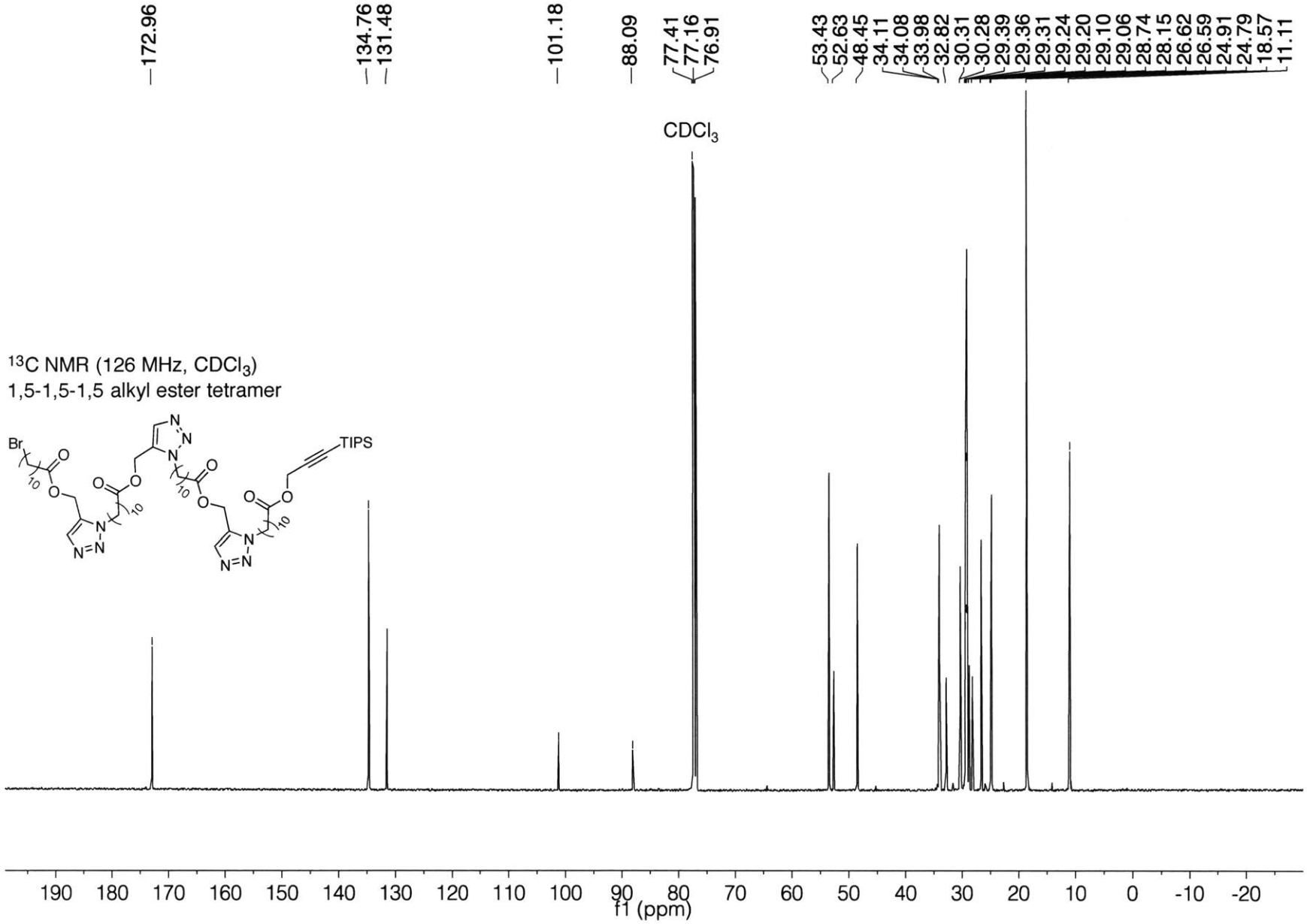
172.96
134.76
131.48
101.18
88.09
77.41
77.16
76.91
53.43
52.63
48.45
34.11
34.08
33.98
32.82
30.31
30.28
29.39
29.36
29.31
29.24
29.20
29.10
29.06
28.74
28.15
26.62
26.59
24.91
24.79
18.57
11.11
CDCl3
13C NMR (126 MHz, CDCl3)
1,5-1,5-1,5 alkyl ester tetramer
Br
TIPS
190 180 170 160 150 140 130 120 110 100 90 80 70 60 50 40 30 20 10 0 -10 -20
f1 (ppm)

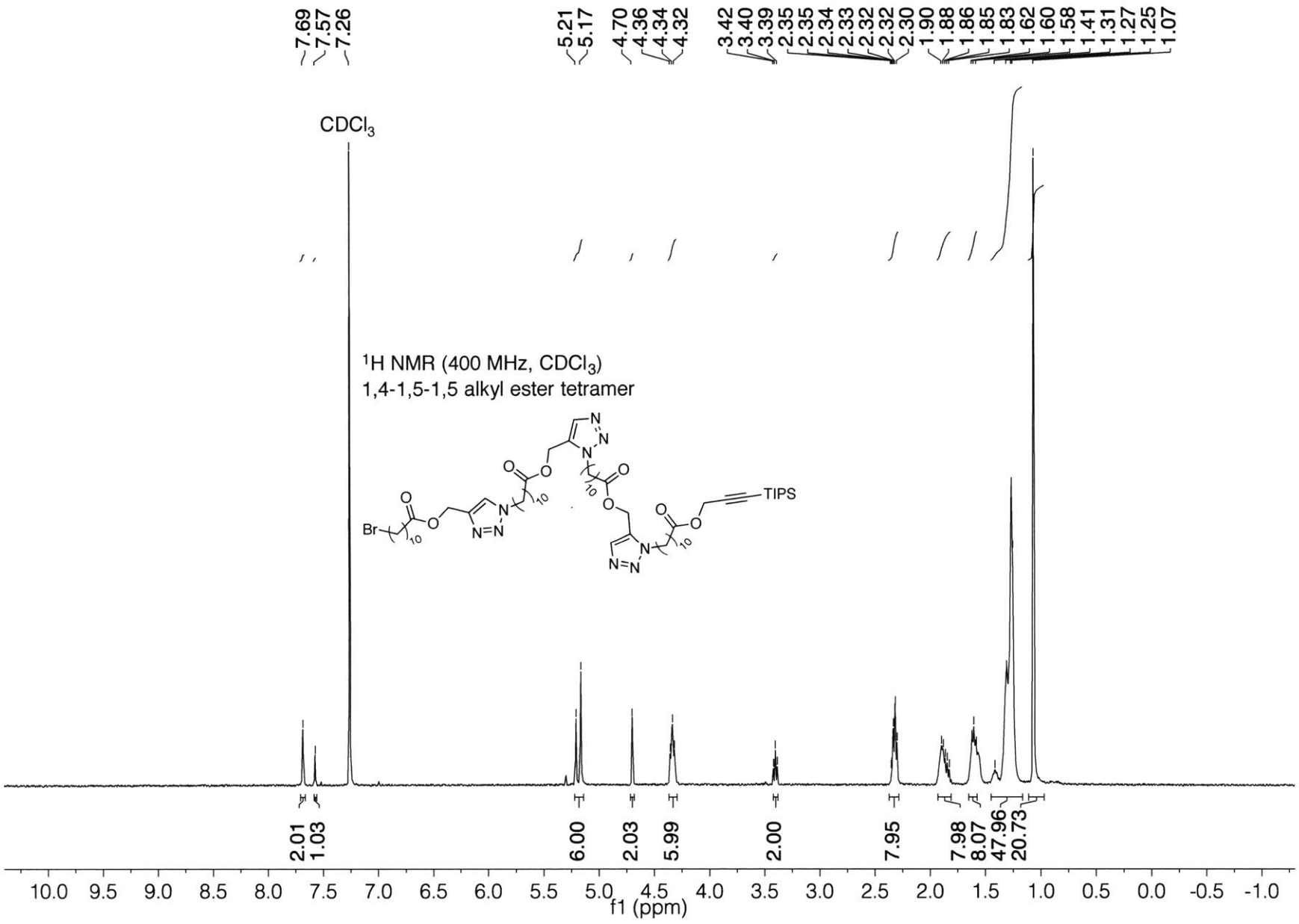
7.69
7.57
7.26
5.21
5.17
4.70
4.36
4.34
4.32
3.42
3.40
3.39
2.35
2.35
2.34
2.33
2.32
2.32
2.30
1.90
1.88
1.86
1.85
1.83
1.62
1.60
1.58
1.41
1.31
1.27
1.25
1.07
CDCl3
1H NMR (400 MHz, CDCl3)
1,4-1,5-1,5 alkyl ester tetramer
TIPS
2.01
1.03
6.00
2.03
5.99
2.00
7.95
7.98
8.07
47.96
20.73
f1 (ppm)

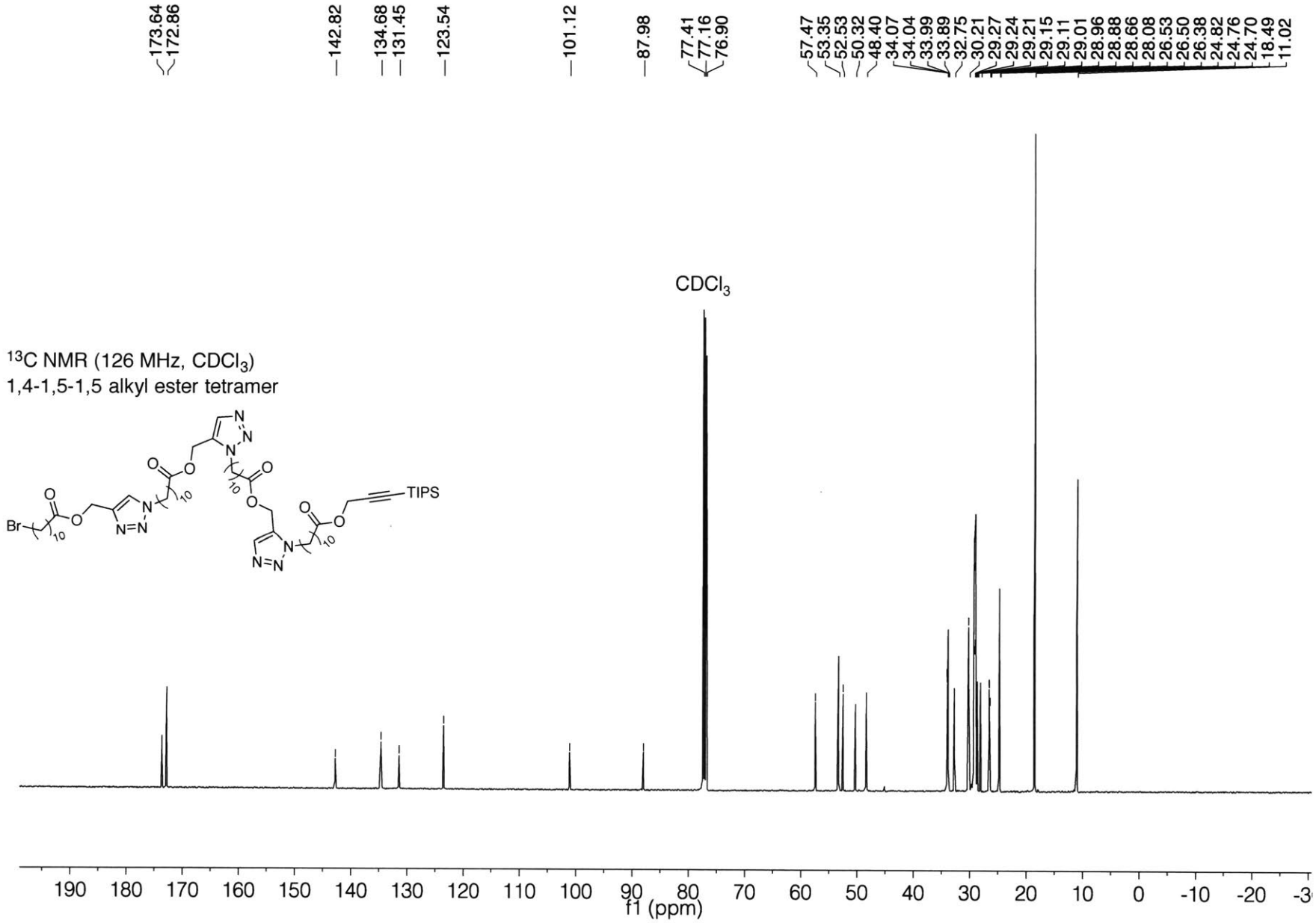
173.64
172.86
142.82
134.68
131.45
123.54
101.12
87.98
77.41
77.16
76.90
57.47
53.35
52.53
50.32
48.40
34.07
34.04
33.99
33.89
32.75
30.21
29.27
29.24
29.21
29.15
29.11
29.01
28.96
28.88
28.66
28.08
26.53
26.50
26.38
24.82
24.76
24.70
18.49
11.02
CDCl3
13C NMR (126 MHz, CDCl3)
1,4-1,5-1,5 alkyl ester tetramer
TIPS
f1 (ppm)

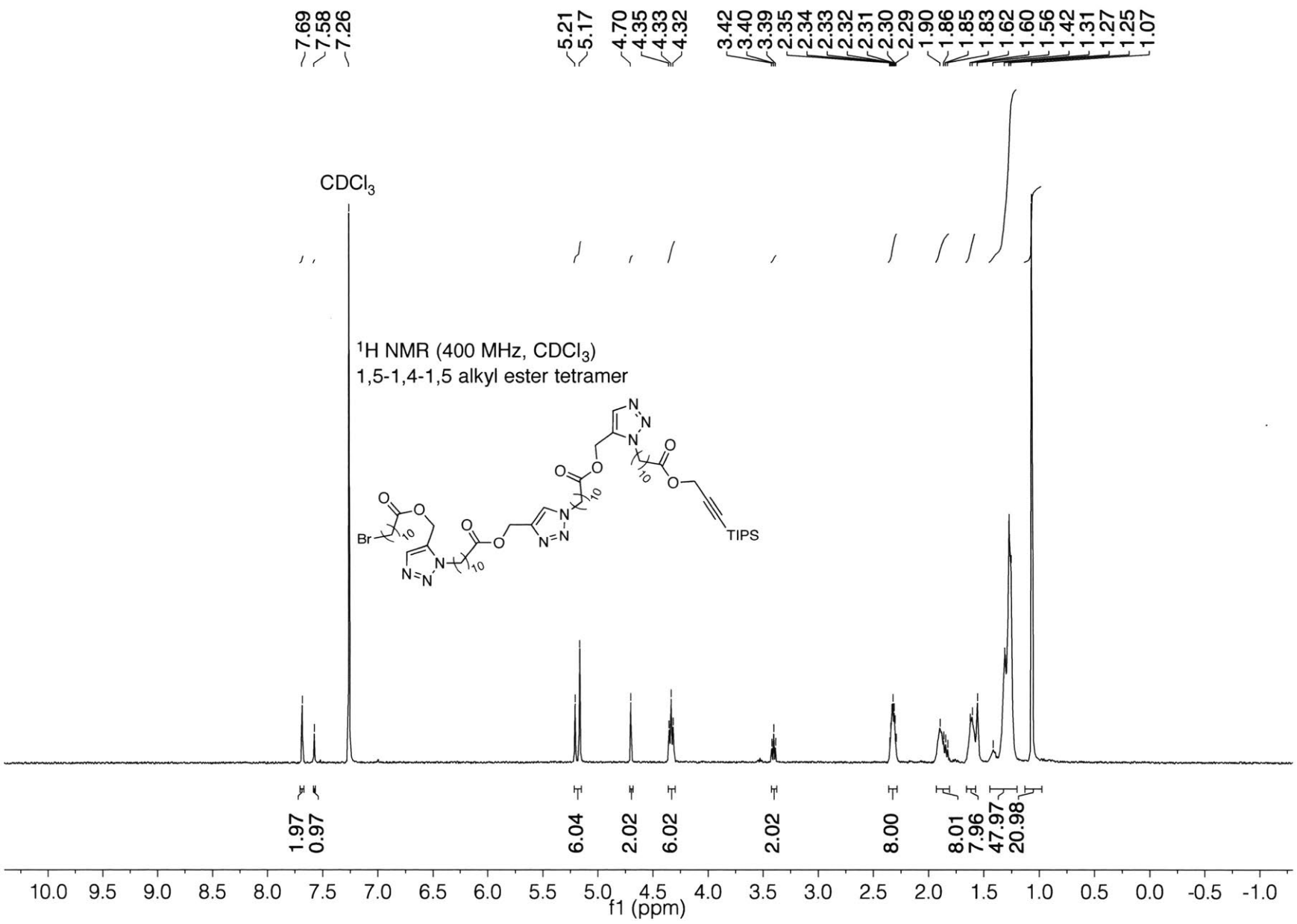
7.69
7.58
7.26
5.21
5.17
4.70
4.35
4.33
4.32
3.42
3.40
3.39
2.35
2.34
2.33
2.32
2.31
2.30
2.29
1.90
1.86
1.85
1.83
1.62
1.60
1.56
1.42
1.31
1.27
1.25
1.07
CDCl3
1H NMR (400 MHz, CDCl3)
1,5-1,4-1,5 alkyl ester tetramer
Br
TIPS
1.97
0.97
6.04
2.02
6.02
2.02
8.00
8.01
7.96
47.97
20.98
f1 (ppm)

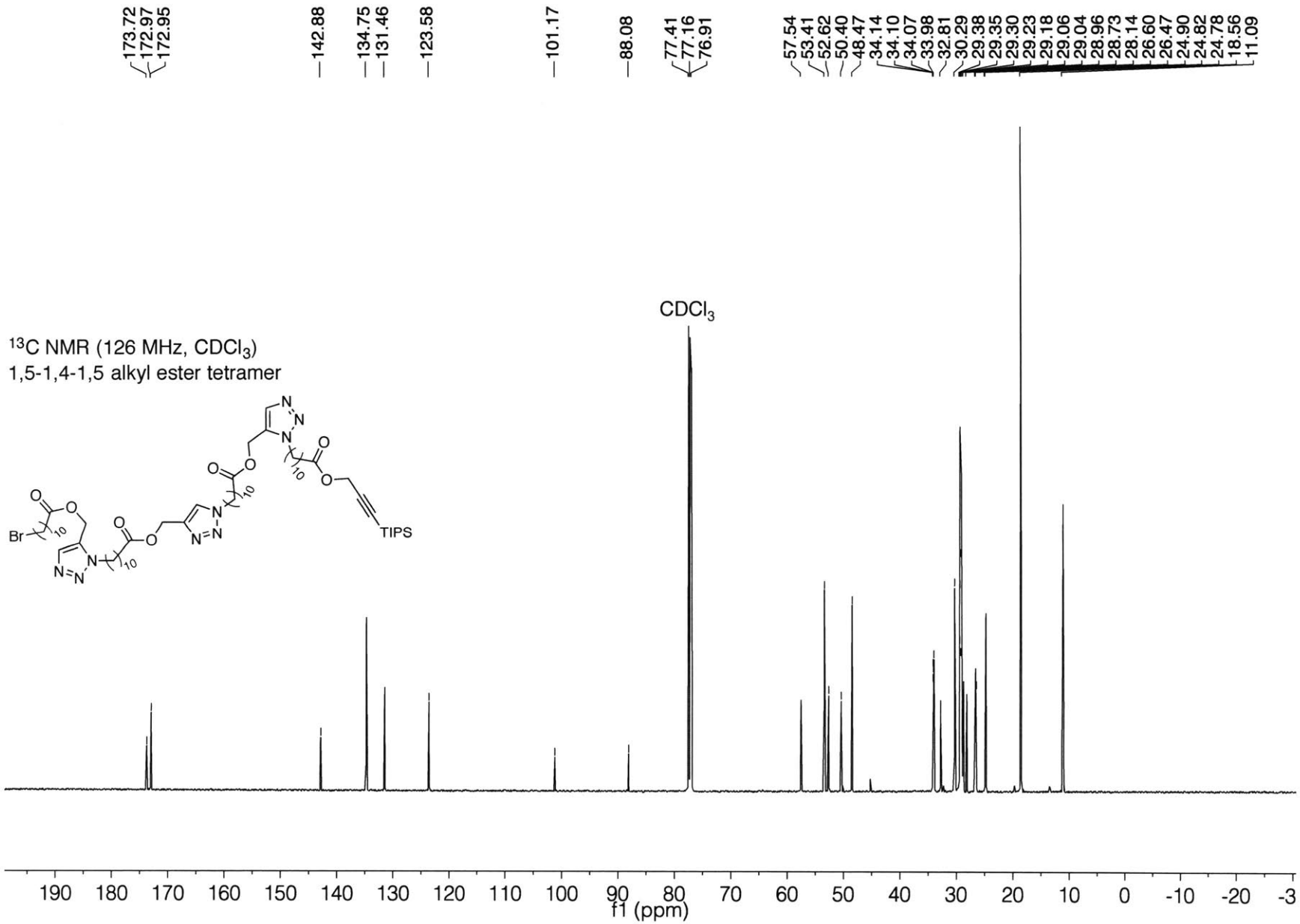
173.72
172.97
172.95
142.88
134.75
131.46
123.58
101.17
88.08
77.41
77.16
76.91
57.54
53.41
52.62
50.40
48.47
34.14
34.10
34.07
33.98
32.81
30.29
29.38
29.35
29.30
29.23
29.18
29.06
29.04
28.96
28.73
28.14
26.60
26.47
24.90
24.82
24.78
18.56
11.09
CDCl3
13C NMR (126 MHz, CDCl3)
1,5-1,4-1,5 alkyl ester tetramer
Br
TIPS
190 180 170 160 150 140 130 120 110 100 90 80 70 60 50 40 30 20 10 0 -10 -20 -3
f1 (ppm)

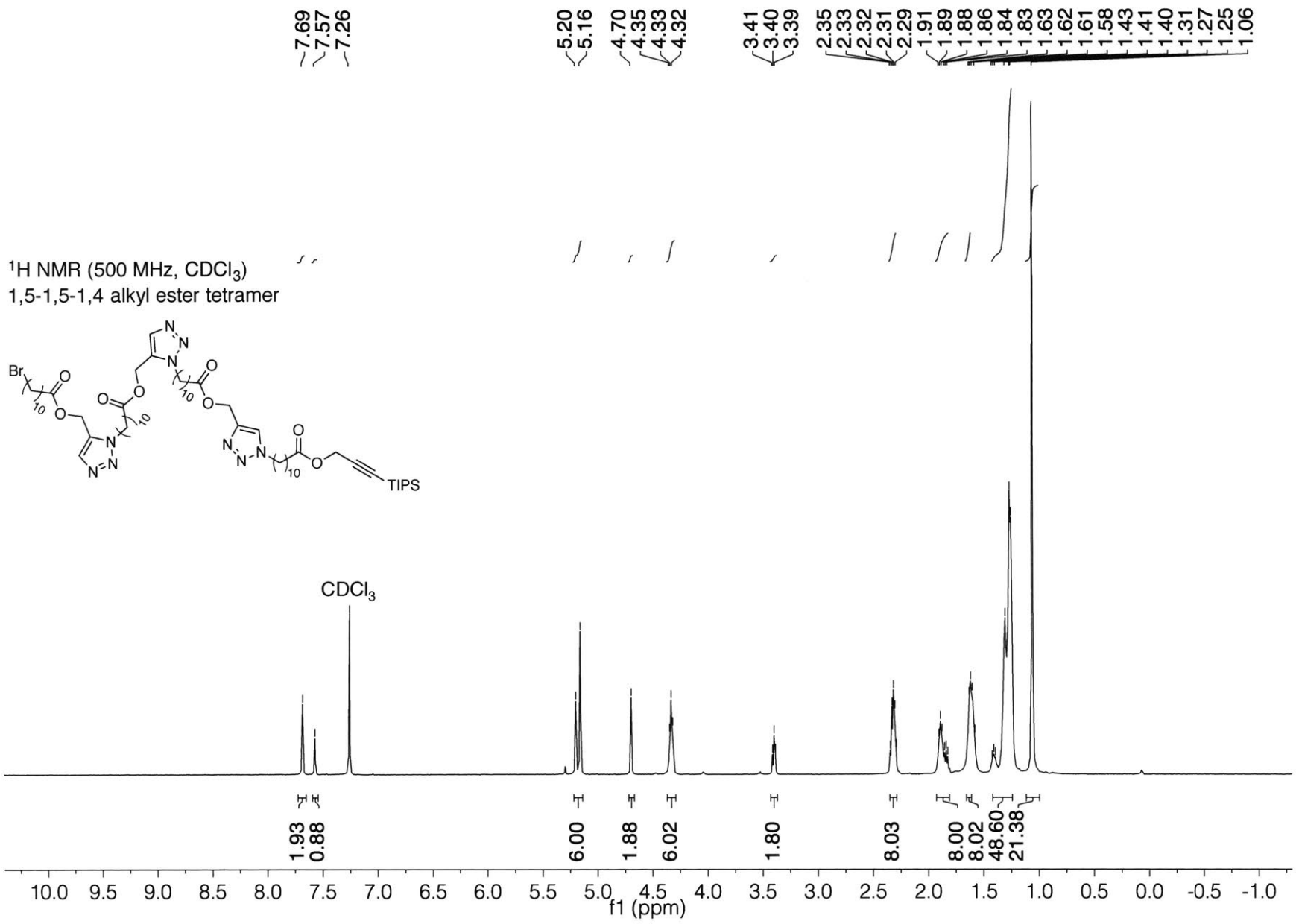
7.69
7.57
7.26
5.20
5.16
4.70
4.35
4.33
4.32
3.41
3.40
3.39
2.35
2.33
2.32
2.31
2.29
1.91
1.89
1.88
1.86
1.84
1.83
1.63
1.62
1.61
1.58
1.43
1.41
1.40
1.31
1.27
1.25
1.06
^{1}H NMR (500 MHz, $CDCl_3$)
1,5-1,5-1,4 alkyl ester tetramer
Br
TIPS
$CDCl_3$
1.93
0.88
6.00
1.88
6.02
1.80
8.03
8.00
8.02
48.60
21.38
10.0 9.5 9.0 8.5 8.0 7.5 7.0 6.5 6.0 5.5 5.0 4.5 4.0 3.5 3.0 2.5 2.0 1.5 1.0 0.5 0.0 -0.5 -1.0
f1 (ppm)

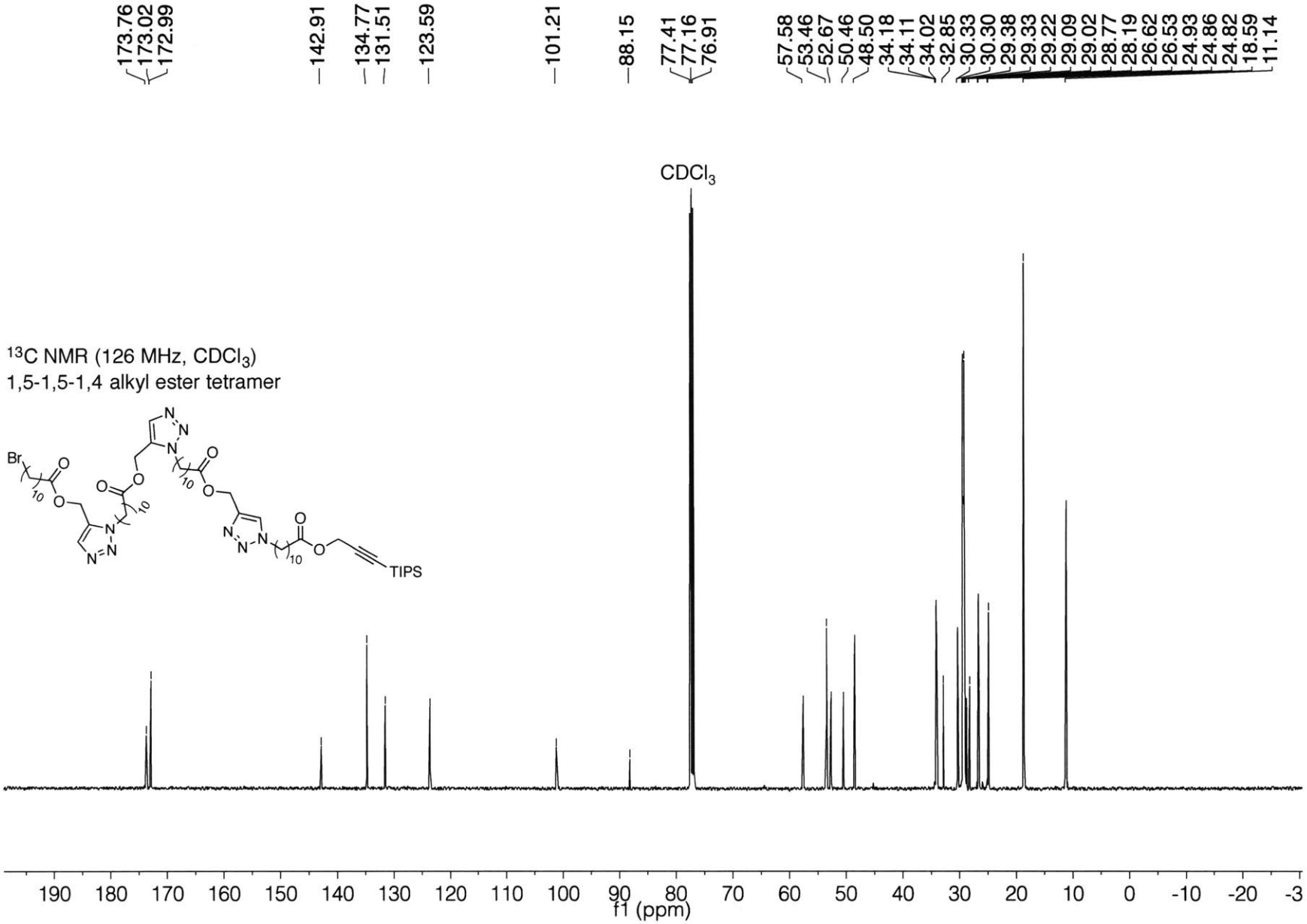
173.76
173.02
172.99
142.91
134.77
131.51
123.59
101.21
88.15
77.41
77.16
76.91
57.58
53.46
52.67
50.46
48.50
34.18
34.11
34.02
32.85
30.33
30.30
29.38
29.33
29.22
29.09
29.02
28.77
28.19
26.62
26.53
24.93
24.86
24.82
18.59
11.14
CDCl3
13C NMR (126 MHz, CDCl3)
1,5-1,5-1,4 alkyl ester tetramer
Br
TIPS
190 180 170 160 150 140 130 120 110 100 90 80 70 60 50 40 30 20 10 0 -10 -20 -3
f1 (ppm)

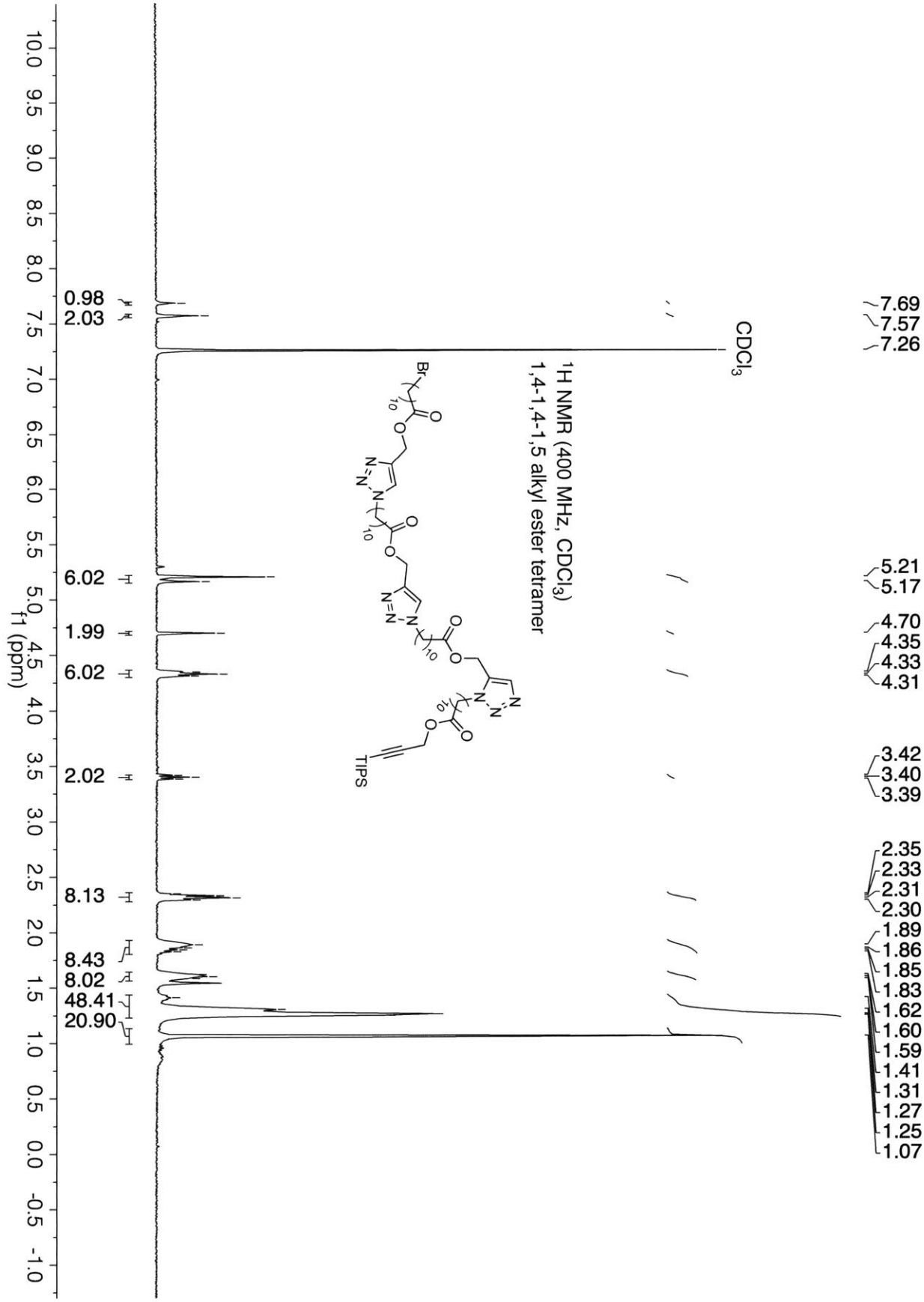
^{1}H NMR (400 MHz, CDCl$_3$)
1,4-1,4-1,5 alkyl ester tetramer
CDCl$_3$
Br
TIPS
7.69
7.57
7.26
5.21
5.17
4.70
4.35
4.33
4.31
3.42
3.40
3.39
2.35
2.33
2.31
2.30
1.89
1.86
1.85
1.83
1.62
1.60
1.59
1.41
1.31
1.27
1.25
1.07
0.98
2.03
6.02
1.99
6.02
2.02
8.13
8.43
8.02
48.41
20.90
f1 (ppm)

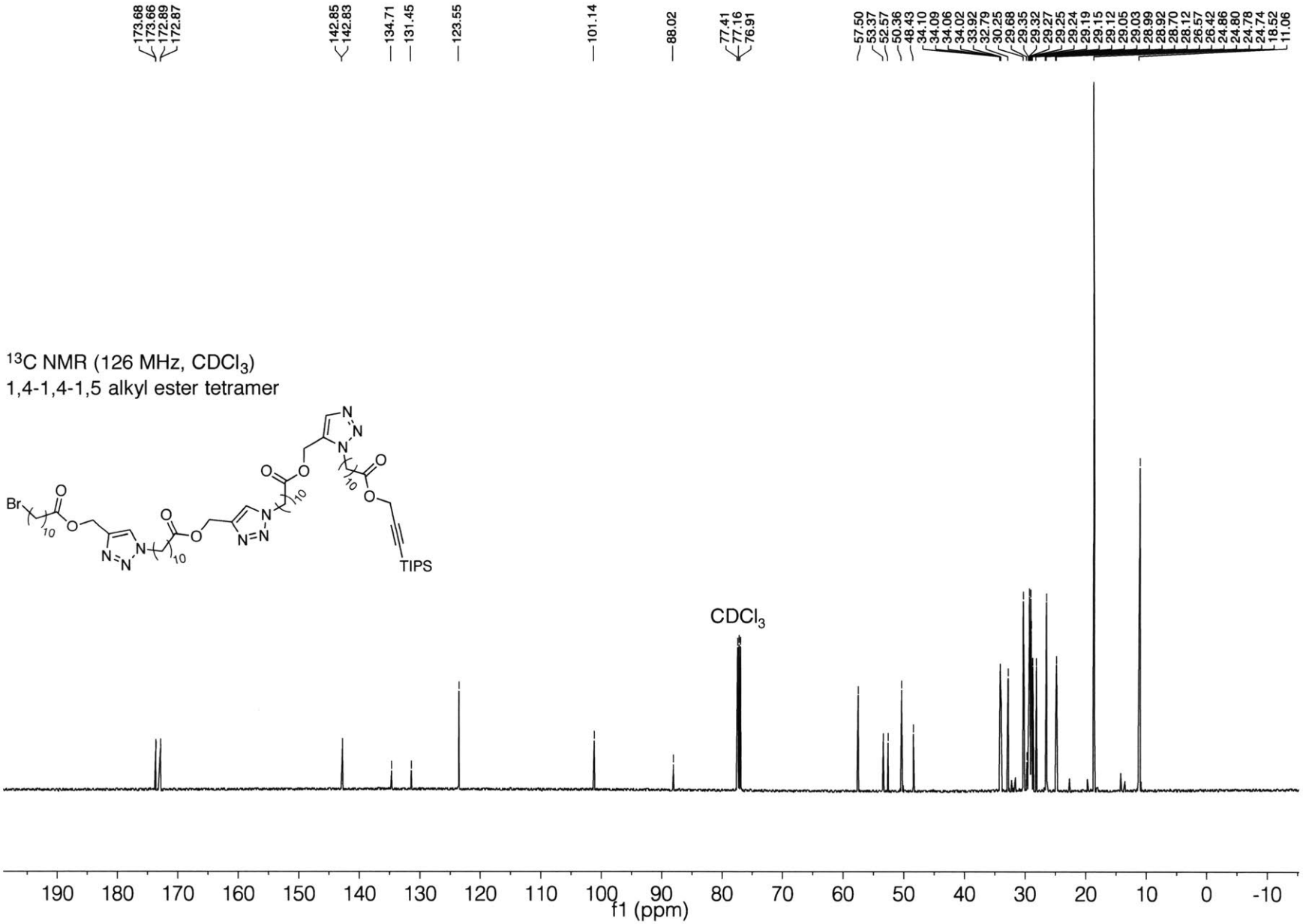
173.68
173.66
172.89
172.87
142.85
142.83
134.71
131.45
123.55
101.14
88.02
77.41
77.16
76.91
57.50
53.37
52.57
50.36
48.43
34.10
34.09
34.06
34.02
33.92
32.79
30.25
29.68
29.35
29.32
29.27
29.25
29.24
29.19
29.15
29.12
29.05
29.03
28.99
28.92
28.70
28.12
26.57
26.42
24.86
24.80
24.78
24.74
18.52
11.06
13C NMR (126 MHz, CDCl3)
1,4-1,4-1,5 alkyl ester tetramer
Br
TIPS
CDCl3
190
180
170
160
150
140
130
120
110
100
90
80
70
60
50
40
30
20
10
0
-10
f1 (ppm)

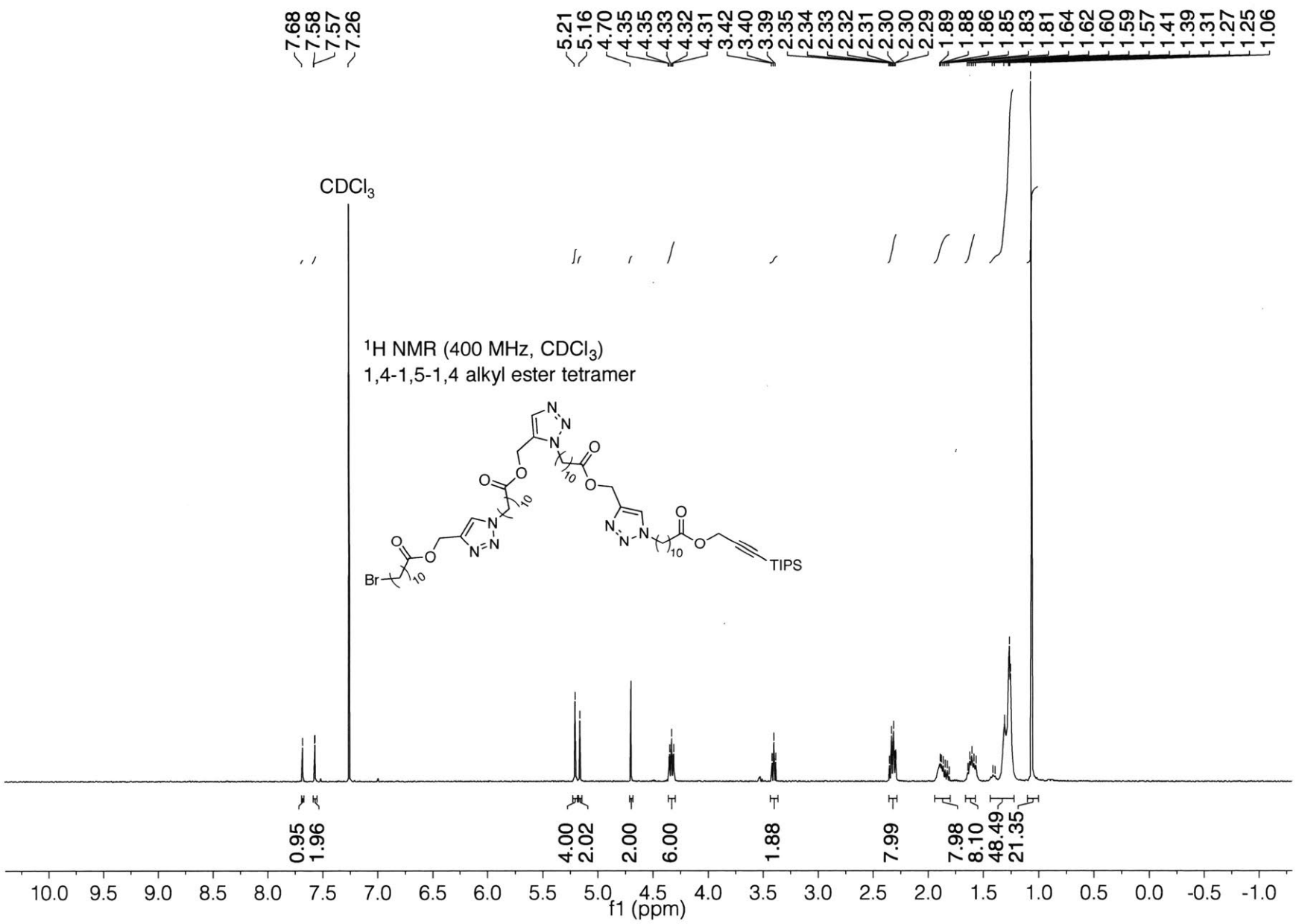
7.68
7.58
7.57
7.26
5.21
5.16
4.70
4.35
4.35
4.33
4.32
4.31
3.42
3.40
3.39
2.35
2.34
2.33
2.32
2.31
2.30
2.30
2.29
1.89
1.88
1.86
1.85
1.83
1.81
1.64
1.62
1.60
1.59
1.57
1.41
1.39
1.31
1.27
1.25
1.06
CDCl3
1H NMR (400 MHz, CDCl3)
1,4-1,5-1,4 alkyl ester tetramer
Br
TIPS
0.95
1.96
4.00
2.02
2.00
6.00
1.88
7.99
7.98
8.10
48.49
21.35
10.0 9.5 9.0 8.5 8.0 7.5 7.0 6.5 6.0 5.5 5.0 4.5 4.0 3.5 3.0 2.5 2.0 1.5 1.0 0.5 0.0 -0.5 -1.0
f1 (ppm)

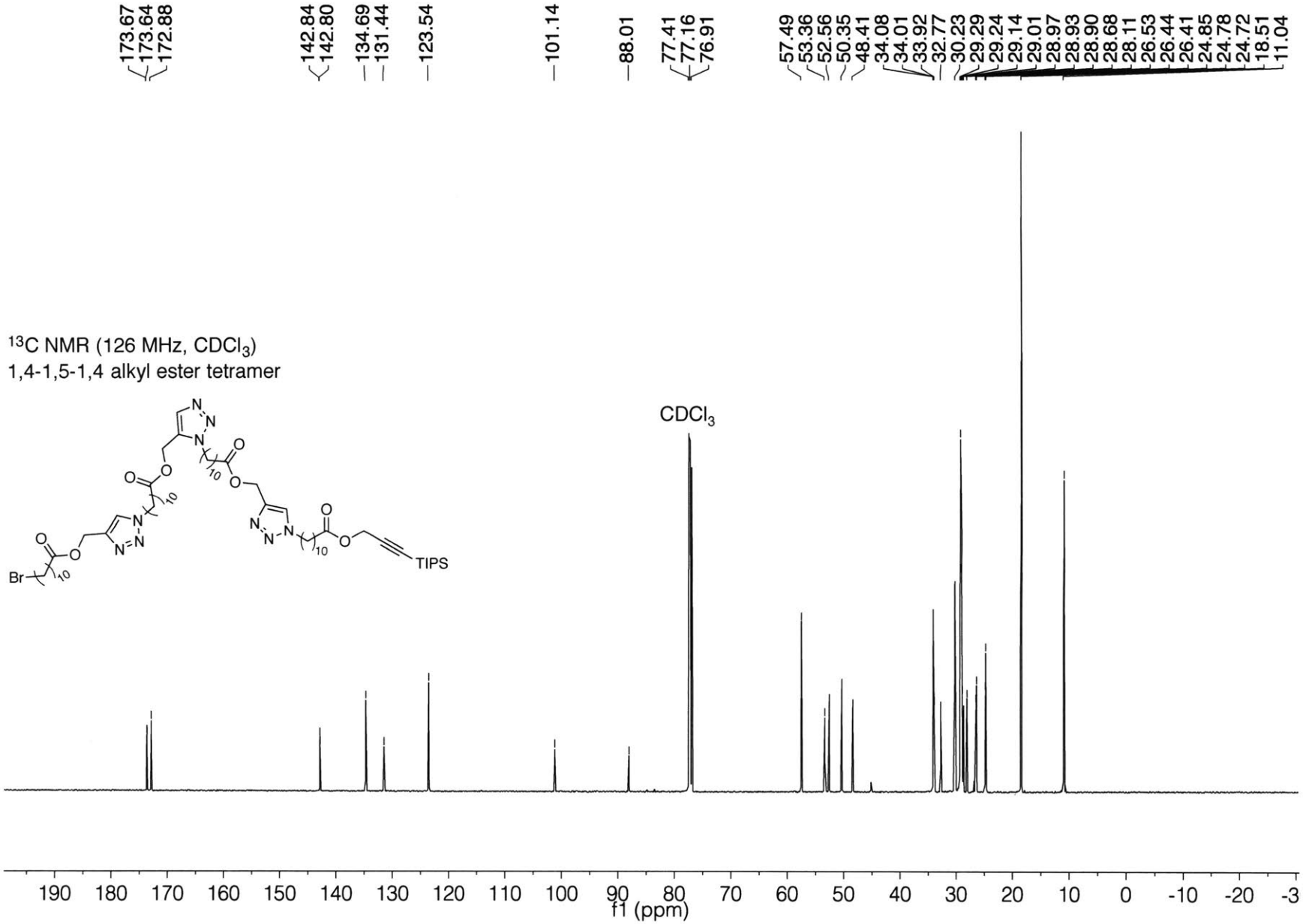
173.67
173.64
172.88
142.84
142.80
134.69
131.44
123.54
101.14
88.01
77.41
77.16
76.91
57.49
53.36
52.56
50.35
48.41
34.08
34.01
33.92
32.77
30.23
29.29
29.24
29.14
29.01
28.97
28.93
28.90
28.68
28.11
26.53
26.44
26.41
24.85
24.78
24.72
18.51
11.04
13C NMR (126 MHz, CDCl3)
1,4-1,5-1,4 alkyl ester tetramer
CDCl3
TIPS
Br
190 180 170 160 150 140 130 120 110 100 90 80 70 60 50 40 30 20 10 0 -10 -20 -3
f1 (ppm)

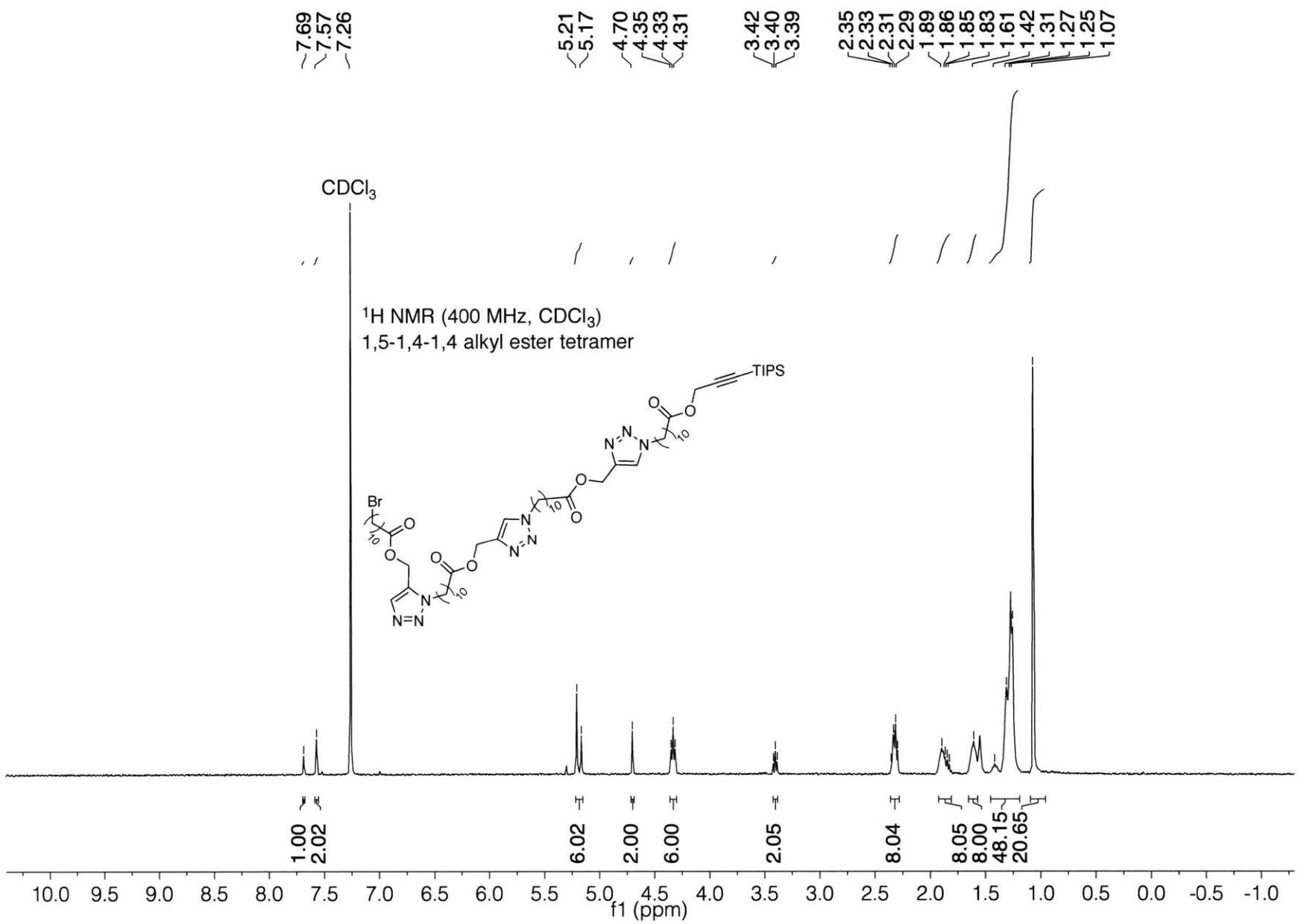
7.69
7.57
7.26
5.21
5.17
4.70
4.35
4.33
4.31
3.42
3.40
3.39
2.35
2.33
2.31
2.29
1.89
1.86
1.85
1.83
1.61
1.42
1.31
1.27
1.25
1.07
CDCl3
1H NMR (400 MHz, CDCl3)
1,5-1,4-1,4 alkyl ester tetramer
TIPS
Br
1.00
2.02
6.02
2.00
6.00
2.05
8.04
8.05
8.00
48.15
20.65
f1 (ppm)

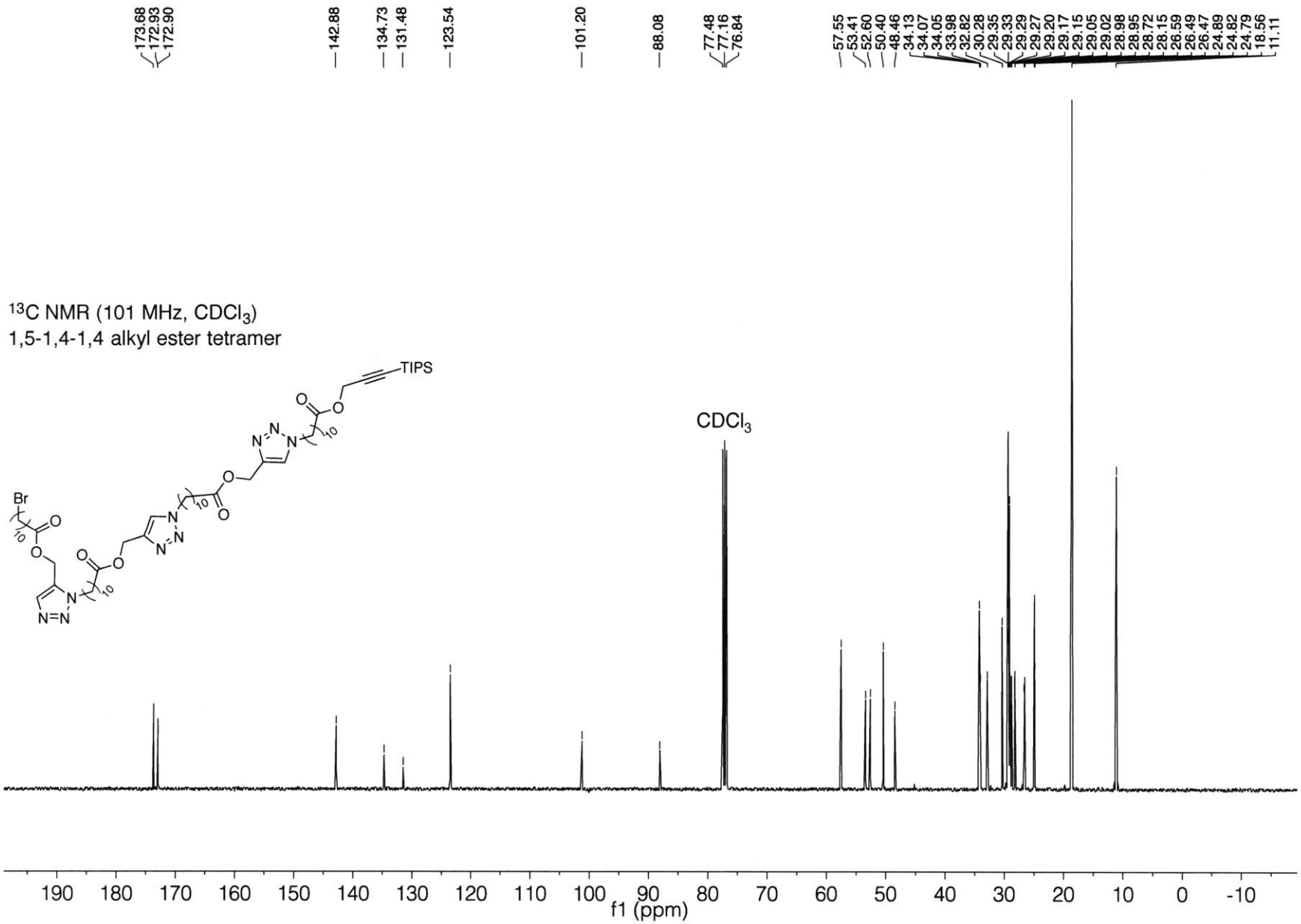
173.68
172.93
172.90
142.88
134.73
131.48
123.54
101.20
88.08
77.48
77.16
76.84
57.55
53.41
52.60
50.40
48.46
34.13
34.07
34.05
33.98
32.82
30.28
29.35
29.33
29.29
29.27
29.20
29.17
29.15
29.05
29.02
28.98
28.95
28.72
28.15
26.59
26.49
26.47
24.89
24.82
24.79
18.56
11.11
13C NMR (101 MHz, CDCl3)
1,5-1,4-1,4 alkyl ester tetramer
TIPS
Br
CDCl3
190 180 170 160 150 140 130 120 110 100 90 80 70 60 50 40 30 20 10 0 -10
f1 (ppm)

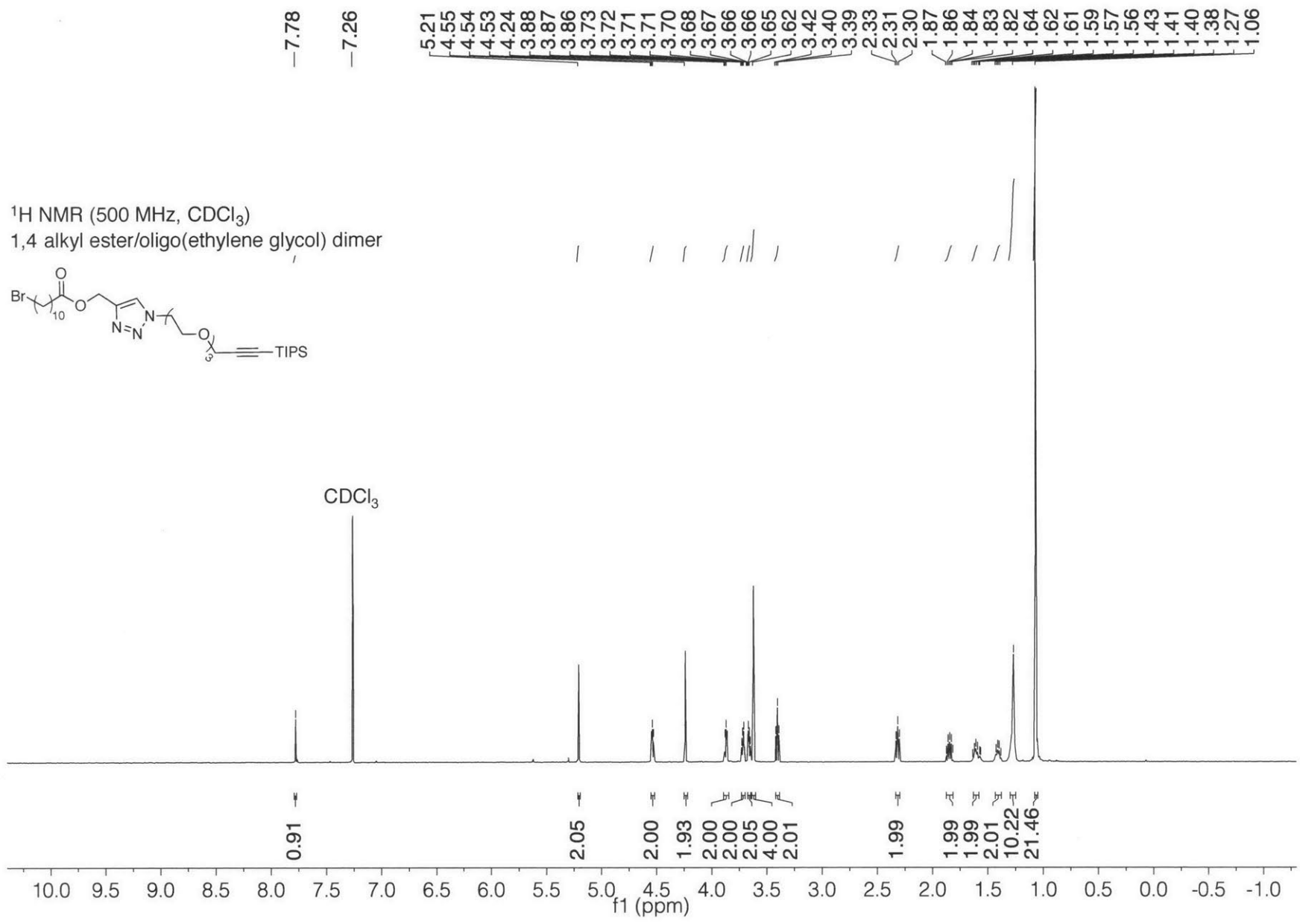
7.78
7.26
5.21
4.55
4.54
4.53
4.24
3.88
3.87
3.86
3.73
3.72
3.71
3.71
3.70
3.68
3.67
3.66
3.66
3.65
3.62
3.42
3.40
3.39
2.33
2.31
2.30
1.87
1.86
1.84
1.83
1.82
1.64
1.62
1.61
1.59
1.57
1.56
1.43
1.41
1.40
1.38
1.27
1.06
1H NMR (500 MHz, CDCl3)
1,4 alkyl ester/oligo(ethylene glycol) dimer
Br
10
O
O
N
N
N
O
3
TIPS
CDCl3
0.91
2.05
2.00
1.93
2.00
2.00
2.05
4.00
2.01
1.99
1.99
1.99
2.01
10.22
21.46
10.0 9.5 9.0 8.5 8.0 7.5 7.0 6.5 6.0 5.5 5.0 4.5 4.0 3.5 3.0 2.5 2.0 1.5 1.0 0.5 0.0 -0.5 -1.0
f1 (ppm)

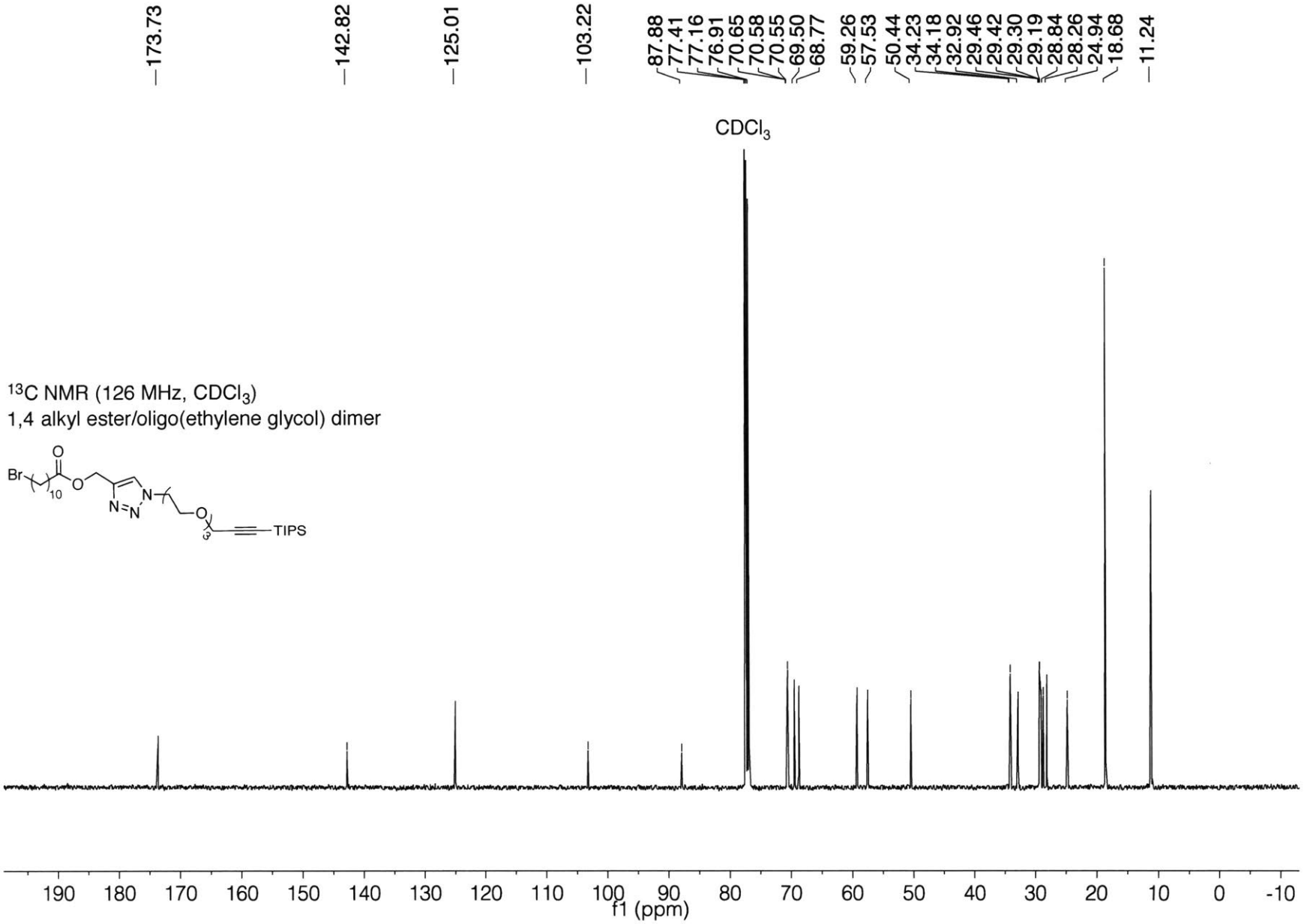
173.73
142.82
125.01
103.22
87.88
77.41
77.16
76.91
70.65
70.58
70.55
69.50
68.77
59.26
57.53
50.44
34.23
34.18
32.92
29.46
29.42
29.30
29.19
28.84
28.26
24.94
18.68
11.24
CDCl3
13C NMR (126 MHz, CDCl3)
1,4 alkyl ester/oligo(ethylene glycol) dimer
Br
10
O
N
N
TIPS
f1 (ppm)

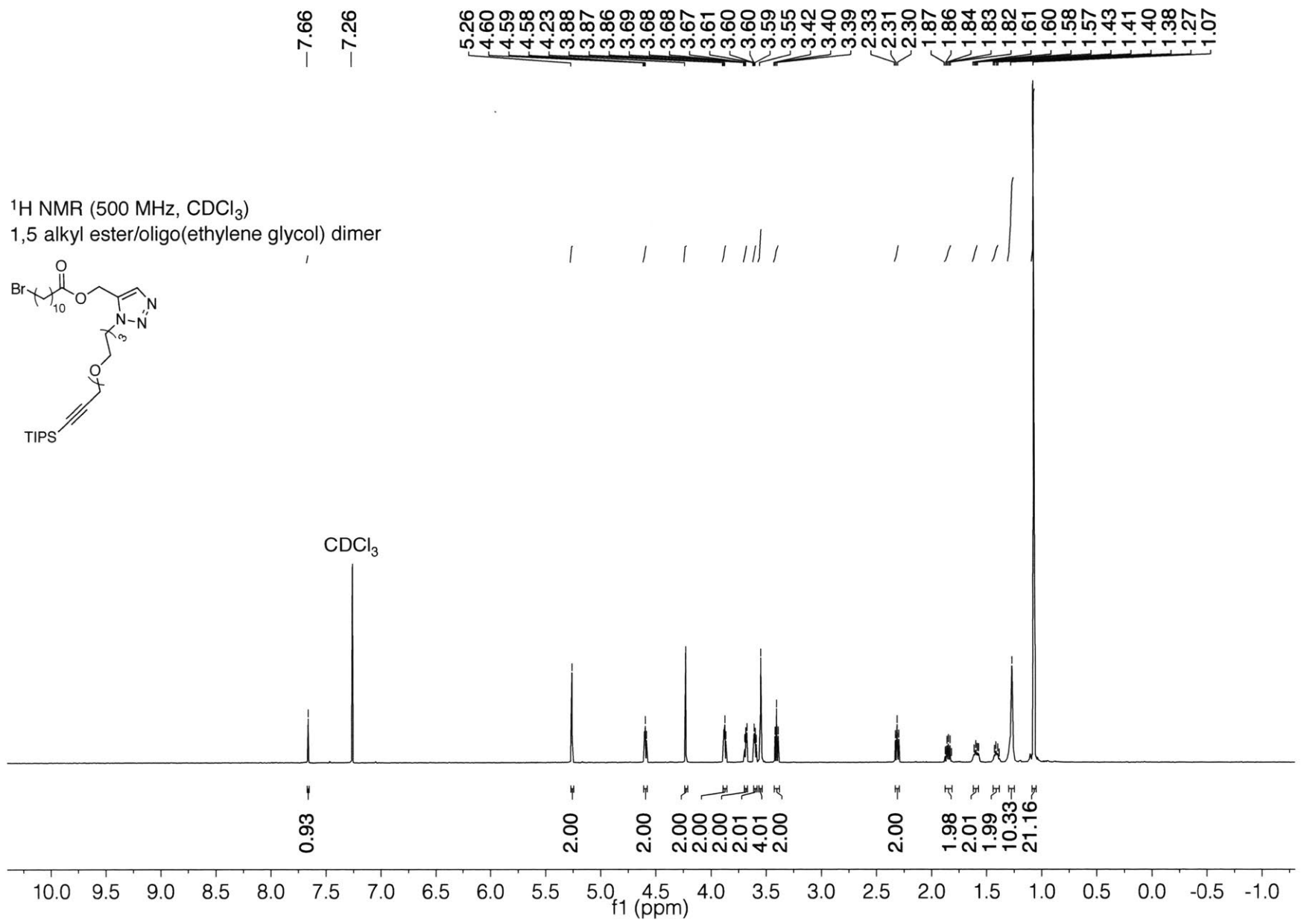
7.66
7.26
5.26
4.60
4.59
4.58
4.23
3.88
3.87
3.86
3.69
3.68
3.68
3.67
3.61
3.60
3.60
3.59
3.55
3.42
3.40
3.39
2.33
2.31
2.30
1.87
1.86
1.84
1.83
1.82
1.61
1.60
1.58
1.57
1.43
1.41
1.40
1.38
1.27
1.07
1H NMR (500 MHz, CDCl3)
1,5 alkyl ester/oligo(ethylene glycol) dimer
Br
10
O
N
N
N
3
O
TIPS
CDCl3
0.93
2.00
2.00
2.00
2.00
2.00
2.01
4.01
2.00
2.00
1.98
2.01
1.99
10.33
21.16
10.0 9.5 9.0 8.5 8.0 7.5 7.0 6.5 6.0 5.5 5.0 4.5 4.0 3.5 3.0 2.5 2.0 1.5 1.0 0.5 0.0 -0.5 -1.0
f1 (ppm)

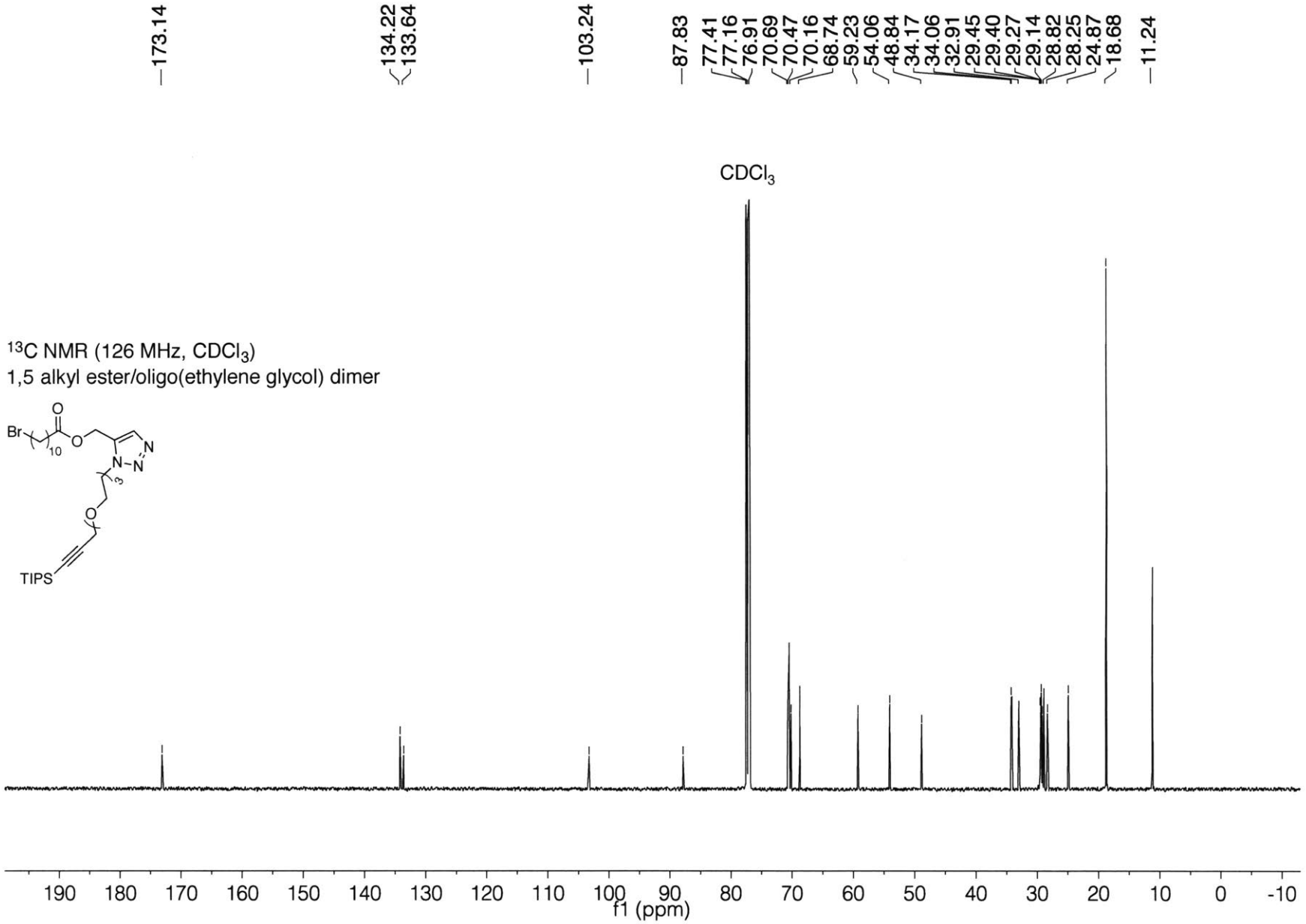
173.14
134.22
133.64
103.24
87.83
77.41
77.16
76.91
70.69
70.47
70.16
68.74
59.23
54.06
48.84
34.17
34.06
32.91
29.45
29.40
29.27
29.14
28.82
28.25
24.87
18.68
11.24
CDCl3
13C NMR (126 MHz, CDCl3)
1,5 alkyl ester/oligo(ethylene glycol) dimer
Br
10
O
N
N
N
3
O
TIPS
190
180
170
160
150
140
130
120
110
100
90
80
70
60
50
40
30
20
10
0
-10
f1 (ppm)

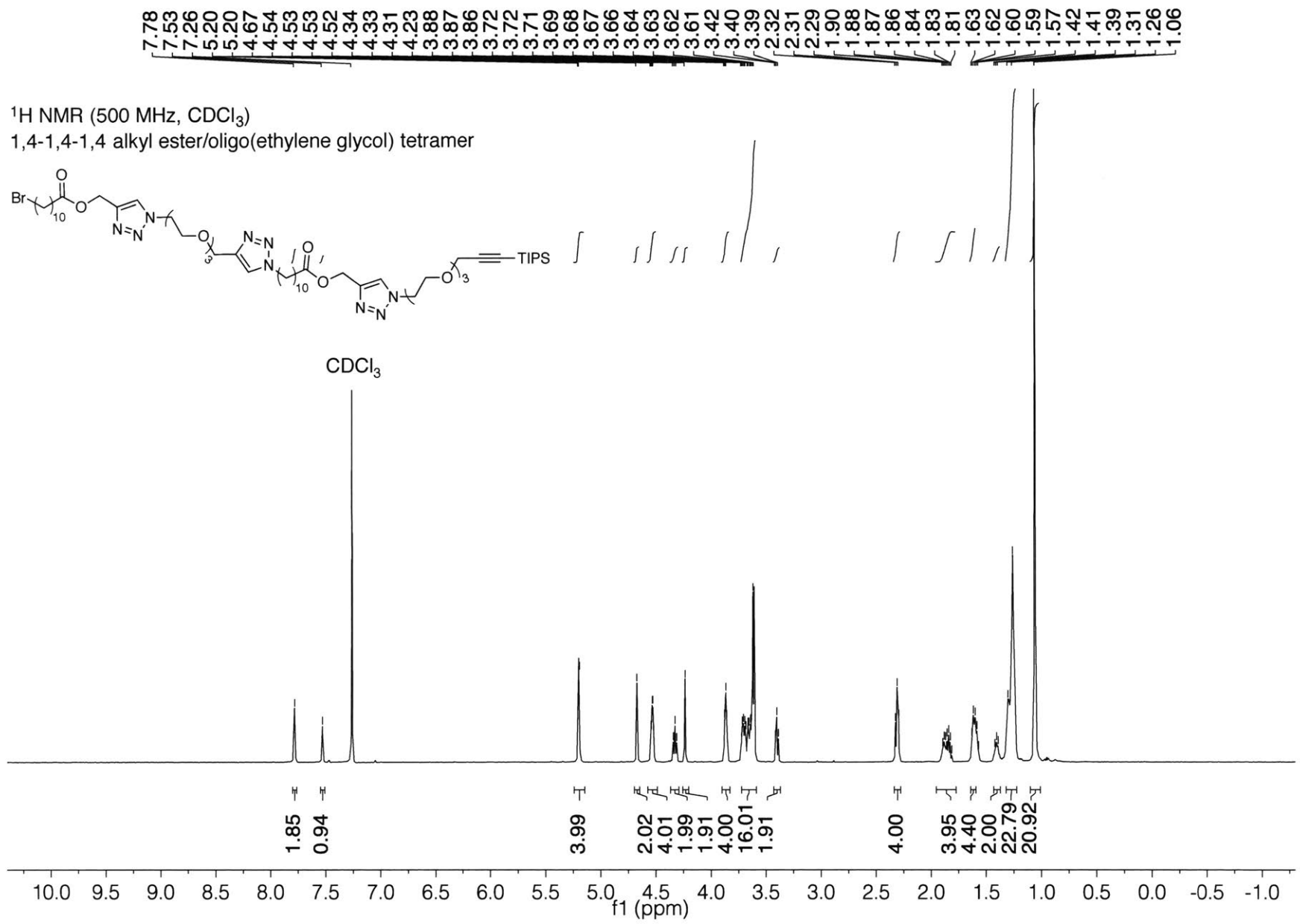
7.78
7.53
7.26
5.20
5.20
4.67
4.54
4.53
4.53
4.52
4.34
4.33
4.31
4.23
3.88
3.87
3.86
3.72
3.72
3.71
3.69
3.68
3.67
3.66
3.64
3.63
3.62
3.61
3.42
3.40
3.39
2.32
2.31
2.29
1.90
1.88
1.87
1.86
1.84
1.83
1.81
1.63
1.62
1.60
1.59
1.57
1.42
1.41
1.39
1.31
1.26
1.06
1H NMR (500 MHz, CDCl3)
1,4-1,4-1,4 alkyl ester/oligo(ethylene glycol) tetramer
Br
TIPS
CDCl3
1.85
0.94
3.99
2.02
4.01
1.99
1.91
4.00
16.01
1.91
4.00
3.95
4.40
2.00
22.79
20.92
10.0 9.5 9.0 8.5 8.0 7.5 7.0 6.5 6.0 5.5 5.0 4.5 4.0 3.5 3.0 2.5 2.0 1.5 1.0 0.5 0.0 -0.5 -1.0
f1 (ppm)

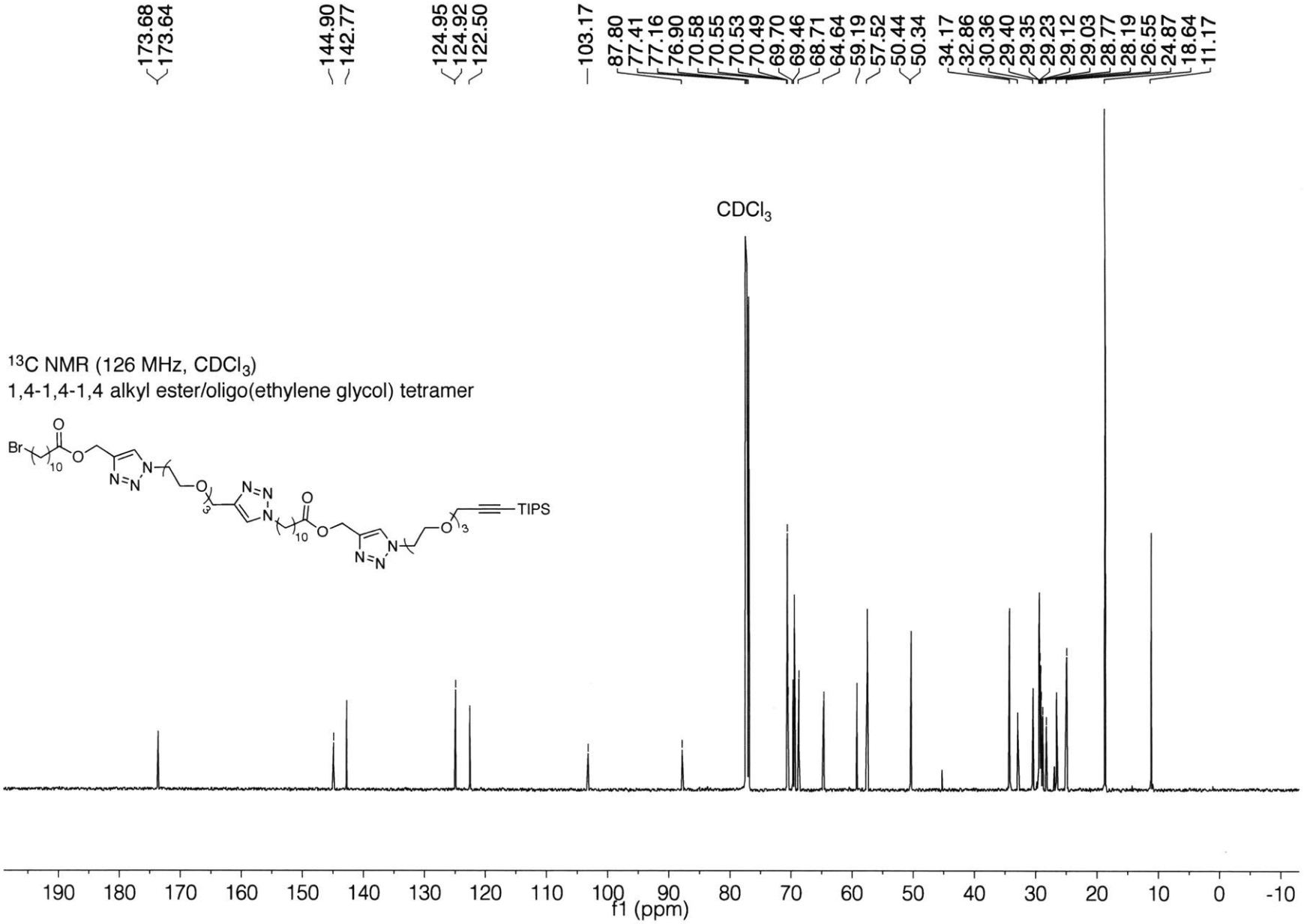
173.68
173.64
144.90
142.77
124.95
124.92
122.50
103.17
87.80
77.41
77.16
76.90
70.58
70.55
70.53
70.49
69.70
69.46
68.71
64.64
59.19
57.52
50.44
50.34
34.17
32.86
30.36
29.40
29.35
29.23
29.12
29.03
28.77
28.19
26.55
24.87
18.64
11.17
CDCl3
13C NMR (126 MHz, CDCl3)
1,4-1,4-1,4 alkyl ester/oligo(ethylene glycol) tetramer
Br
TIPS
190
180
170
160
150
140
130
120
110
100
90
80
70
60
50
40
30
20
10
0
-10
f1 (ppm)

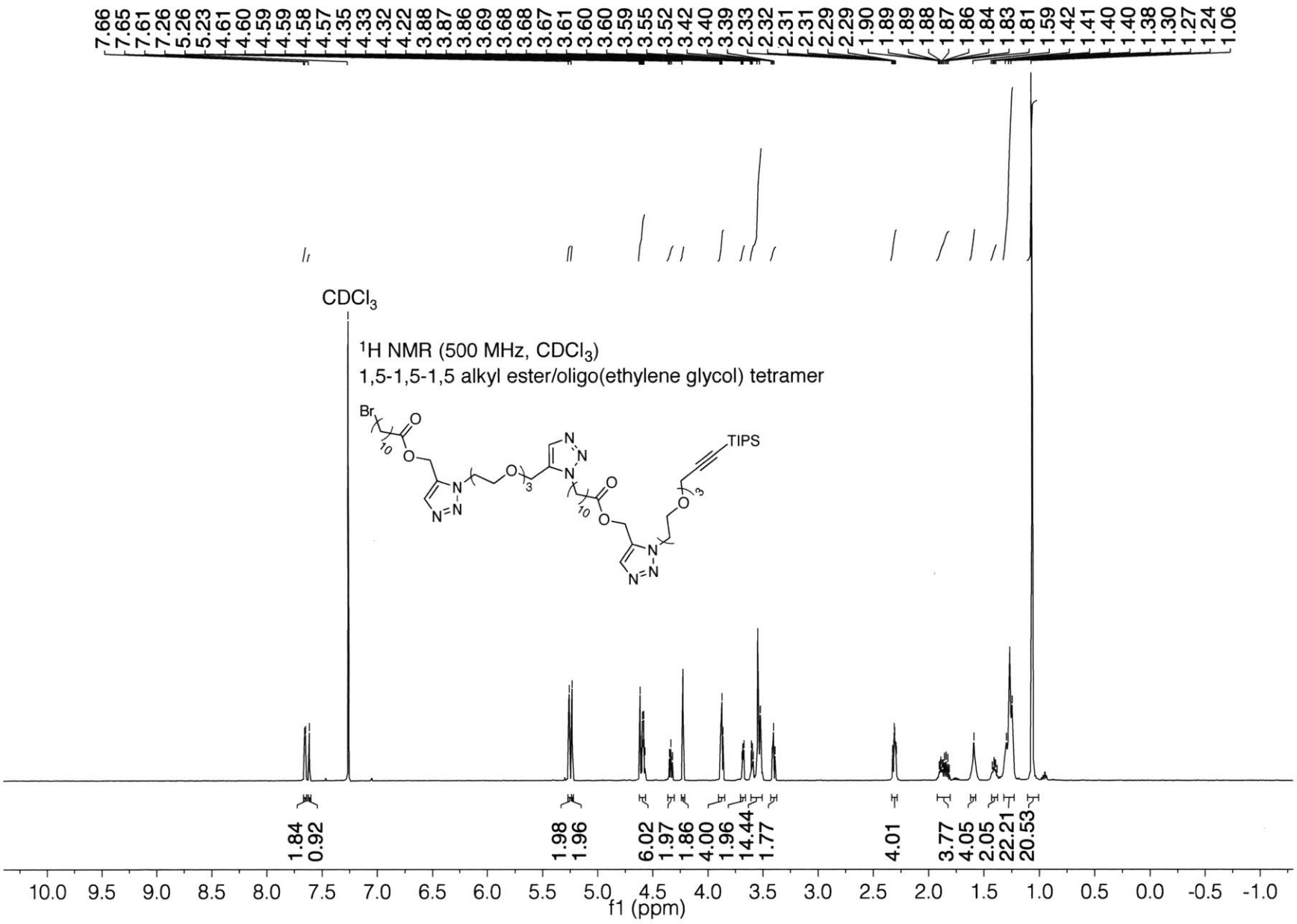
7.66 7.65 7.61 7.26 5.26 5.23 4.61 4.60 4.59 4.59 4.58 4.57 4.35 4.33 4.32 4.22 3.88 3.87 3.86 3.69 3.68 3.68 3.67 3.61 3.60 3.60 3.59 3.55 3.52 3.42 3.40 3.39 2.33 2.32 2.31 2.31 2.29 2.29 1.90 1.89 1.89 1.88 1.87 1.86 1.84 1.83 1.81 1.59 1.42 1.41 1.40 1.40 1.38 1.30 1.27 1.24 1.06
CDCl3
1H NMR (500 MHz, CDCl3)
1,5-1,5-1,5 alkyl ester/oligo(ethylene glycol) tetramer
Br
TIPS
1.84 0.92 1.98 1.96 6.02 1.97 1.86 4.00 1.96 14.44 1.77 4.01 3.77 4.05 2.05 22.21 20.53
10.0 9.5 9.0 8.5 8.0 7.5 7.0 6.5 6.0 5.5 5.0 4.5 4.0 3.5 3.0 2.5 2.0 1.5 1.0 0.5 0.0 -0.5 -1.0
f1 (ppm)

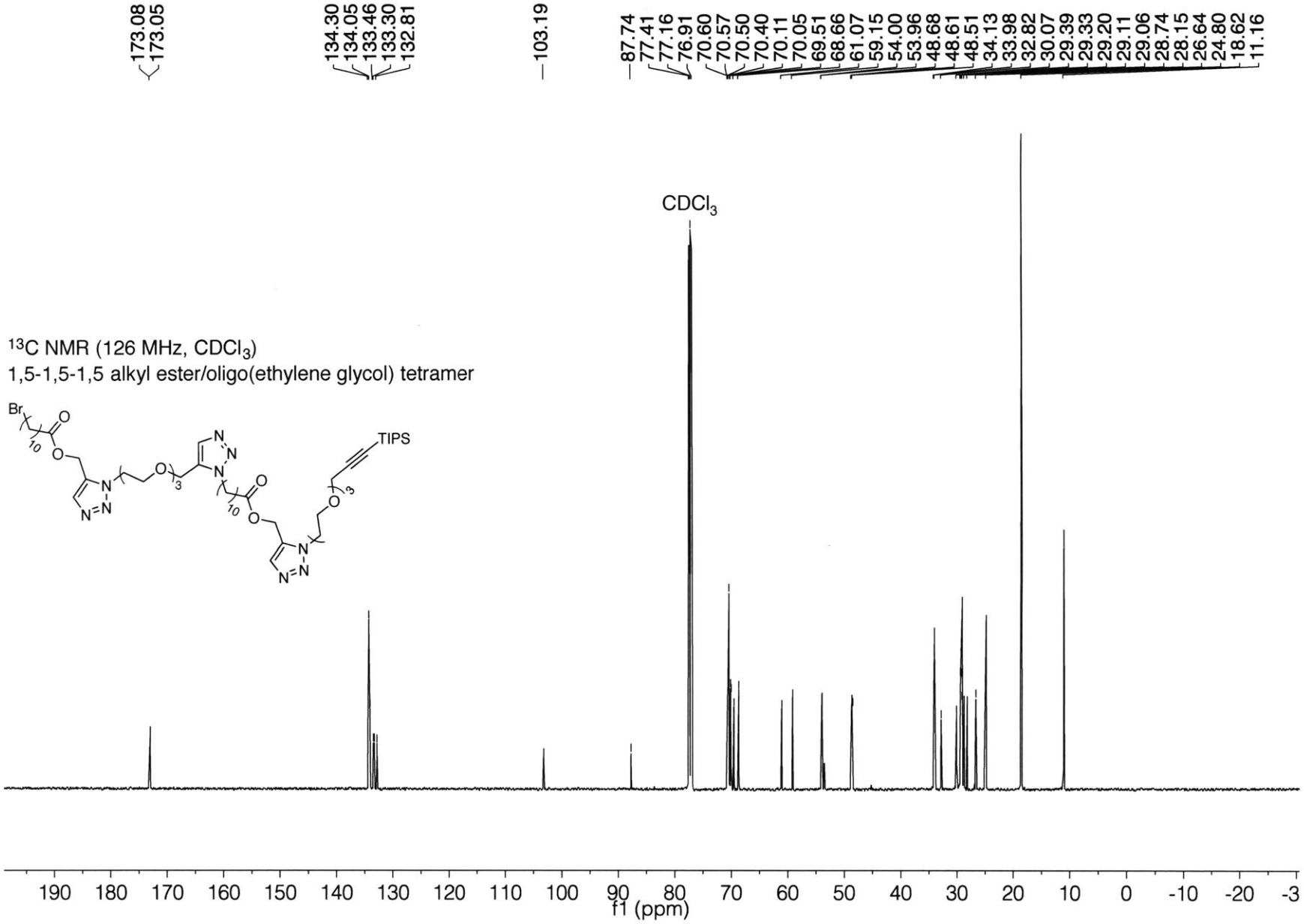
173.08
173.05
134.30
134.05
133.46
133.30
132.81
103.19
87.74
77.41
77.16
76.91
70.60
70.57
70.50
70.40
70.11
70.05
69.51
68.66
61.07
59.15
54.00
53.96
48.68
48.61
48.51
34.13
33.98
32.82
30.07
29.39
29.33
29.20
29.11
29.06
28.74
28.15
26.64
24.80
18.62
11.16
CDCl3
13C NMR (126 MHz, CDCl3)
1,5-1,5-1,5 alkyl ester/oligo(ethylene glycol) tetramer
Br
TIPS
f1 (ppm)

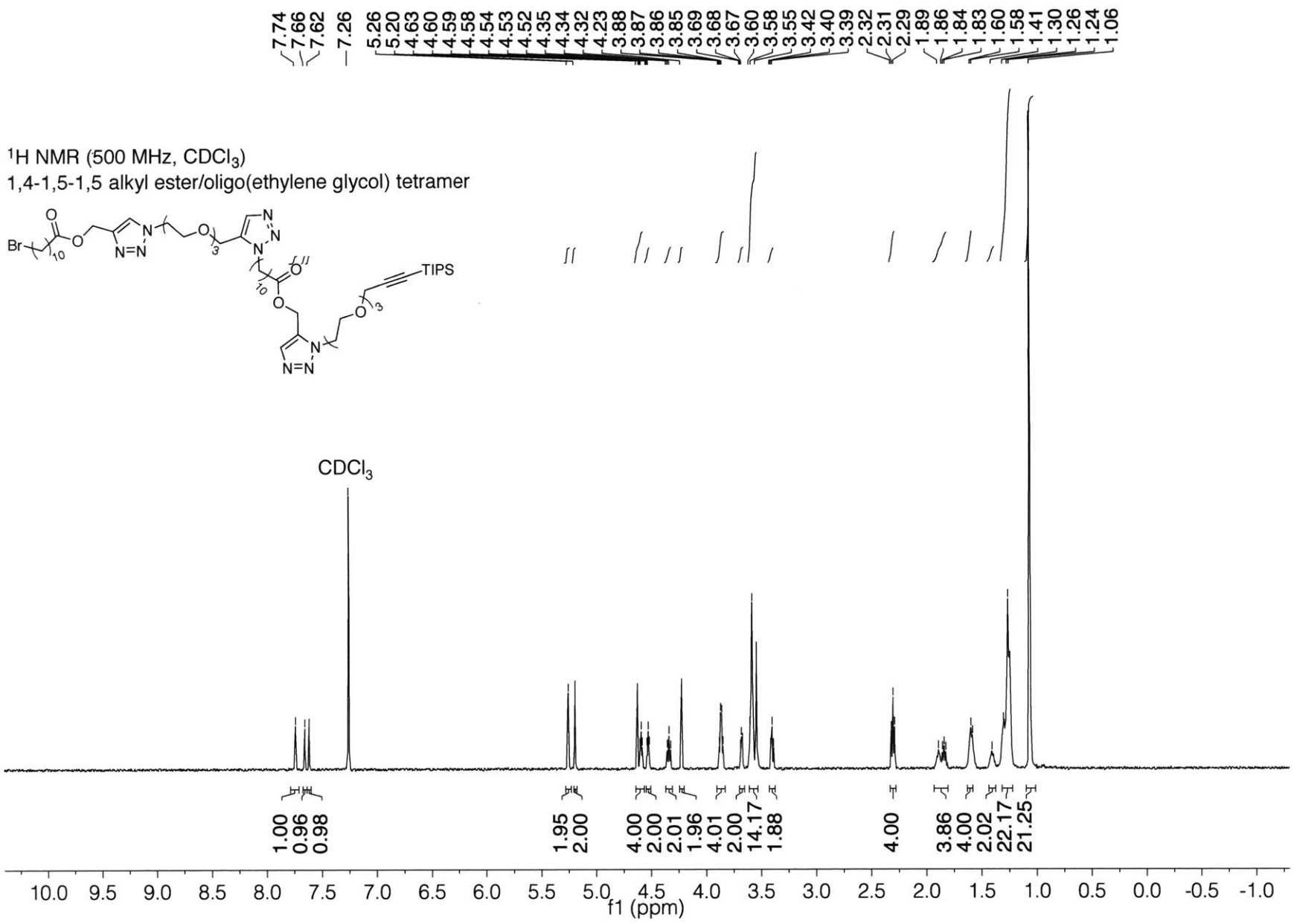
7.74
7.66
7.62
7.26
5.26
5.20
4.63
4.60
4.59
4.58
4.54
4.53
4.52
4.35
4.34
4.32
4.23
3.88
3.87
3.86
3.85
3.69
3.68
3.67
3.60
3.58
3.55
3.42
3.40
3.39
2.32
2.31
2.29
1.89
1.86
1.84
1.83
1.60
1.58
1.41
1.30
1.26
1.24
1.06
1H NMR (500 MHz, CDCl3)
1,4-1,5-1,5 alkyl ester/oligo(ethylene glycol) tetramer
Br
TIPS
CDCl3
1.00
0.96
0.98
1.95
2.00
4.00
2.00
2.01
1.96
4.01
2.00
14.17
1.88
4.00
3.86
4.00
2.02
22.17
21.25
10.0 9.5 9.0 8.5 8.0 7.5 7.0 6.5 6.0 5.5 5.0 4.5 4.0 3.5 3.0 2.5 2.0 1.5 1.0 0.5 0.0 -0.5 -1.0
f1 (ppm)

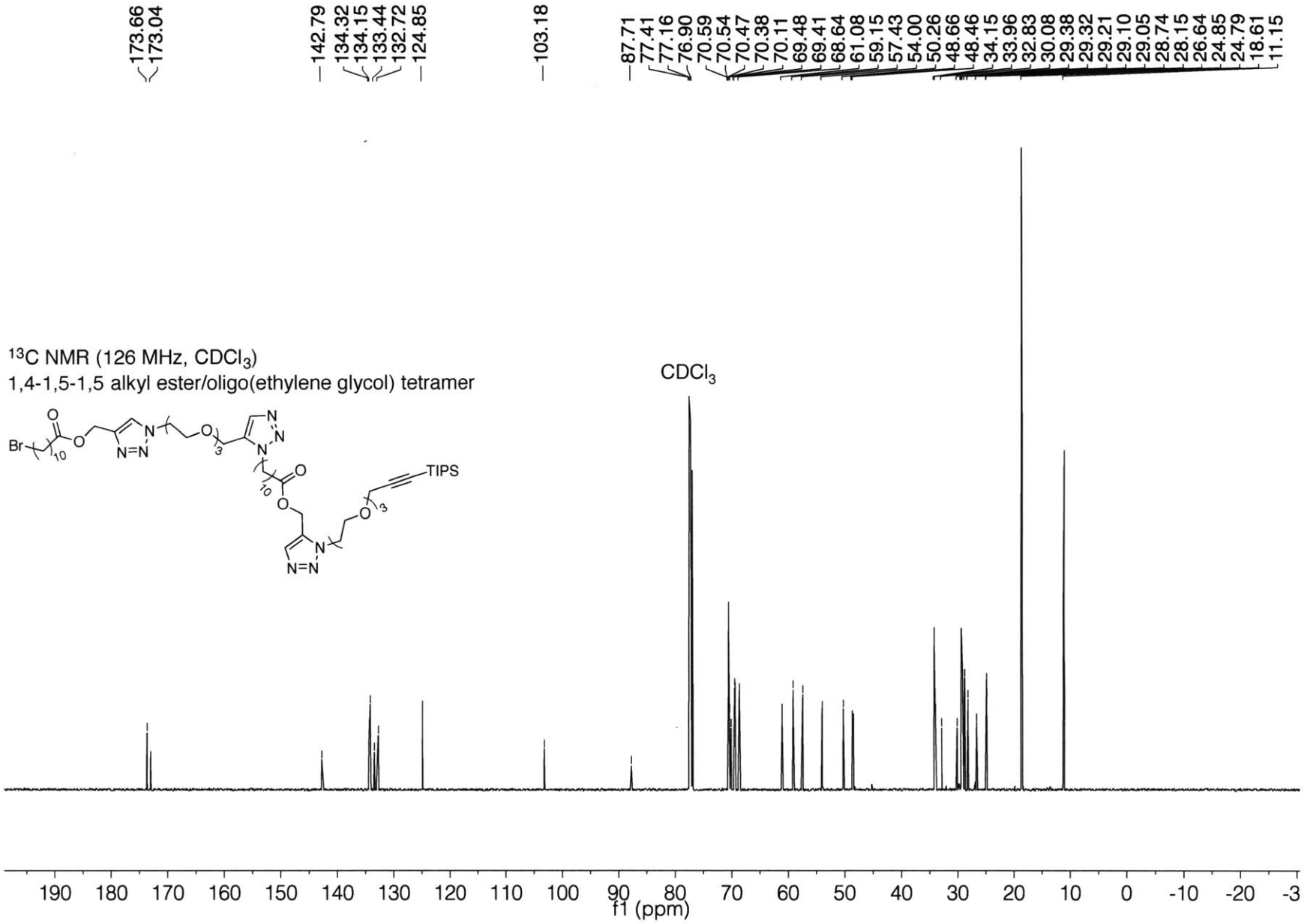
173.66
173.04
142.79
134.32
134.15
133.44
132.72
124.85
103.18
87.71
77.41
77.16
76.90
70.59
70.54
70.47
70.38
70.11
69.48
69.41
68.64
61.08
59.15
57.43
54.00
50.26
48.66
48.46
34.15
33.96
32.83
30.08
29.38
29.32
29.21
29.10
29.05
28.74
28.15
26.64
24.85
24.79
18.61
11.15
13C NMR (126 MHz, CDCl3)
1,4-1,5-1,5 alkyl ester/oligo(ethylene glycol) tetramer
CDCl3
TIPS
f1 (ppm)

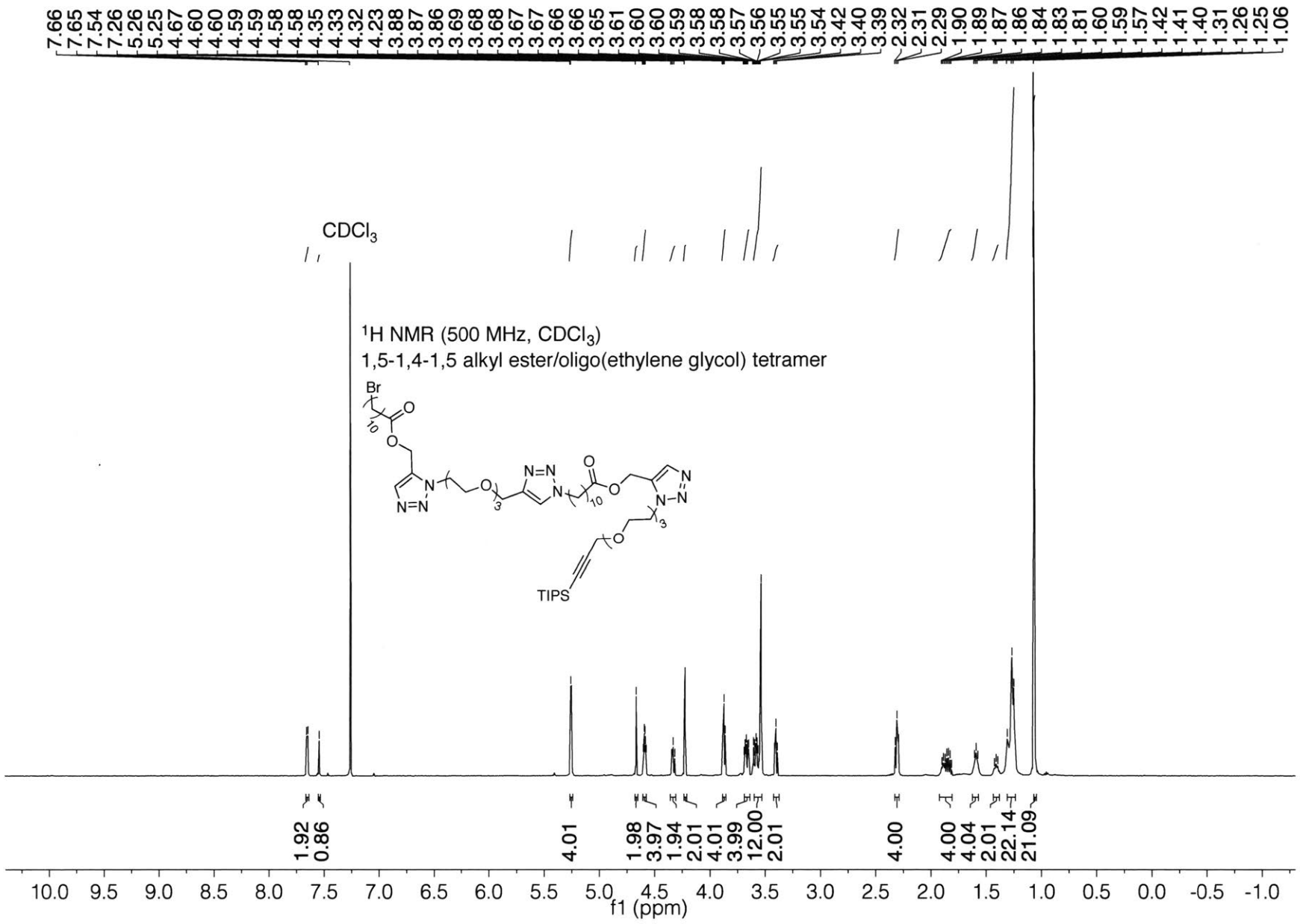
7.66 7.65 7.54 7.26 5.25 4.67 4.60 4.60 4.59 4.59 4.58 4.58 4.35 4.33 4.32 4.23 3.88 3.87 3.86 3.69 3.68 3.68 3.67 3.67 3.66 3.66 3.65 3.61 3.60 3.60 3.59 3.58 3.58 3.57 3.56 3.55 3.55 3.54 3.42 3.40 3.39 2.32 2.31 2.29 1.90 1.89 1.87 1.86 1.84 1.83 1.81 1.60 1.59 1.57 1.42 1.41 1.40 1.31 1.26 1.25 1.06
CDCl3
1H NMR (500 MHz, CDCl3)
1,5-1,4-1,5 alkyl ester/oligo(ethylene glycol) tetramer
Br
TIPS
1.92 0.86 4.01 1.98 3.97 1.94 2.01 4.01 3.99 12.00 2.01 4.00 4.00 4.04 2.01 22.14 21.09
10.0 9.5 9.0 8.5 8.0 7.5 7.0 6.5 6.0 5.5 5.0 4.5 4.0 3.5 3.0 2.5 2.0 1.5 1.0 0.5 0.0 -0.5 -1.0
f1 (ppm)

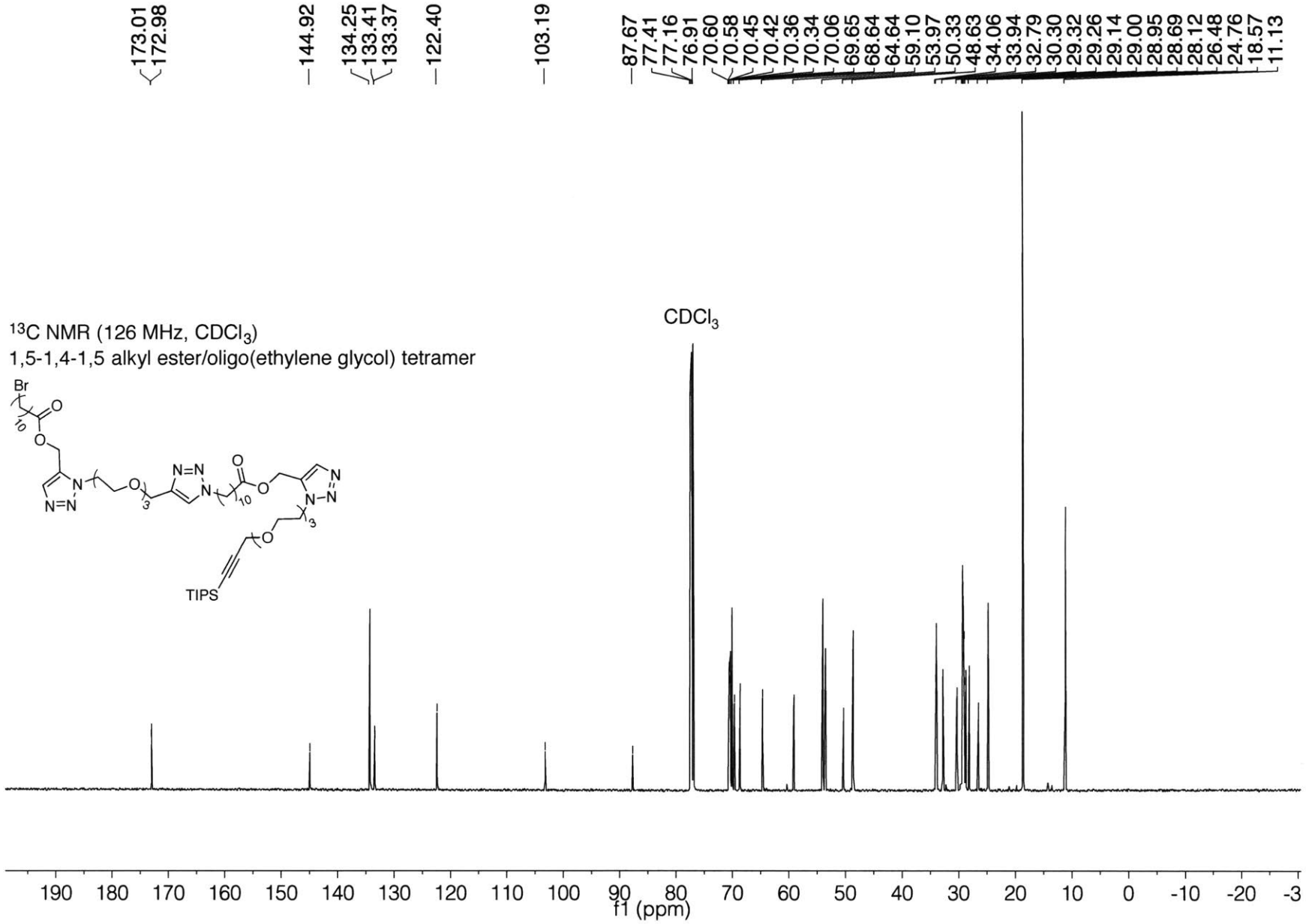
173.01
172.98
144.92
134.25
133.41
133.37
122.40
103.19
87.67
77.41
77.16
76.91
70.60
70.58
70.45
70.42
70.36
70.34
70.06
69.65
68.64
64.64
59.10
53.97
50.33
48.63
34.06
33.94
32.79
30.30
29.32
29.26
29.14
29.00
28.95
28.69
28.12
26.48
24.76
18.57
11.13
CDCl3
13C NMR (126 MHz, CDCl3)
1,5-1,4-1,5 alkyl ester/oligo(ethylene glycol) tetramer
Br
TIPS
190 180 170 160 150 140 130 120 110 100 90 80 70 60 50 40 30 20 10 0 -10 -20 -3
f1 (ppm)

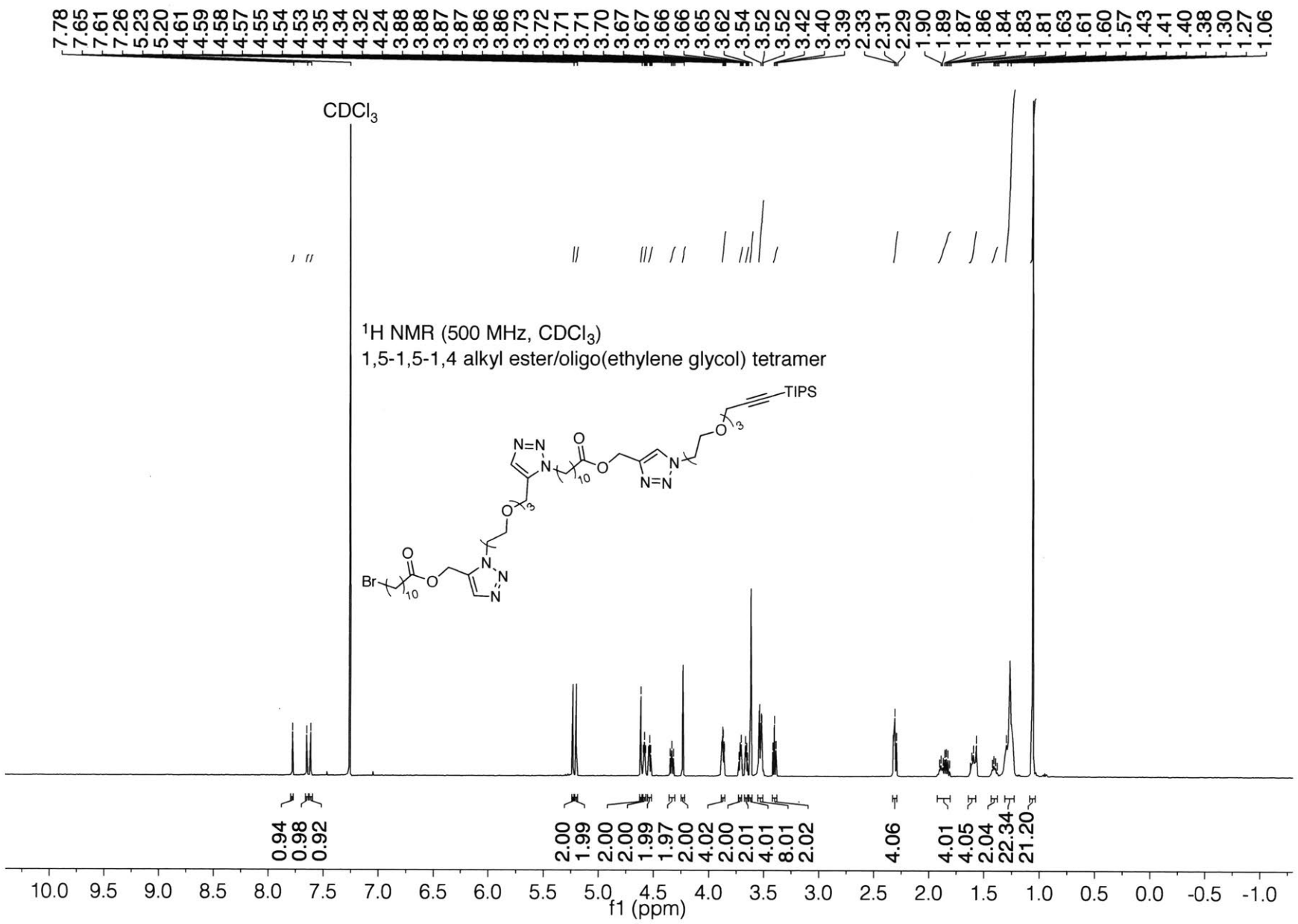
7.78 7.65 7.61 7.26 5.23 5.20 4.61 4.59 4.58 4.57 4.55 4.54 4.53 4.35 4.34 4.32 4.24 3.88 3.88 3.87 3.87 3.86 3.86 3.73 3.72 3.71 3.71 3.70 3.67 3.67 3.66 3.66 3.65 3.62 3.54 3.52 3.52 3.42 3.40 3.39 2.33 2.31 2.29 1.90 1.89 1.87 1.86 1.84 1.83 1.81 1.63 1.61 1.60 1.57 1.43 1.41 1.40 1.38 1.30 1.27 1.06
CDCl3
1H NMR (500 MHz, CDCl3)
1,5-1,5-1,4 alkyl ester/oligo(ethylene glycol) tetramer
TIPS
Br
0.94 0.98 0.92 2.00 1.99 2.00 2.00 1.99 1.97 2.00 4.02 2.00 2.01 4.01 8.01 2.02 4.06 4.01 4.05 2.04 22.34 21.20
10.0 9.5 9.0 8.5 8.0 7.5 7.0 6.5 6.0 5.5 5.0 4.5 4.0 3.5 3.0 2.5 2.0 1.5 1.0 0.5 0.0 -0.5 -1.0
f1 (ppm)

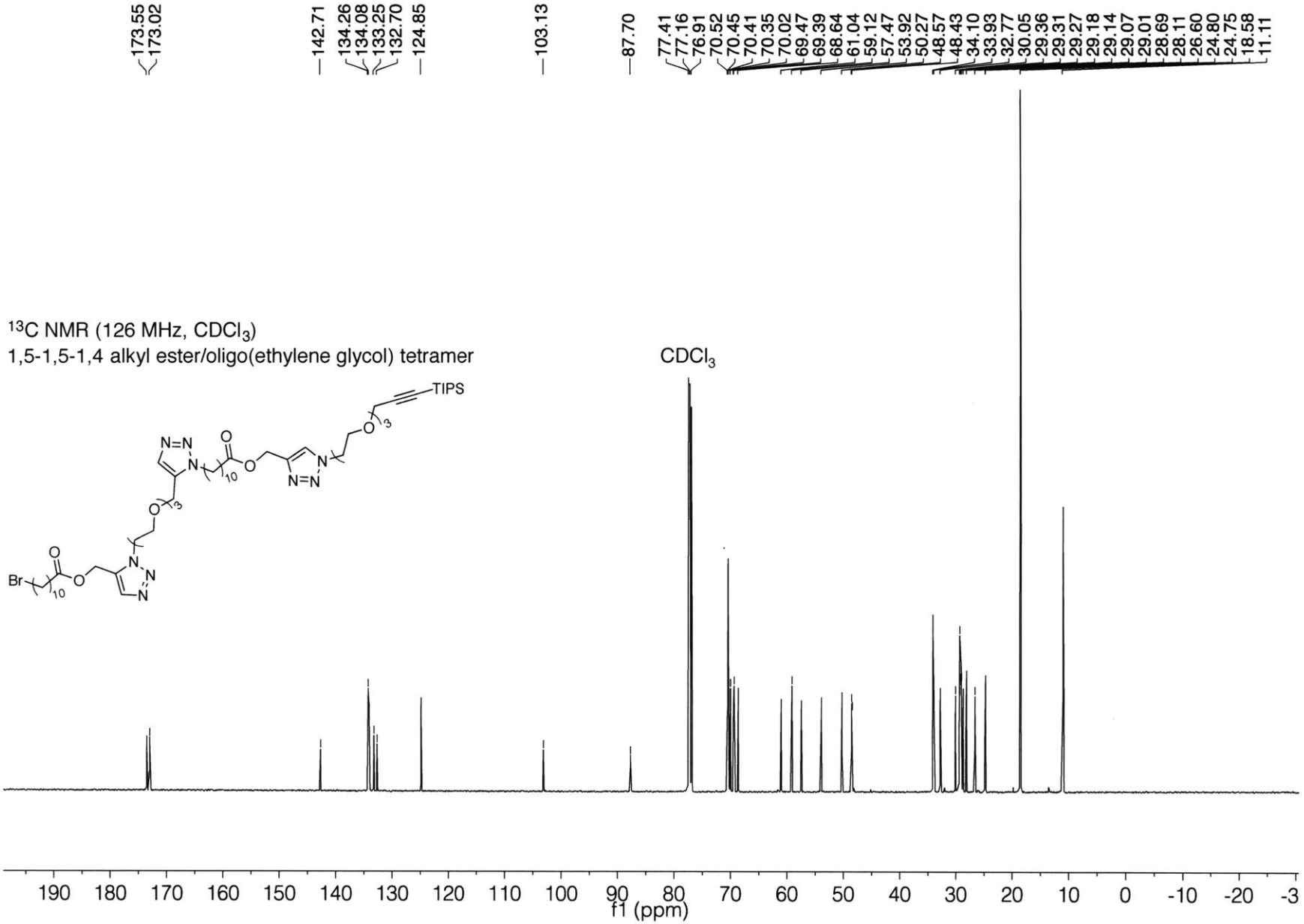
173.55
173.02
142.71
134.26
134.08
133.25
132.70
124.85
103.13
87.70
77.41
77.16
76.91
70.52
70.45
70.41
70.35
70.02
69.47
69.39
68.64
61.04
59.12
57.47
53.92
50.27
48.57
48.43
34.10
33.93
32.77
30.05
29.36
29.31
29.27
29.18
29.14
29.07
29.01
28.69
28.11
26.60
24.80
24.75
18.58
11.11
13C NMR (126 MHz, CDCl3)
1,5-1,5-1,4 alkyl ester/oligo(ethylene glycol) tetramer
CDCl3
TIPS
Br
190 180 170 160 150 140 130 120 110 100 90 80 70 60 50 40 30 20 10 0 -10 -20 -3
f1 (ppm)

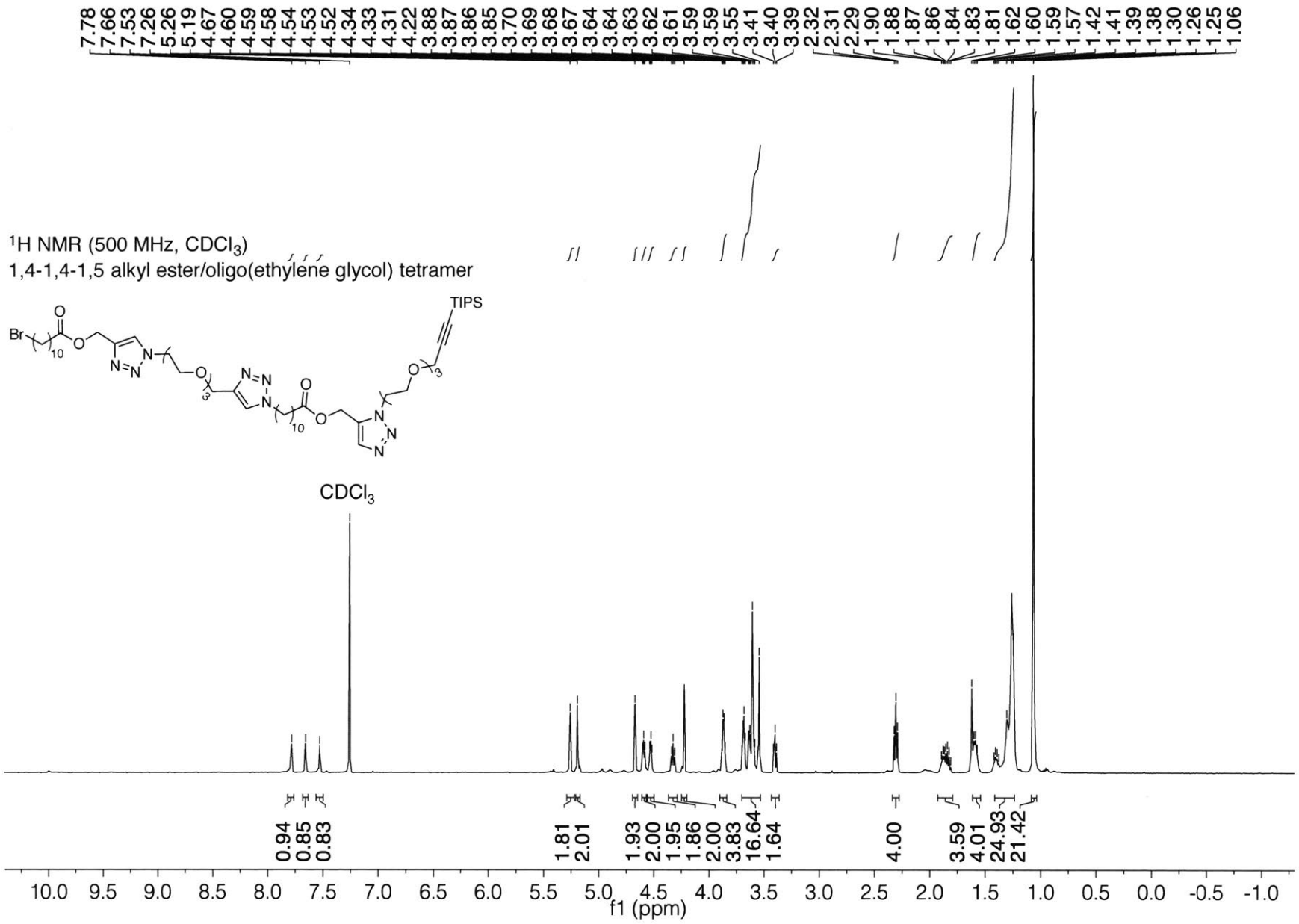
7.78
7.66
7.53
7.26
5.26
5.19
4.67
4.60
4.59
4.58
4.54
4.53
4.52
4.34
4.33
4.31
4.22
3.88
3.87
3.86
3.85
3.70
3.69
3.68
3.67
3.64
3.64
3.63
3.62
3.61
3.59
3.59
3.55
3.41
3.40
3.39
2.32
2.31
2.29
1.90
1.88
1.87
1.86
1.84
1.83
1.81
1.62
1.60
1.59
1.57
1.42
1.41
1.39
1.38
1.30
1.26
1.25
1.06
1H NMR (500 MHz, CDCl3)
1,4-1,4-1,5 alkyl ester/oligo(ethylene glycol) tetramer
Br
TIPS
CDCl3
0.94
0.85
0.83
1.81
2.01
1.93
2.00
1.95
1.86
2.00
3.83
16.64
1.64
4.00
3.59
4.01
24.93
21.42
10.0 9.5 9.0 8.5 8.0 7.5 7.0 6.5 6.0 5.5 5.0 4.5 4.0 3.5 3.0 2.5 2.0 1.5 1.0 0.5 0.0 -0.5 -1.0
f1 (ppm)

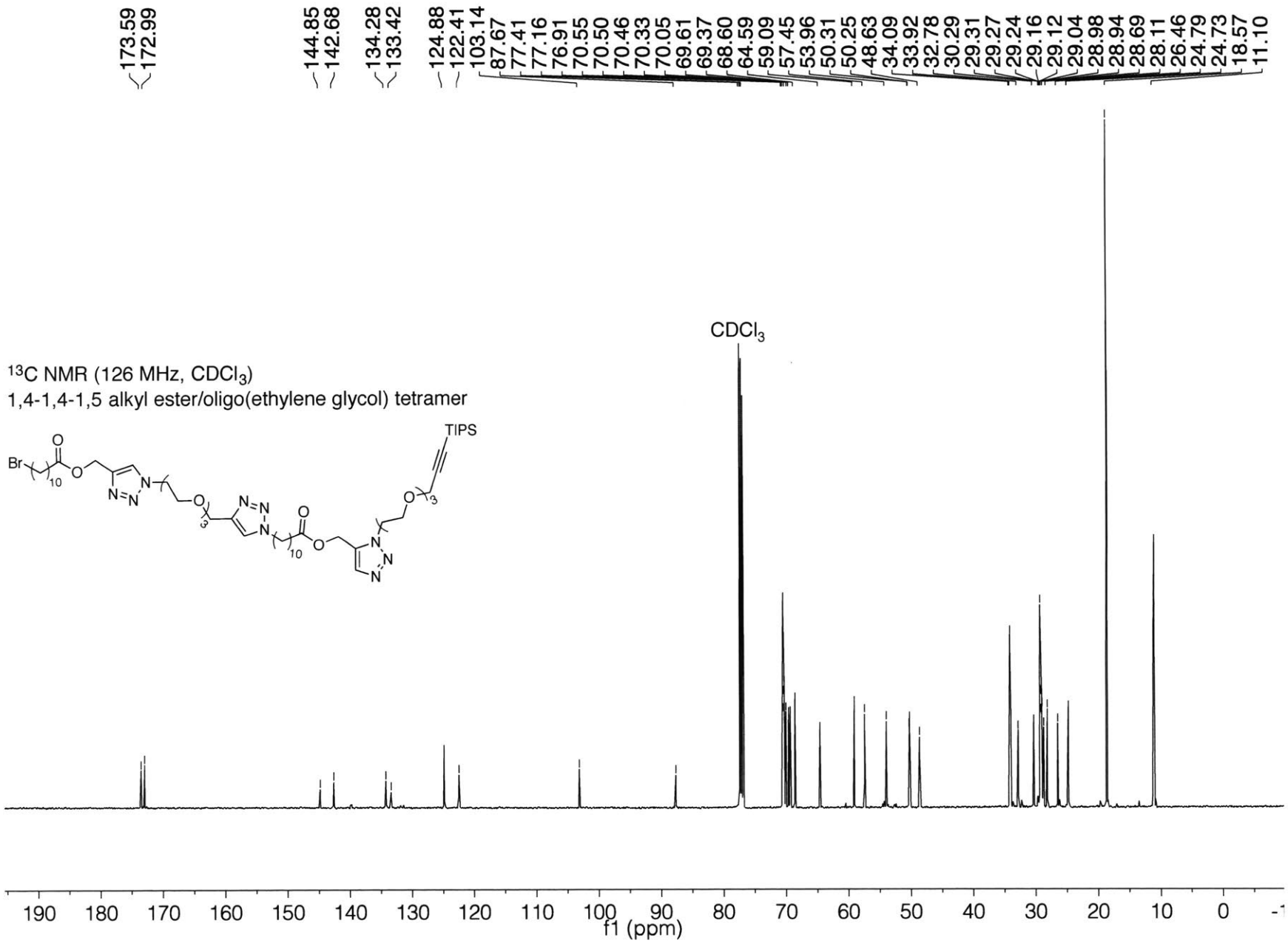
173.59
172.99
144.85
142.68
134.28
133.42
124.88
122.41
103.14
87.67
77.41
77.16
76.91
70.55
70.50
70.46
70.33
70.05
69.61
69.37
68.60
64.59
59.09
57.45
53.96
50.31
50.25
48.63
34.09
33.92
32.78
30.29
29.31
29.27
29.24
29.16
29.12
29.04
28.98
28.94
28.69
28.11
26.46
24.79
24.73
18.57
11.10
CDCl3
13C NMR (126 MHz, CDCl3)
1,4-1,4-1,5 alkyl ester/oligo(ethylene glycol) tetramer
TIPS
Br
f1 (ppm)

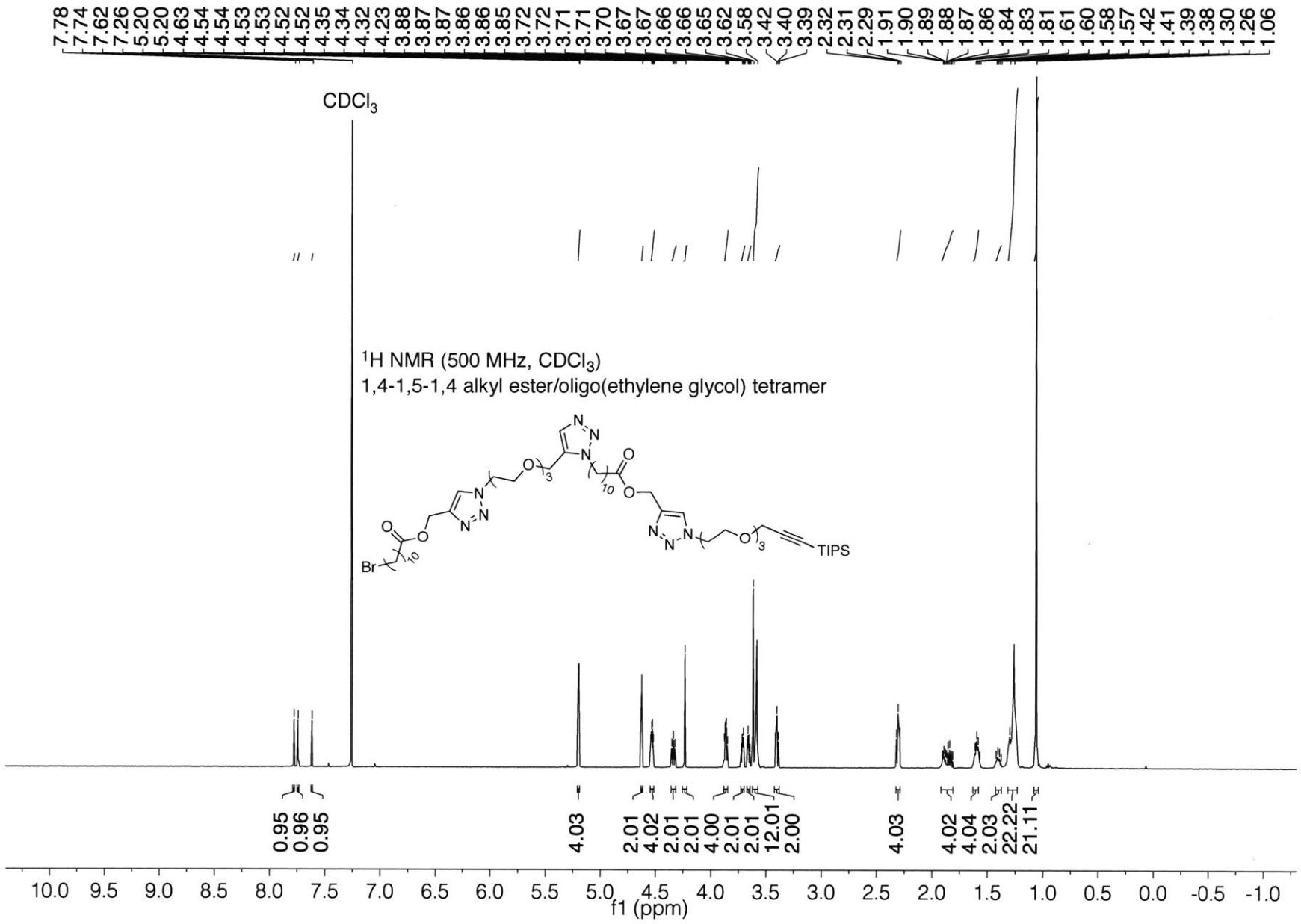
7.78
7.74
7.62
7.26
5.20
5.20
4.63
4.54
4.54
4.53
4.53
4.52
4.52
4.35
4.34
4.32
4.23
3.88
3.87
3.87
3.86
3.86
3.85
3.72
3.72
3.71
3.71
3.70
3.67
3.67
3.66
3.66
3.65
3.62
3.58
3.42
3.40
3.39
2.32
2.31
2.29
1.91
1.90
1.89
1.88
1.87
1.86
1.84
1.83
1.81
1.61
1.60
1.58
1.57
1.42
1.41
1.39
1.38
1.30
1.26
1.06
CDCl3
1H NMR (500 MHz, CDCl3)
1,4-1,5-1,4 alkyl ester/oligo(ethylene glycol) tetramer
Br
TIPS
0.95
0.96
0.95
4.03
2.01
4.02
2.01
2.01
4.00
2.01
2.01
12.01
2.00
4.03
4.02
4.04
2.03
22.22
21.11
10.0 9.5 9.0 8.5 8.0 7.5 7.0 6.5 6.0 5.5 5.0 4.5 4.0 3.5 3.0 2.5 2.0 1.5 1.0 0.5 0.0 -0.5 -1.0
f1 (ppm)

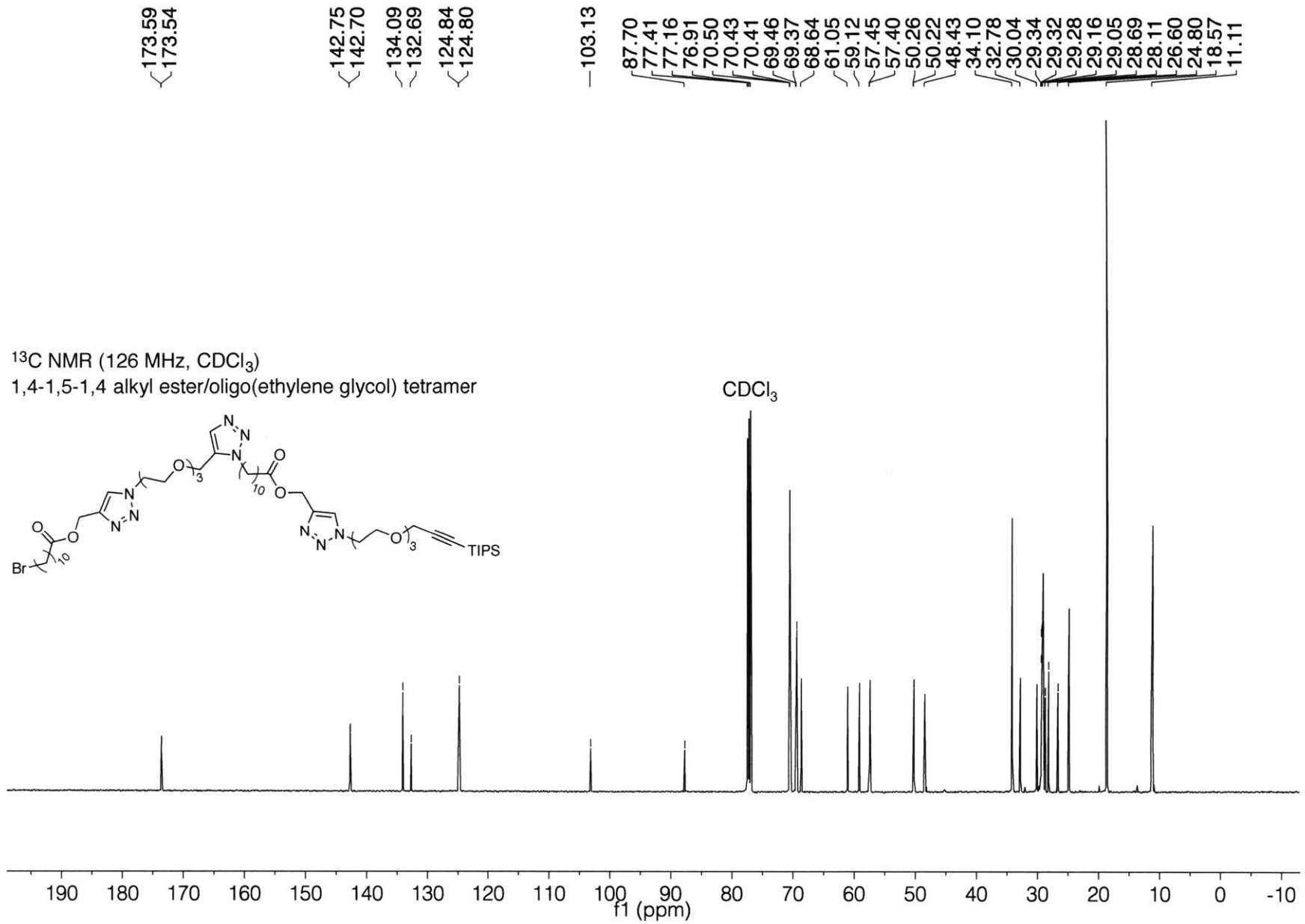
173.59
173.54
142.75
142.70
134.09
132.69
124.84
124.80
103.13
87.70
77.41
77.16
76.91
70.50
70.43
70.41
69.46
69.37
68.64
61.05
59.12
57.45
57.40
50.26
50.22
48.43
34.10
32.78
30.04
29.34
29.32
29.28
29.16
29.05
28.69
28.11
26.60
24.80
18.57
11.11
13C NMR (126 MHz, CDCl3)
1,4-1,5-1,4 alkyl ester/oligo(ethylene glycol) tetramer
CDCl3
Br
TIPS
190
180
170
160
150
140
130
120
110
100
90
80
70
60
50
40
30
20
10
0
-10
f1 (ppm)

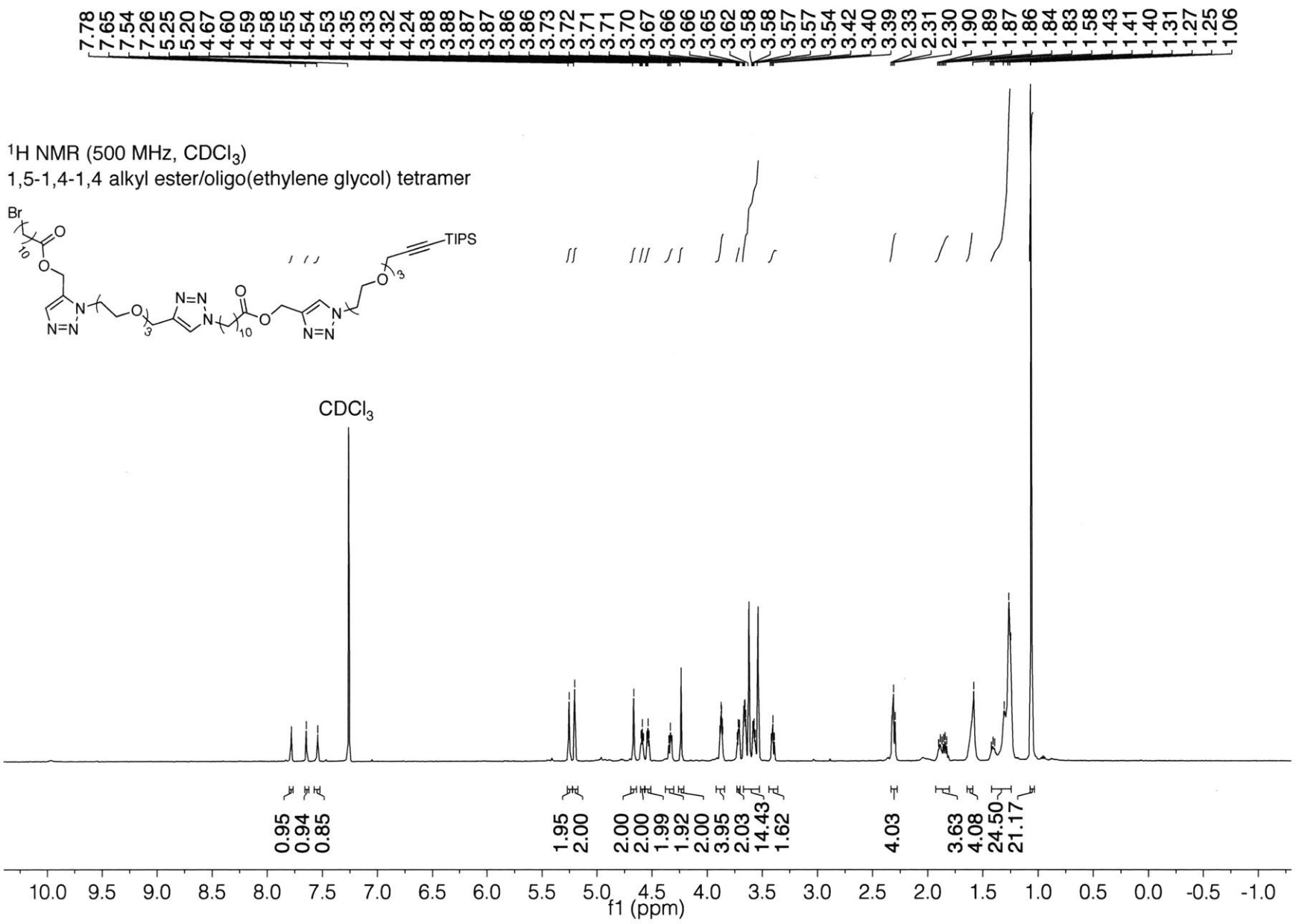
7.78 7.65 7.54 7.26 5.25 5.20 4.67 4.60 4.59 4.58 4.55 4.54 4.53 4.35 4.33 4.32 4.24 3.88 3.88 3.87 3.87 3.86 3.86 3.73 3.72 3.71 3.71 3.70 3.67 3.66 3.66 3.65 3.62 3.58 3.58 3.57 3.57 3.54 3.42 3.40 3.39 2.33 2.31 2.30 1.90 1.89 1.87 1.86 1.84 1.83 1.58 1.43 1.41 1.40 1.31 1.27 1.25 1.06
1H NMR (500 MHz, CDCl3)
1,5-1,4-1,4 alkyl ester/oligo(ethylene glycol) tetramer
Br
TIPS
CDCl3
0.95 0.94 0.85 1.95 2.00 2.00 2.00 1.99 1.92 2.00 3.95 2.03 14.43 1.62 4.03 3.63 4.08 24.50 21.17
10.0 9.5 9.0 8.5 8.0 7.5 7.0 6.5 6.0 5.5 5.0 4.5 4.0 3.5 3.0 2.5 2.0 1.5 1.0 0.5 0.0 -0.5 -1.0
f1 (ppm)

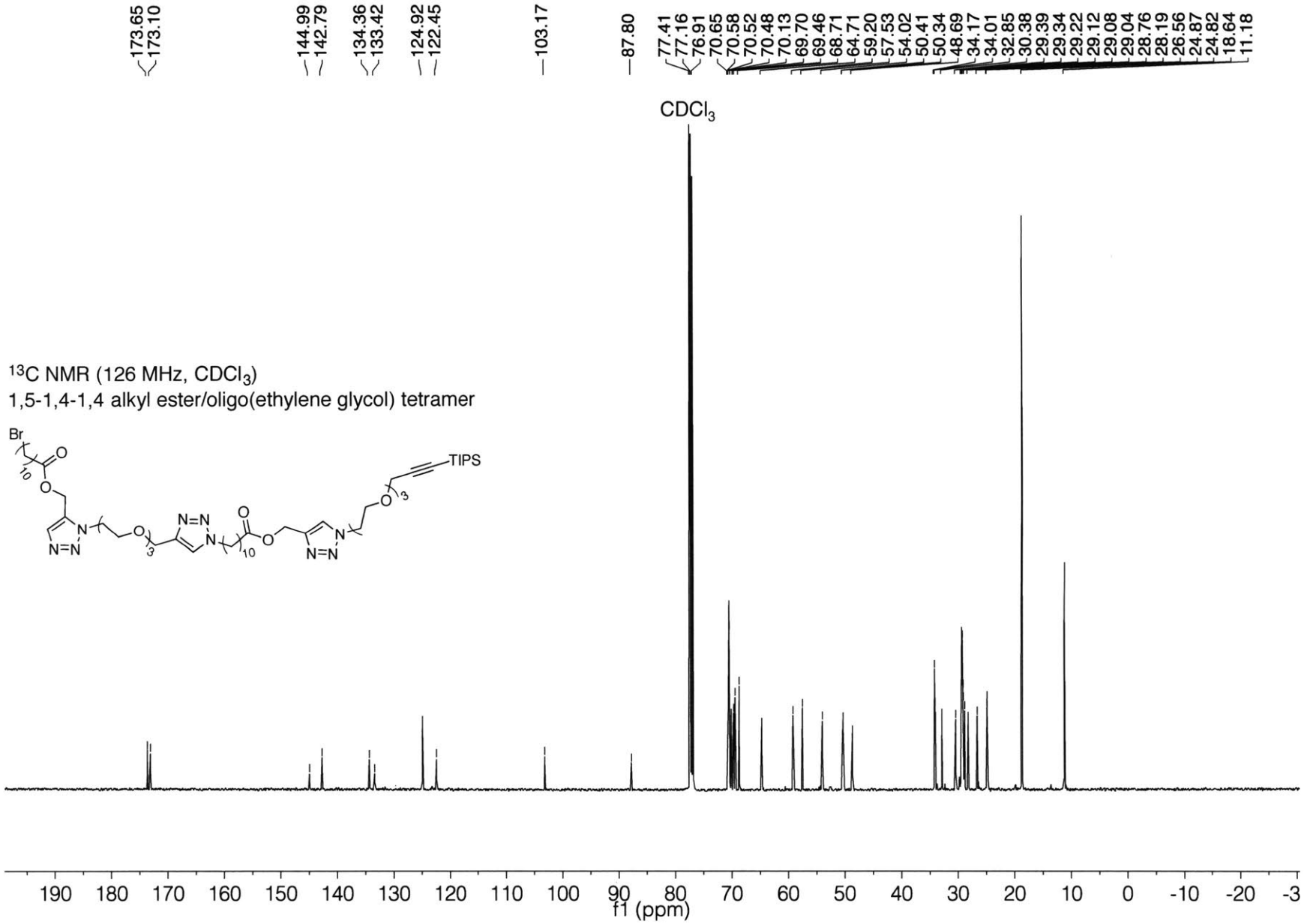
173.65
173.10
144.99
142.79
134.36
133.42
124.92
122.45
103.17
87.80
77.41
77.16
76.91
70.65
70.58
70.52
70.48
70.13
69.70
69.46
68.71
64.71
59.20
57.53
54.02
50.41
50.34
48.69
34.17
34.01
32.85
30.38
29.39
29.34
29.22
29.12
29.08
29.04
28.76
28.19
26.56
24.87
24.82
18.64
11.18
CDCl3
13C NMR (126 MHz, CDCl3)
1,5-1,4-1,4 alkyl ester/oligo(ethylene glycol) tetramer
Br
TIPS
190 180 170 160 150 140 130 120 110 100 90 80 70 60 50 40 30 20 10 0 -10 -20 -3
f1 (ppm)